MODELING THE IMPACT OF ENVIRONMENTAL FACTORS, DIAPAUSE AND CONTROL STRATEGIES ON TICK AND TICK-BORNE DISEASE DYNAMICS

MARCO TOSATO

A DISSERTATION SUBMITTED TO THE FACULTY OF GRADUATE STUDIES
IN PARTIAL FULFILMENT OF THE REQUIREMENTS
FOR THE DEGREE OF
DOCTOR OF PHILOSOPHY

GRADUATE PROGRAM IN MATHEMATICS AND STATISTICS
YORK UNIVERSITY
TORONTO, ONTARIO

JULY 2022

Abstract

In this thesis, we focus on mathematical formulation and analyses for a specific vector responsible for a wide variety of diseases: ticks. Due to climate change, various tick species are rapidly spreading northward from the United States and have increasingly affected the Canadian population through a variety of tick-borne diseases including Lyme disease. In order to address this problem, the Public Health Agency of Canada has dedicated an entire section of its website to discuss the risks and the possibility of preventing, recognising and treating tick-bites. It is therefore important to analyse tick and tick-borne disease dynamics in order to better understand, study and prevent possible new outbreaks.

We aim to achieve this by using mathematical and epidemiological tools including dynamical systems, ordinary and delay differential equations, basic reproduction numbers and Hopf bifurcation theory. For this purpose, we produce three different models to study the effect of physiological features such as diapause, control strategies and the effect of environmental conditions on tick and tick-borne disease persistence and periodicity.

The first model we propose is a two-patch tick population model in which we show how the tick reproduction number $R_{T,c}$ affects the long-term behaviours of tick population and how it might lead to extinction, convergence to a coexistent or to a periodic solution. The second model is a single tick population model with switching delays. In this, we prove how oscillations of different frequencies caused by two delays might produce multi-cycle periodic solutions. The last model we analyse is a tick-host model including host control strategies. In this work, we find that there are situations in which the improper application of repellent and acaricide may lead to unexpected results and improve disease spread instead of reducing it.

Acknowledgements

I would like to thank all the people that I have encountered throughout this PhD journey. In a way, all of you have contributed to my personal growth which lead to this important achievement.

First, I want to thank Dr. Jianhong Wu for his supervision and guidance during these past five years. Although he did not have much time to dedicate to all his students, he was there in the moments of need and supported me when I needed it the most. Also he was responsible of creating a very familiar environment in the LIAM lab which made my experience very enjoyable. I want to thank also Dr. Xue Zhang and Dr. Kyeongah Nah for collaborating in some of the projects; Dr. Neal Madras and Dr. Huaiping Zhu for being part of my supervisory committee throughout my PhD journey; Dr. Jude Kong, Dr. Jean-Paul Paluzzi, Dr. Xingfu Zou for the useful feedback provided in the final defense; Dr. Woldegebriel Assefa Woldegerima, Dr. Jummy David, Dr. Martin Grunnill and Dr. Pengfei Song for their collaboration in our vector-borne disease and climate change group work.

Of course, my family has played a great role in this life-changing experience in Canada so I would like to thank immensely my parents Bruno and Carla and my younger brother Jacopo. They are a continuous source of inspiration for me and I never stop learning from them. Without their continuous love, patience and support, it would have been much harder to reach this achievement.

Also I would like to mention my friends that have significantly participated and helped me throughout these years. A few of them managed to share the journey with me at some point of my Canadian experience: Abdullah, Allysa, Ben, Elena, Justin, Kelvin, Mirko, Neda,

Vishal and Yohana. Others have supported me from far: Alessandra, Damiano, Eduardo, Frizz, Giovanna, Giulia, Kornelia, Marco, Mirtza, Nicola, Stefano and Toni. Note that there are many other people not included in this list that are worth thanking.

In the last few years, I viewed the lab not only as a workplace, but also as a family. For this reason, there are several more people I would like to mention with which I created a strong relation and which have helped me also in a professional way. First, I would like to thank Qiuyi for her support and patience that helped me overcome some moments of difficulty and for the great experiences we shared in these years. Also, I would like to mention other LIAM members such as Francesca, Kyeongah and Mahnaz with which I shared part of my adventures. Finally, I wanted to mention also Bushra and Mina which were very helpful in the moment of need and Gregoire and Farah which are newcomers to the lab and wish them the brightest future.

Last but not least, I would like to thank the maths department for the opportunity offered, the professors that I have had a chance to communicate with and to learn from, and in general all those that have been helpful including Ann-Marie, Anne Marie, Madeline and Primrose.

Table of Contents

List of Tables

List of Figures

Chapter 1

Introduction

1.1 Introduction to ticks

Vector-borne diseases are among the most important public health problems and account for more than 17% of all infectious diseases according to the World Health Organisation (WHO) [1]. These have a great impact worldwide due to the large geographical range of vector movements even though the main issues can be viewed in poorer countries. WHO has approved a "Global Vector Control Response (GVCR) 2017–2030" where guidelines have been put in practice to help strengthening vector control [2].

Ticks are one of the main vectors (after mosquitoes) responsible for this matter and have been considered a worldwide concern due to the variety and range to which they are responsible of disease transmission. Along with climate change, public concerns over vector-borne diseases have been growing due to the drastic increase of disease incidence in endemic areas or the emergence of diseases in previously non-endemic regions. As an example, *Ixodes scapularis* ticks which were originally just in the Southern parts of Canada have started to spread northward and have reached areas which used to be tick-free and tick-related diseases have started to affect significantly the Canadian population [3].

Ticks are arachnids that belong to the subclass of "Acari" together with mites and they differ substantially from the insect world. Similar to spiders, they are eight-legged organisms

in their adult stage. There are several varieties of ticks but they can all be subdivided in two main classes: hard and soft ticks. The former are characterised by a harder outer layer and are mostly responsible for tick-borne diseases (TBDs) while the latter have a soft outer layer. In this thesis, we will mostly focus on hard ticks since they are more likely to parasitize people and animals and are the main cause of several tick-borne diseases. Their lifecycle consists of four main stages: Eggs, Larvae, Nymphs and Adults, and the stage-to-stage development from larvae to nymphs and from nymphs to adults occurs after ticks blood feed on hosts. There are different substages for each post-egg stage: the questing stage, the feeding stage and the engorged stage. In the questing stage, ticks look for a host to climb on and to feed on. In the feeding stage, they feed on a host before detaching and moulting on the ground. Note that host preferences vary from species to species - there are one-host, two-hosts and three-host ticks species. Most hard ticks are three-hosts species so they need to feed blood from three different hosts before molting at each stage for full development. They usually feed on rodents or small mammals at larval stage and larger mammals at the nymphal and adult stage [4]. Adult females can lay eggs after they feed one last time, usually in the Spring, and they die soon after. In most ticks, mating occurs on the host but certain Ixodid species can mate also on the ground while the female engorges. Tick lifecycle length varies and is for hard ticks generally between two and four years. The number of eggs laid by female hard tick adults is variable and can reach up to tens of thousands [5, 6]. Tick lifecycle may vary depending to several factors. An important aspect to consider is the fact that during their lifecycle ticks have a hormonal mechanism to minimize energy consumption during unfavorable periods called diapause. Diapause can be behavioural or developmental. The former occurs when there is an unfavorable questing condition while the latter occurs while ticks are developing from stage-to-stage (larvae-to-nymphs or nymphs-to-adults). Not much is known about the physiology of diapause in ticks but we know that it is comprised of three different stages and it has a fixed latency period [7].

Ticks are responsible for several diseases brought to mammals, including rodents, deer, cattle and also to humans. The wide variety of possible TBDs and ticks' large and expanding

geographical range constitutes a problem. Two of the main tick-borne diseases are Lyme disease which has been a rather controversial topic in the media and tick-borne encephalitis (TBE). There are several other TBDs worth mentioning which include Heartland virus, spotted fever, paralysis, Q-fever [4].

Lyme disease is a bacterial infection caused by the bacterium *Borrelia burgdorferi* and usually manifests itself in a bull's eye pattern rash. The main vectors are Ixodid ticks and the main species affecting the spread are *Ixodes ricinus* which is mainly present in Europe, *Ixodes pacificus* in Western America, *Ixodes scapularis* in Eastern America and *Ixodes persulcatus* in Asia [4]. A vaccine was available in the United States for Lyme disease between 1998-2002 but it was highly debated and was then discontinued supposedly due to insufficient consumer demand. Now several vaccines are under trial to treat Lyme disease [8] but there are currently only vaccines available for dogs.

TBE is instead a viral infection which is usually asymptomatic. In symptomatic cases, it presents itself into two stages. Generally the first stage symptoms are similar to flu and not life-threatening, but in a second stage it can affect the central nervous system and can cause long-term brain damage. Vaccines are available to prevent TBE in disease-endemic areas like China and Europe [9]. Vaccine has recently been made available also in the United States from August 2021 [10].

The main route of disease transmission is direct when either an infected tick bites on a susceptible host and infects the host or when a susceptible tick bites on an infected host and acquires the pathogen. Small mammals and ticks are active parts in the disease transmission. Note that humans and deer are dead-end hosts in this cycle since they can become infected but do not infect other ticks biting on them and this is due to the different concentration of pathogen in the blood between humans, deer and other smaller mammals. Another possible route of disease transmission is transovarial which may occur when an infected female lays egg and it may transmit the disease to the newly born. This mode of transmission is still under investigation but seems to be irrelevant for certain kinds of tick-borne diseases like Lyme disease [11, 12]. A third indirect disease transmission route is co-feeding and it has

been shown to be a relevant mean of disease transmission in several studies for tick-borne diseases [13, 14, 15]. It is a non-systemic transmission where a susceptible tick (usually at the larval stage) feeds on the same host with an infected tick (usually at the nymphal stage) and acquires the infection by feeding adjacent to each other. This is common since ticks tend to feed on hosts in specific places for example behind the ears so several ticks may be in proximity to each other at the same time. Note that co-feeding transmission may take place even without infecting the host and also if the host is immune from any tick-borne disease [16].

Tick population dynamics depends highly on the habitat's local microclimatic conditions [17] and host abundance is key to sustaining the tick population since ticks must take blood meals from hosts to develop. Ticks at different stages of their life cycles have different host preferences: immature ticks mostly feed on small mammals and rodents while adult ticks tend to have their blood meals from large mammal hosts such as deer [18]. Therefore, the ecosystem and biodiversity can greatly affect tick dynamics and tick-borne disease transmission risk and its effects are still not entirely analysed. Predation is for example a key element that modifies host dynamics for ticks and some studies have tried to show correlation between some species and incidence of Lyme disease. Some works show that predation on small hosts does not change tick population significantly but predation on large hosts such as deer does [19]. The abundance of suitable large mammals in the habitat is therefore important for adult ticks to complete their development and reproduction [20]. These large mammal hosts also provide the mobility of adult ticks as feeding adult ticks may be carried by the hosts and drop off in different locations. If though deer population is above a certain threshold, predation on small mammals becomes highly relevant. In this case, it has been shown [21, 22] that for example foxes have a negative correlation with Lyme disease incidence since they mainly feed on tick hosts such as rodents while coyotes have a positive correlation with it since they compete with foxes on some of other mammal hosts.

Climatic conditions also affect tick population dynamics. Temperature, for example, has been seen to play a crucial role in tick persistence [23]. Low temperatures may lead ticks

to a quiescence period, a state of torpidity in which ticks arrest their development and slow down their progression [7]. It is also well known that ticks cannot survive at really cold temperatures. Therefore, when temperature rises due to climate warming, the geographic range of ticks expands quickly. This led to the observed trend of northward spread of ticks in Canada [3]. Other factors influencing tick development include humidity and daylight exposure. Ticks tend to survive easily in humid environments such as those with thick mat layers in the soil [24]. Several experimental studies show that ticks are very vulnerable to desiccation, therefore they remain questing for a limited time before replenishing their reserves [25]. Ticks are also sensitive to changes of daylight and tend to undergo long diapausing periods in habitats where the amount of light is below an optimal level [26].

For this reason, in a given region, there may be heterogeneity in tick distribution which depends on different combinations of local environmental conditions [27]. The habitat configuration analysis [28], aiming to identify potentially favorable areas for tick development and examining how connectivity between different patches impacts the tick population distribution, has shown that hosts play a key role since ticks have very limited mobility by themselves, but they can move between different patches when they are attached to hosts during their blood meals. In a work by Estrada-Peña et al. [29], geographical areas are classified according to certain micro-habitat and climatic conditions into being favorable or unfavorable for tick growth and spread. Certain woodland areas are both less exposed to daylight and contain a dense shrub layer that guarantees a high level of humidity and can keep the ticks protected from sub-zero temperatures, so they are highly favorable for tick growth [17, 30]. On the other hand, grasslands do not have any protection from sunlight and can be drier in comparison to woodlands, so they are generally less favorable for tick development [31]. Several studies have found a higher density of ticks in woodlands than in grasslands, for example in Spain [29] and Sweden [32] for *Ixodes ricinus*, and in the United States [33] for *Ixodes scapularis*. All the ecological factors mentioned above have been shown to influence tick development by modifying not only their survival rates but also their diapause probabilities [34]. This means that ticks in general take less time to develop and have a higher survival

rate in favorable areas than in unfavorable areas.

Therefore, human interventions can alter the tick population dynamics. The two main types of control are host-related and habitat-related. Host control strategies can be classified into rodent-targeting strategies and deer-targeting strategies. The rodent-targeting strategies include bait boxes and tick tubes which are designed to treat rodents with acaricides using different baits: food in the former and nest material in the latter [35, 36]. The deer-targeting strategies include the application of acaricide on a food bait and a pesticide-impregnated collar [37], removal of deer population in overpopulated areas or fencing [38]. Depending on the chemical used on the acaricide, it can be useful to kill ticks on the host or to repel ticks from feeding on that host. As for habitat-related control strategies, they can be divided into tick habitat modification strategies [39] including controlled burns [40] or interventions to decrease humidity levels in tick-populated areas [41]; and tick-targeted strategies to capture ticks such as TickBots, which are robots fitted with a cloth which attract ticks [42]. It is difficult to find a universal control strategy as there are several area-specific factors affecting the control outcomes, such as local habitat, temperature and humidity level. Also, several other complications arise including tick behaviour change and acquired immunity that would render some of these strategies less effective or ineffective. Another important aspect to keep in mind is overcompensation, which might happen when some of these host control strategies cause adult tick reduction. This in turn leads to a reduced competition among adults that causes an increase in the juvenile population which may act as a reservoir for the disease to establish. An explanation of this process in perch is described in the paper by Ohlberger et al [43]. Finally, there are several tick species transmitting the same type of tick-borne diseases which have different feeding preferences, behaviours (can be aggressive or passive in questing for hosts) and lifecycles so the most effective control strategy should also be species-specific.

1.2 Mathematical models for ticks

There has been intensive studies on ticks, ranging from experimental work to mathematical models where the aim is mainly to understand and analyse tick ecological population dynamics and tick-borne disease epidemiological transmission dynamics in order to reduce disease transmission. Most of the models included in this section are compartmental models that involve tick population densities at each, or some integrated parts, of the different tick stages: egg, questing larvae, feeding larvae, engorged larvae, questing nymphs, feeding nymphs, engorged nymphs, questing adults, feeding adults, engorged adults and egg-laying adults. Most of these works present novel approaches or ideas to study specific aspects of tick ecological and tick-borne disease epidemiological dynamics.

A few of the models proposed were reaction-diffusion models using partial differential equations. Caraco et al. [44] introduced such a model to study Lyme disease epidemics. The idea was to consider the epidemic wave deriving from this model and use it to study the effect of introduction of new cases on a highly susceptible population through perturbation analysis. Here the main finding was that the addition of a single case could cause the dynamics to reach a disease-endemic equilibrium starting from a disease-free one. This study was then extended by Zhang et al. [45] with the inclusion of periodicity in the biting and developmental rates. In this work, results are presented both for a bounded and unbounded environment and a case study with Ontario tick data is analysed.

A relevant review on previous works is the paper by Lou and Wu [46] which analyses the effect of three different tick host-seeking behaviours chosen in previous models: a frequency-dependent case in which seeking time for ticks does not depend on host density, a linear density-dependent case where the searching time for ticks is inversely proportional to the host density and a Holling 2 type of interaction where there is a dependence on density but it saturates as host density grows large. We see that the implications for disease control are completely different in all cases. For the frequency-dependent case, host reduction would increase disease transmission, for the density-dependent case it would reduce transmission. For the Holling 2 case, host reduction could either increase or decrease transmission depending

on the circumstances. So it follows that we need to be very careful on the choice of the host functional response since it completely modifies the model dynamics.

Other tick models study the transmission dynamics of Lyme disease using delay differential equations (DDEs) where the delay term represents the effect of inter-stadial development of ticks. Here parameters are considered to be constant as in Fan et al. [47] and Shu et al. [48] or time-dependent due to seasonality as in Wang et al. [49] and the aim is to analyse the tick basic reproduction number. In the first two papers, great emphasis is given to the study of global Hopf bifurcations in the model while the latter mainly shows how to compute the reproduction number using Floquet multipliers and functional analysis tools in a periodic setting and describes a case study in Ontario.

Another category of papers describe the importance of climate change in tick population. As pointed out by Fisman et al. [50], the effect of climate change and of climate oscillations phenomena such as ENSO (El Nino Southern Oscillation) has had great repercussions on infectious diseases and in particular on vector borne diseases in North America. In case of tick-borne diseases, the range of tick spread has widened in North America and the northward range expansion of ticks has increased over time and is predicted to increase also in the future. Specifically regarding ticks, there are several papers documenting on this matter. A series of papers by Ogden and collaborators focus on this matter starting with a paper from 2004 [23] which focuses on the relation between temperature and tick development rates. This paper derives from some experimental work on *Ixodes scapularis* ticks showing how long it would take them to develop from stage to stage under different temperatures in a lab setting. This work is then extended by the same author in [51] to create a difference equations model for tick dynamics where temperature plays a key role. In the long run, the model would result in either one of the two options: it can reach extinction or a cyclical equilibrium depending on the temperatures at input. This model has then been used to formulate predictions on tick establishment in Canada [52]. This idea is then used in Wu et al. [3] with a system of differential equations where the basic reproduction number of *Ixodes scapularis* ticks in different areas of Canada can be computed according to the temperatures in each area. From

this, a few more works such as Ogden et al. [53] and especially McPherson et al. [54] have tried to use different climate models to predict tick and tick-borne disease expansion in the future. It turns out that in most climate predictions, due to global warming, ticks are predicted to expand northward more and more and lead to persistence in a large portion of Canada. In a similar time, other works have described the effect of climate change including the increasing temperature on tick northward expansion in Canada using remote sensing data like Cheng et al. [55] or including statistical analysis on predictions for tick spread like Clow et al [56].

Another relevant aspect influencing tick-borne diseases is the effect of hosts in tick-borne disease spread. Levi et al. [21] studied the importance of host predation in modifying the host structure and tick dynamics. For this purpose, a host-tick ordinary differential equation (ODE) model focusing on small mammal dynamics has been produced and predation has been included in the model. Also Cobbold et al. [19] included host predation and environmental conditions on hosts by including seasonality in host abundance. Another interesting idea is derived in Jennings et al. [57] whose goal is to study how tick dynamics are influenced by host immune reactions. This is an ODE model for general tick-host dynamics where hosts are divided into rodents and deer and each of these contain two subclasses: the so-called "good" hosts which have no/little immunity to ticks and "bad" hosts which are instead immune. This theoretical study describes four different reproduction ratios which involve different combinations of rodent and deer hosts (where rodents and deer are respectively either all "good" or all "bad") and shows how immunity in hosts would affect the tick population and lead either to unlimited growth, to a constant persistence or to extinction.

There is also a tick-related development factor that greatly influences tick-borne disease dynamics which is diapause. Several models have taken into account this possibility for ticks to pause their development. Ghosh and Pugliese [58] have included the presence of diapause through a parameter p in a two season ODE tick dynamical model. It turns out that this parameter is key in determining the long-run behaviour of the model and can cause extinction or convergence to a positive equilibrium. In this paper, tick population densities are shown to

be positively correlated to hosts. An interesting phenomenon observed there is the dilution effect where large host numbers would help in disease eradication since several tick bites would be wasted in biting non-infected hosts. In two separate works, Rosà et al. and Ludwig et al. [59, 60] have described how diapause is significant in the model through statistical studies with field data respectively in Italy and USA since there is a high correlation between larvae in a year and nymphs in the following year. Dobson et al. [61] has included co-feeding in the model including nymphs in both behavioural and developmental diapause. In recent years, Zhang and other authors have worked in studying diapause and considering a fraction of the tick population to undergo diapause and therefore take longer to develop. Such models are quite challenging to study and analyse since they contain two different delays which lead to interesting patterns. In 2019, Zhang and Wu [62] studied periodic solutions by analysing Hopf bifurcations in such a model and on a later paper Zhang et al. have considered what happens to the global continuation of periodic solutions [63].

Another tick-related aspect worth considering is co-feeding which has been considered in several works. Rosà et al. for example included co-feeding transmission in a two-host tick epidemic model, since research showed the relevance of co-feeding in tick-borne disease transmission in Italy [64]. Harrison and Bennett [13] have simulated theoretical datasets on tick dynamics using statistical techniques and analysed the relevance of co-feeding in the disease basic reproduction number. A similar model to Rosà has been ideated by Wu et al. in 2015 [65] where the system of ODEs has been replaced by a system of DDEs. Zhang et al. [66, 67] have considered both co-feeding and diapause and showed how both are involved in periodic and irregular oscillations that take place for certain parameter values. In the first paper, hosts are just separated into hosts that admit co-feeding and those that cannot. In the second paper, hosts are further divided according to how many nymphs are feeding on them and a basic reproduction number of infestation is described which is the average number of ticks biting on a generic host. Nah et al. [15] have shown how co-feeding is also relevant in Hungarian TBE virus transmission dynamics and estimated some parameters by fitting temperature and incidence data to a complex hidden Markov model.

Another aspect studied in this thesis is the effect of control strategies to modify tick population and transmission dynamics. In Australia and Cuba, works by Sutherst et al. in 1979 [68] and Labarta et al. in 1996 [69] have analysed the effect of the cattle tick *Boophilus microplus* responsible for spreading babesia (a parasite that infects red blood cells) on cattle. The plan was to maximize the earning using control methods for cattle to avoid tick infestation which causes disease transmission. In the former paper, control methods considered include acaricide on sheep and pasture spelling. In the latter, also the possibility of a vaccine is considered and combinations between vaccine and acaricide applications have been analysed. Gaff et al. analysed in their papers [70, 71] the impact of feeding corn with acaricide to deer through a control strategy model. In the latter, the aim was to determine the optimal time at which the acaricide should be applied.

Understanding how ticks would behave spatially when feeding on large mammals is another important aspect to consider. Works by Zhang et al. [72, 73] propose a multi-patch environment for ticks including an element of migration. In the first paper [72], the aim is to show how movement, co-feeding and seasonal variation impact on tick and tick-borne disease dynamics. This is accomplished by studying the effect of the parameters in modifying the two reproduction numbers that are defined: the net reproduction number of tick growth and the basic reproduction number for disease spread. In this model, migration is supposed to occur only in hosts and not in ticks. In the second paper [73], numerical simulations are used to show how host mobility may modify the model dynamics. In certain cases, the addition of this parameter leads from a complicated oscillatory pattern (without mobility), to an asymptotically synchronised periodic solution around the unique positive equilibrium (with mobility).

1.3 Structure and main contributions of the dissertation

As ticks' ranges are expanding in Canada due to climate change and are responsible for the transmission of a variety of several diseases, it is important to analyse how tick population dynamics and disease spread dynamics takes place in order to understand, predict and limit the impact on humans. Therefore, this thesis aims to develop mathematical models using delay differential equations to better understand the dynamics of tick-borne diseases. As discussed earlier, this has been a widely studied topic in literature so our specific goals and novel contributions would be to analyse the integrative effects of several factors such as diapause, mobility, environment and control strategies on the modeling outcomes.

In the second chapter, we propose a two-patch model for ticks using a system of coupled delay and ordinary differential equations incorporating just two life stages for ticks per patch: the feeding and the egg-laying female adult ticks. Here we consider different habitats in each patch (respectively woodlands and grasslands) and the ability for ticks to move when feeding on adult hosts. We introduce the concept of patch-dependent reproduction numbers and show how mobility and environmental factors affect the outcomes of the model: tick extinction, convergence to a coexistence equilibrium or convergence to a periodic solution and illustrate possible outcomes using simulations.

In the third chapter, we take inspiration from the work by Zhang and Wu [62] and analyse the periodic solutions of a scalar delay differential equation with two constant delays which are periodically switching. This equation represents the adult tick population where the two delays represent the development times for ticks not undergoing diapause (shortest delay) and for ticks that go through a diapause period (longest delay). Since we have seen that development is affected by factors such as temperature and daylight, we consider this shift to be periodic. We rigorously prove how to generate multi-cycle periodic solutions given oscillations of different frequencies produced by the two delays.

In the fourth chapter, we study the effect of two control methods for ticks: application

of acaricide (tick-killing chemical) or repellent on the host population. Here, we propose a tick-host ODE model including susceptible and infected hosts, larvae, susceptible and infected nymphs, and adult ticks. We introduce two different reproduction numbers: tick and disease and show the effect of applying acaricide and repellent on hosts in the model dynamics. It turns out that improper application of repellent and acaricide, under specific assumptions, may lead to unexpected results and improve disease spread instead of reducing it.

1.4 Author contributions for the published and submitted papers

Chapters of the thesis are based on the following publications and pre-prints:

Chapter 2:

- Tosato M., Zhang X. and Wu J., A patchy model for tick population dynamics with patch-specific developmental delays, Mathematical Biosciences and Engineering, 19(5), 5329-5360 (2022).

  Author contribution: J. W. and X. Z. originated the research idea. The model formulation was carried out by M. T. and J. W. Numerical simulation were performed by M. T. with the help of a student: Ning Yu. The writing of the manuscript was completed by M. T. after feedback from X. Z. and J. W. The project was supervised by J. W.

- Tosato M., Asymptotic expansion and Hopf bifurcations of a two-delay tick model, invited session paper for the 17th IFAC Workshop on Time Delay Systems, under review (2022).

Chapter 3:

- Tosato M., Zhang X. and Wu J., Multi-cycle periodic solutions of a differential equation with delay that switches periodically, Differential Equations and Dynamical Systems (2020).

  Author contribution: M. T., J. W. and X. Z. originated the research idea. The model formulation was carried out by M. T. and J. W. Numerical simulation were performed by M. T. The writing of the manuscript was completed by M. T. after feedback from X. Z. and J. W. The project was supervised by J. W.

Chapter 4:

- Tosato M., Nah K. and Wu J., Are host control strategies effective to eradicate tick-borne diseases (TBD)?, Journal of Theoretical Biology 508, 110483 (2021).

  Author contribution: M. T. and K. N. originated the research idea. Theoretical results were completed by M. T. and K. N. A literature review on control mechanisms was mainly completed by M. T. Numerical simulations were mainly performed by K. N. The writing of the manuscript was completed by M. T. and K. N. after feedback from J. W. The project was supervised by J. W.

Chapter 2

A tick population dynamics model in a patchy environment with patch-specific developmental delays

Tick infestation and tick-borne disease spread in a region of multiple adjacent patches with different environmental conditions depend heavily on the host mobility and patch-specific suitability for tick growth. Here we introduce a two-patch model where environmental conditions differ in patches and yield different tick developmental delays, and where feeding adult ticks can be dispersed by the movement of larger mammal hosts. We obtain a coupled system of four delay differential equations with two delays, and we examine how the dynamical behaviours depend on patch-specific basic reproduction numbers and host mobility by using singular perturbation analyses and monotone dynamical systems theory. Our theoretical results and numerical simulations provide useful insights for tick population control strategies.

2.1 Introduction to the two-patch tick model

Our focus here is the population dynamics of ticks, such as *Ixodes ricinus* and *Ixodes scapularis*, which are responsible respectively in Europe and Northeastern America for transmitting

tick-borne diseases including Lyme disease and tick-borne encephalitis. As we have described in the introduction, tick population dynamics is greatly dependent on three main factors: the metereological conditions of the area, the habitat's local microclimatic conditions and host abundance. These factors are incorporated in the model introduced in this chapter. Metereological conditions include temperature, humidity and daylight exposure which are seen to be relevant factors in tick dynamics. Local microclimatic conditions include the existence of favourable and unfavourable areas for ticks to survive. Certain woodland areas are considered to be favourable for tick persistence while most grasslands are disadvantageous for tick growth. Host abundance includes the presence of different varieties of hosts. Here, we focus mainly on large mammal hosts such as deer which can provide mobility of adult ticks as feeding adult ticks may be carried by the hosts and drop off in different locations.

In this chapter, we first introduce the model and show some of its key properties. We then introduce tick reproduction numbers when patches are isolated, semi-connected and fully connected, show how patch-dependent survival probabilities and migration parameters affect these and demonstrate their relevance in the study of equilibria and stability of the model. Finally, we present some simulations, describe implications of our results in terms of human interventions, and comment on further studies.

2.2 Two-patch tick model formulation

We consider a simplified habitat configuration containing two patches connected together and geographically close which are classified according to the possibility of tick development: a favourable area for tick spread (ex. woodland), and an unfavourable one (ex. grassland). We plan to model the dynamics of the female tick population considering the possible movement from one patch to the other whenever feeding adults are attached to large-sized hosts such as deer. We do not consider movement of immature ticks since we assume deer have a wider geographical range with respect to smaller mammals fed by immature ticks.

This can be modelled by a coupled system of ordinary and delay differential equations

(ODEs and DDEs). We suppose there is a faster tick development (normal delay) in the favourable environment and slower (diapause delay) in the unfavourable one. Also the survival rate would be higher in the former, reflecting the higher survival chance for ticks. The rest of the parameters on the other hand, are chosen to be identical in both patches. We now list standing assumptions and formalize some parameters for the tick population dynamics involving two patches. We assume these patches are distinguished by the length of life cycle of inhabiting ticks, and the two patches are connected by large size mammals which provide blood meals to feeding adult ticks. We assume that large size mammals move between the two patches and therefore engorged adult ticks can drop off to either of the two patches due to host mobility. We ignore host mobility for larval and nymphal ticks, so in our patchy model, only feeding adult ticks and egg-laying adult ticks are explicitly incorporated while ticks in other stages can be calculated from the production rate and the survival probability. In particular, we assume that

H1. The host density, for ticks at each stage, in each patch remains constant.

H2. The movement of large mammals between two patches is considered, so a portion α_{ij} of feeding adult ticks in patch i can drop off to patch j to become egg-laying adults in patch j. We also consider this movement to be instantaneous.

H3. Ticks grow up from the eggs in a given patch and remain in the patch until they reach the stage of feeding adults, in other words, hosts for larval and nymphal ticks do move within the patch but not between two different patches.

H4. The two patches are distinct by the developmental delays from eggs to feeding adults, one with normal developmental delay τ_1 and another with diapause developmental delay $\tau_2 > \tau_1$.

H5. The probability of survival from eggs to feeding adults ρ_i depends exclusively on the patchy environment ($\rho_1 > \rho_2$), although this can be relaxed to allowing delay-dependent probability.

H6. The birth rate is assumed to be dependent on the egg-laying adult density in the same patch by the Ricker reproduction function $f(x) = pxe^{-qx}$ [74].

H7. The transition time from feeding adult ticks to engorged ticks is relatively short, so the probability for the engorged adult ticks to drop off to the same patch where the feeding ticks come from is relatively large, and hence $\alpha_{12} + \alpha_{21} < 1$.

H8. Feeding adults either die out with the death rate μ or develop into egg-laying adults with the development rate γ.

H9. Feeding adults advance to the egg-laying stage with rate $\gamma_F = \gamma\theta$, where θ represents the survival probability of female adult ticks in the engorged stage.

The parameters are incorporated in Figure 2.1 and have been summarized in Table 2.1.

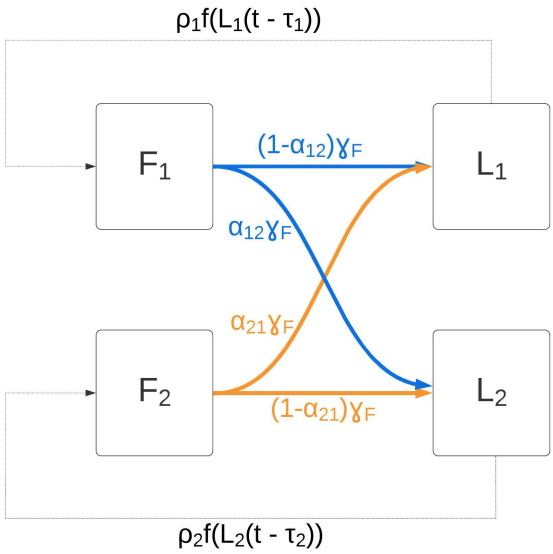

Figure 2.1: **Flowchart for the model** - The parameters are indicated in the parameter table below. Note that death rates have not been incorporated in the diagram.

Parameter	Explanation
ρ_i	Survival probability from eggs to feeding adults in patch i.
τ_i	Development delay from eggs to feeding adults in patch i.
γ	Development rate from feeding to engorged adults.
μ	Mortality rate for feeding adults.
γ_F	Transfer rate from feeding adults to egg-laying adults.
α_{ij}	Probability for feeding adult ticks in patch i to drop off to patch j.
p	Maximal number of eggs produced by an egg-laying adult per unit time.
q	Density-dependent effect parameter in the Ricker function.
δ	Exit rate for egg-laying ticks.

Table 2.1: Table including parameters in the model for $i = 1, 2$ and their explanation.

With the above assumptions and parameters, we can now formulate the patchy model with multiple delays as follows:

$$\begin{cases} F_1'(t) = \rho_1 f(L_1(t-\tau_1)) - (\gamma+\mu)F_1(t), \\ F_2'(t) = \rho_2 f(L_2(t-\tau_2)) - (\gamma+\mu)F_2(t), \\ L_1'(t) = (1-\alpha_{12})\gamma_F F_1(t) + \alpha_{21}\gamma_F F_2(t) - \delta L_1(t), \\ L_2'(t) = \alpha_{12}\gamma_F F_1(t) + (1-\alpha_{21})\gamma_F F_2(t) - \delta L_2(t). \end{cases} \tag{2.1}$$

In the above formulation, we use $F_i(t)$ to denote the number of feeding adults in patch i, and $L_i(t)$ for the number of egg-laying adults in patch i.

2.3 Properties of the two-patch model

In this section, we show that solutions to (2.1) are non-negative (given non-negative initial conditions) and bounded.

First, we define the phase space

$$X^+ := \{(z_1, z_2, \phi_1, \phi_2) : z_i \in [0, \infty); \phi_i \in C([-\tau_i, 0], [0, \infty)), i = 1, 2\},$$

with norm

$$||\phi|| = \sum_{i=1}^{2}(|z_i| + \sup_{s\in[-\tau_i,0]}|\phi_i(s)|).$$

Given the initial data $\phi \in X^+$, we obtain a unique solution to (2.1) $x^\phi(t)$ for positive times (Theorem 2.3 of [75]) and it generates a semiflow on X^+.

Proposition 1. *Solutions to* (2.1) *with non-negative initial conditions remain non-negative.*

Proof. Given our semiflow, we know solutions are continuous, so we show equivalently that all the compartments (F_1, F_2, L_1, L_2) remain non-negative.

Suppose there exists solutions that are not always non-negative. Since solutions are continuous, at a certain time t^* one of the following has to be true for solutions to become negative:

1. $F_i(t^*) = 0$ either for $i = 1$ or for $i = 2$. In this case $F_i'(t^*) = \rho_i f(L_i(t^* - \tau_i)) \geq 0$ which contradicts with the crossing of the x-axis.

2. $L_i(t^*) = 0$ either for $i = 1$ or for $i = 2$. But $L_i'(t^*) \geq 0$ which contradicts with the crossing of the x-axis.

Therefore solutions remain non-negative. □

Proposition 2. *Solutions to* (2.1) *with non-negative initial conditions are uniformly bounded.*

Proof. We show that there exists a positively invariant set

$$\Gamma := \{(F_1, F_2, L_1, L_2) \in \mathbb{R}^4_+ : F_1 \leq F_1^\infty,\, F_2 \leq F_2^\infty,\, L_1 \leq L_1^\infty,\, L_2 \leq L_2^\infty\}, \tag{2.2}$$

where

$$\begin{aligned} F_1^\infty &= \frac{\rho_1 p}{qe(\gamma+\mu)}, \\ F_2^\infty &= \frac{\rho_2 p}{qe(\gamma+\mu)}, \\ L_1^\infty &= \frac{\gamma_F p}{qe\delta(\gamma+\mu)}[(1-\alpha_{12})\rho_1 + \alpha_{21}\rho_2], \end{aligned}$$

$$L_2^\infty = \frac{\gamma_F p}{qe\delta(\gamma+\mu)}[\rho_1\alpha_{12} + \rho_2(1-\alpha_{21})].$$

To show this, consider the Ricker function $f(x) = pxe^{-qx}$. This function is bounded for $x \geq 0$ and has its maximum at $x = \frac{1}{q}$. Let

$$f_\infty := \max_{x\geq 0}(f(x)) = f\left(\frac{1}{q}\right) = \frac{p}{qe}.$$

Following the definition of f_∞,

$$\begin{cases} F_1'(t) \leq \rho_1 f_\infty - (\gamma+\mu)F_1(t), \\ F_2'(t) \leq \rho_2 f_\infty - (\gamma+\mu)F_2(t), \end{cases} \tag{2.3}$$

Using the method of variation of constants to solve the inequalities of (2.3) with initial conditions $F_1(0) = F_1^0$ and $F_2(0) = F_2^0$, we have

$$F_1(t) \leq (F_1^0 - F_1^\infty)e^{-(\gamma+\mu)t} + F_1^\infty,$$
$$F_2(t) \leq (F_2^0 - F_2^\infty)e^{-(\gamma+\mu)t} + F_2^\infty.$$

In particular, if $F_i^0 \leq F_i^\infty$, then $F_i(t) \leq F_i^\infty \ \forall t \geq 0, \ \text{for } i = 1, 2.$ Then

$$\begin{cases} L_1'(t) \leq (1-\alpha_{12})\gamma_F F_1^\infty + \alpha_{21}\gamma_F F_2^\infty - \delta L_1(t), \\ L_2'(t) \leq \alpha_{12}\gamma_F F_1^\infty + (1-\alpha_{21})\gamma_F F_2^\infty - \delta L_2(t). \end{cases} \tag{2.4}$$

Using the method of variation of constants again for (2.4) with initial conditions $L_1(0) = L_1^0$ and $L_2(0) = L_2^0$, we have

$$L_1(t) \leq (L_1^0 - L_1^\infty)e^{-\delta t} + L_1^\infty,$$
$$L_2(t) \leq (L_2^0 - L_2^\infty)e^{-\delta t} + L_2^\infty.$$

In a similar way, if $L_i^0 \leq L_i^\infty$, then $L_i(t) \leq L_i^\infty \ \forall t \geq 0, \ \text{for } i = 1, 2.$ The above argument

implies that all solutions of the model system remain bounded for all $t \geq 0$ and solutions are in fact ultimately uniformly bounded since

$$\limsup_{t\to\infty} F_i(t) \leq F_i^{\infty}, \quad \limsup_{t\to\infty} L_i(t) \leq L_i^{\infty}. \tag{2.5}$$

Let

$$X_\Gamma^+ := \{\phi \in X^+; z_i \leq F_i^{\infty}; \phi(s) \in [0, L_i^{\infty}], s \in [-\tau_i, 0], i = 1, 2\}.$$

Then we have shown that X_Γ^+ is a positively invariant set in X^+ which attracts solutions of (2.1) with initial data in X^+. □

Note that (2.5) guarantees that the ω-limit of solutions to (2.1) is contained in Γ.

2.4 Tick reproduction numbers

2.4.1 Isolated patches

We start with a special case where two patches are isolated from each other, and we have for $i = 1, 2$, the decoupled system

$$\begin{cases} F_i'(t) = \rho_i f(L_i(t-\tau_i)) - (\gamma+\mu)F_i(t), \\ L_i'(t) = \gamma_F F_i(t) - \delta L_i(t). \end{cases} \tag{2.6}$$

We compute the tick basic reproduction number $R_{T,i}$ for a single patch i which allows us to study the average number of female ticks that are born by a single female tick in that patch. The procedure is similar to calculating the basic reproduction number for epidemics where in the ecological case we consider linearization at the tick-free equilibrium. Note that if $R_{T,i} < 1$, ticks will die out; while if $R_{T,i} > 1$ the population will reach a non-trivial equilibrium. The existence of a positive feedback $f'(0) = p > 0$ guarantees that monotone dynamical theory can be applied. Therefore, the stability of the trivial solution of (2.6) is equivalent to that of the linear ordinary differential equation system associated (where $\tau_i = 0$) [76]. $R_{T,i}$ can

be therefore calculated as the spectral radius of the Next Generation Matrix (NGM) of the ODE model where new births are included in the transmission matrix and tick development and deaths are part of the transition matrix [77, 78].

We first linearize system (2.6) at the trivial equilibrium, where $\tau_1 = \tau_2 = 0$, to get

$$\begin{pmatrix} F_i' \\ L_i' \end{pmatrix} = (T + \Sigma) \begin{pmatrix} F_i \\ L_i \end{pmatrix},$$

with the transmission matrix T and the transition matrix Σ

$$T = \begin{pmatrix} 0 & \rho_i p \\ 0 & 0 \end{pmatrix}$$

and

$$\Sigma = \begin{pmatrix} -(\gamma + \mu) & 0 \\ \gamma_F & -\delta \end{pmatrix},$$

where $p = f'(0)$. To use the next generation matrix approach, we note that the inverse of Σ and the next generation matrix $K = -T\Sigma^{-1}$ are given by

$$\Sigma^{-1} = \begin{pmatrix} -\frac{1}{\gamma+\mu} & 0 \\ -\frac{\gamma_F}{\delta(\gamma+\mu)} & -\frac{1}{\delta} \end{pmatrix}, \quad K = \begin{pmatrix} \frac{\gamma_F \rho_i p}{\delta(\gamma+\mu)} & \frac{\rho_i p}{\delta} \\ 0 & 0 \end{pmatrix}.$$

Therefore the characteristic equation is

$$\lambda \left(\lambda - \frac{\gamma_F \rho_i p}{\delta(\gamma + \mu)} \right) = 0,$$

and the spectral radius is

$$R_{T,i} = \frac{\gamma_F \rho_i p}{\delta(\gamma + \mu)}. \tag{2.7}$$

The basic reproduction number has a clear biological meaning. $\frac{\rho_1 p}{\gamma+\mu}$ represents the number of eggs that survive to feeding adult stage per unit time produced by an egg-laying female

multiplied by the average time in the feeding adult compartment. $\frac{\gamma_F}{\delta}$ instead is the proportion of feeding adults that move into the egg-laying compartment per unit time multiplied by the average time of ticks in egg-laying stage. We see that $R_{T,i}$ is a key quantity since it allows tick persistence if $R_{T,i} > 1$, or tick extinction in the area if $R_{T,i} < 1$.

In this paper, we consider patch 1 to be favourable environment for ticks which translates mathematically into the condition $R_{T,1} > 1$ since ticks would persist in absence of movement. In addition we suppose ticks also have a shorter development phase due to lack of diapause with respect to the other patch, therefore $\tau_1 < \tau_2$.

On the other hand, we consider patch 2 to be unfavourable, therefore ticks would not be able to survive if the environment were isolated or in other words $R_{T,2} < 1$ and ticks would take longer to develop since they would undergo diapause.

2.4.2 Interconnected patches

We now consider the case when two patches are connected by mobility of feeding adults (α_{12}, $\alpha_{21} \neq 0$). Similar to the isolated case, the stability of the trivial solution of (2.1) is equivalent to that of the linear ordinary differential equation system associated (where $\tau_1 = \tau_2 = 0$) [76]. We linearize model (2.1) at the trivial equilibrium to get a linear system of ordinary differential equations for $X = (F_1, F_2, L_1, L_2)^T$, with $\tau_1 = \tau_2 = 0$

$$X' = (T + \Sigma)X.$$

We now use the next generation approach to introduce the so-called basic reproduction number. The transmission matrix T and the transition matrix Σ are given by

$$T = \begin{pmatrix} 0 & 0 & \rho_1 p & 0 \\ 0 & 0 & 0 & \rho_2 p \\ 0 & 0 & 0 & 0 \\ 0 & 0 & 0 & 0 \end{pmatrix}, \quad \Sigma = \begin{pmatrix} -(\gamma+\mu) & 0 & 0 & 0 \\ 0 & -(\gamma+\mu) & 0 & 0 \\ (1-\alpha_{12})\gamma_F & \alpha_{21}\gamma_F & -\delta & 0 \\ \alpha_{12}\gamma_F & (1-\alpha_{21})\gamma_F & 0 & -\delta \end{pmatrix},$$

respectively.

The inverse of Σ is given by

$$\Sigma^{-1} = \begin{pmatrix} -\frac{1}{\gamma+\mu} & 0 & 0 & 0 \\ 0 & -\frac{1}{\gamma+\mu} & 0 & 0 \\ -\frac{(1-\alpha_{12})\gamma_F}{\delta(\gamma+\mu)} & -\frac{\alpha_{21}\gamma_F}{\delta(\gamma+\mu)} & -\frac{1}{\delta} & 0 \\ -\frac{\alpha_{12}\gamma_F}{\delta(\gamma+\mu)} & -\frac{(1-\alpha_{21})\gamma_F}{\delta(\gamma+\mu)} & 0 & -\frac{1}{\delta} \end{pmatrix},$$

so the next generation matrix $K = -T\Sigma^{-1}$ is given by

$$K = \begin{pmatrix} \frac{(1-\alpha_{12})\gamma_F\rho_1 p}{\delta(\gamma+\mu)} & \frac{\alpha_{21}\gamma_F\rho_1 p}{\delta(\gamma+\mu)} & \frac{\rho_1 p}{\delta} & 0 \\ \frac{\alpha_{12}\gamma_F\rho_2 p}{\delta(\gamma+\mu)} & \frac{(1-\alpha_{21})\gamma_F\rho_2 p}{\delta(\gamma+\mu)} & 0 & \frac{\rho_2 p}{\delta} \\ 0 & 0 & 0 & 0 \\ 0 & 0 & 0 & 0 \end{pmatrix}.$$

We define the tick reproduction number $R_{T,c} = \rho(K_{12})$, where ρ denotes the spectral radius and

$$K_{12} = \begin{pmatrix} \frac{(1-\alpha_{12})\gamma_F\rho_1 p}{\delta(\gamma+\mu)} & \frac{\alpha_{21}\gamma_F\rho_1 p}{\delta(\gamma+\mu)} \\ \frac{\alpha_{12}\gamma_F\rho_2 p}{\delta(\gamma+\mu)} & \frac{(1-\alpha_{21})\gamma_F\rho_2 p}{\delta(\gamma+\mu)} \end{pmatrix} = \begin{pmatrix} (1-\alpha_{12})R_{T,1} & \alpha_{21}R_{T,1} \\ \alpha_{12}R_{T,2} & (1-\alpha_{21})R_{T,2} \end{pmatrix}.$$

Therefore the characteristic equation of K_{12} is

$$\left[\lambda^2 - \lambda\left(\frac{\gamma_F\rho_1 p(1-\alpha_{12}) + \gamma_F\rho_2 p(1-\alpha_{21})}{\delta(\gamma+\mu)}\right) + \frac{\gamma_F^2\rho_1\rho_2 p^2(1-\alpha_{12}-\alpha_{21})}{\delta^2(\gamma+\mu)^2}\right] = 0,$$

and can be rewritten as

$$\lambda^2 - b\lambda + c = 0,$$

where

$$b = (1-\alpha_{12})R_{T,1} + (1-\alpha_{21})R_{T,2}, \quad c = R_{T,1}R_{T,2}[1-(\alpha_{12}+\alpha_{21})].$$

Note that both eigenvalues are real since

$$\begin{aligned}\Delta_1 &= [(1-\alpha_{12})R_{T,1} + (1-\alpha_{21})R_{T,2}]^2 - 4R_{T,1}R_{T,2}[1-(\alpha_{12}+\alpha_{21})],\\ &\geq [(1-\alpha_{12})R_{T,1} + (1-\alpha_{21})R_{T,2}]^2 - 4R_{T,1}R_{T,2}[1-\alpha_{12}][1-\alpha_{21}],\\ &= [(1-\alpha_{12})R_{T,1} - (1-\alpha_{21})R_{T,2}]^2,\\ &> 0.\end{aligned}$$

Therefore the tick reproduction number is

$$R_{T,c} = \rho(K_{12}) = \frac{b+\sqrt{\Delta_1}}{2}. \tag{2.8}$$

There are two interesting special cases of semi-connectedness of two patches.

2.4.3 Escalating up

This is the case when hosts for feeding adults move only from patch 2 (tick-unfavorable patch) to patch 1 (tick-favorable patch), so $\alpha_{12} = 0$. In this case, we have

$$\begin{aligned}\Delta_2 &= [R_{T,1} + (1-\alpha_{21})R_{T,2}]^2 - 4R_{T,1}R_{T,2}(1-\alpha_{21}),\\ &= [R_{T,1} - (1-\alpha_{21})R_{T,2}]^2,\end{aligned}$$

and

$$\begin{aligned}R_{T,eu} &= \frac{1}{2}[R_{T,1} + (1-\alpha_{21})R_{T,2} + R_{T,1} - (1-\alpha_{21})R_{T,2}]\\ &= R_{T,1}.\end{aligned}$$

In other words, in the escalating-up case, the tick reproduction number is exactly the same as in the favourable isolated case since the inward movement in patch 1 would not provide a relevant change in the overall dynamics.

2.4.4 Cascading down

This is the case when hosts for feeding adults move only from patch 1 (tick-favorable patch) to patch 2 (tick-unfavorable patch), so $\alpha_{21} = 0$. In this case, we have

$$\begin{aligned}\Delta_3 &= [(1-\alpha_{12})R_{T,1} + R_{T,2}]^2 - 4R_{T,1}R_{T,2}(1-\alpha_{12}),\\ &= [(1-\alpha_{12})R_{T,1} - R_{T,2}]^2,\end{aligned}$$

and

$$R_{T,cd} = \max\{R_{T,1}(1-\alpha_{12}), R_{T,2}\}.$$

In the cascading down case, the tick reproduction number depends on the mobility parameter - in particular the smaller α_{12}, the larger the tick reproduction number.

2.5 Model equilibrium analyses

The equilibria $(F_1^*, F_2^*, L_1^*, L_2^*)$ of (2.1) satisfy the following system of equations

$$\begin{cases} 0 = \rho_1 f(L_1^*) - (\gamma+\mu)F_1^*,\\ 0 = \rho_2 f(L_2^*) - (\gamma+\mu)F_2^*,\\ 0 = (1-\alpha_{12})\gamma_F F_1^* + \alpha_{21}\gamma_F F_2^* - \delta L_1^*,\\ 0 = \alpha_{12}\gamma_F F_1^* + (1-\alpha_{21})\gamma_F F_2^* - \delta L_2^*. \end{cases}$$

This can be rewritten as:

$$\begin{cases} F_1^* = \dfrac{\rho_1 f(L_1^*)}{\gamma+\mu},\\ F_2^* = \dfrac{\rho_2 f(L_2^*)}{\gamma+\mu},\\ L_1^* = \dfrac{(1-\alpha_{12})\gamma_F F_1^* + \alpha_{21}\gamma_F F_2^*}{\delta},\\ L_2^* = \dfrac{\alpha_{12}\gamma_F F_1^* + (1-\alpha_{21})\gamma_F F_2^*}{\delta}. \end{cases} \tag{2.9}$$

2.5.1 Isolated patches

Without host mobility ($\alpha_{12} = \alpha_{21} = 0$), (2.9) is given by

$$\begin{cases} F_1^* = \dfrac{\rho_1 f(L_1^*)}{\gamma + \mu}, \\ F_2^* = \dfrac{\rho_2 f(L_2^*)}{\gamma + \mu}, \\ L_1^* = \dfrac{\gamma_F F_1^*}{\delta}, \\ L_2^* = \dfrac{\gamma_F F_2^*}{\delta}. \end{cases}$$

In this case the two-patches do not interact with each other which means that we can treat the two patches independently. In addition, we consider the basic reproduction numbers defined in the previous section and this yields

$$\begin{cases} L_1^* = \dfrac{\gamma_F \rho_1 f(L_1^*)}{\delta(\gamma + \mu)} = \dfrac{R_{T,1} f(L_1^*)}{p}, \\ L_2^* = \dfrac{\gamma_F \rho_2 f(L_2^*)}{\delta(\gamma + \mu)} = \dfrac{R_{T,2} f(L_2^*)}{p}. \end{cases}$$

Note that $(0, 0, 0, 0)$ is always an equilibrium. We then look for conditions that guarantee the existence of a non-trivial solution $(F_1^*, F_2^*, L_1^*, L_2^*)$.

In this case, we know that $\frac{f(x)}{x} = pe^{-qx}$, so

$$L_1^* = q^{-1} \ln\left(\frac{\gamma_F \rho_1 p}{\delta(\gamma + \mu)}\right) = q^{-1} \ln(R_{T,1}),$$

and

$$L_2^* = q^{-1} \ln\left(\frac{\gamma_F \rho_2 p}{\delta(\gamma + \mu)}\right) = q^{-1} \ln(R_{T,2}).$$

Since only non-negative solutions are biologically reasonable and we have already shown that $(0, 0, 0, 0)$ is an equilibrium, we study the conditions for which L_1^* and L_2^* are both strictly positive. In particular, we know that $\rho_1 \geq \rho_2$ because the survival probability will be higher in a favourable environment ($R_{T,1} \geq R_{T,2}$), so we distinguish three different cases:

1. $R_{T,1} < 1$ - Unique equilibrium is $E_0 = (0, 0, 0, 0)$;

2. $R_{T,2} < 1 < R_{T,1}$ - There is also a nontrivial equilibrium $E_1 = (F_1^*, 0, L_1^*, 0)$;

3. $R_{T,2} > 1$ - There are three nontrivial equilibria: $E_1 = (F_1^*, 0, L_1^*, 0)$, $E_2 = (0, F_2^*, 0, L_2^*)$ and the coexistence equilibrium $E_C = (F_1^*, F_2^*, L_1^*, L_2^*)$.

As stated before, we will consider the second case. The equilibria of the system can also be shown as intersections of the two functions shown in Figure 2.2. We also can observe that there are other relevant threshold values in addition to $R_{T,i} = 1$:

- $R_{T,i} = e$ at which the system changes its feedback nature from positive ($R_{T,i} < e$) to negative ($R_{T,i} > e$). At this point, the resulting equilibrium $L_i^* = \frac{1}{q}$ is the peak of the red curve, therefore it maximizes the birth function $f(L_i)$ and separates the cases for which $f'(L_i^*) > 0$ (for $R_{T,i} < e$) and $f'(L_i^*) < 0$ (for $R_{T,i} > e$).

- $R_{T,i} = e^2$ which represents the case in which the slope of the line and the derivative of the function at the equilibrium are both equal in absolute value to pe^{-2} and this will be crucial in studying stability and Hopf bifurcations.

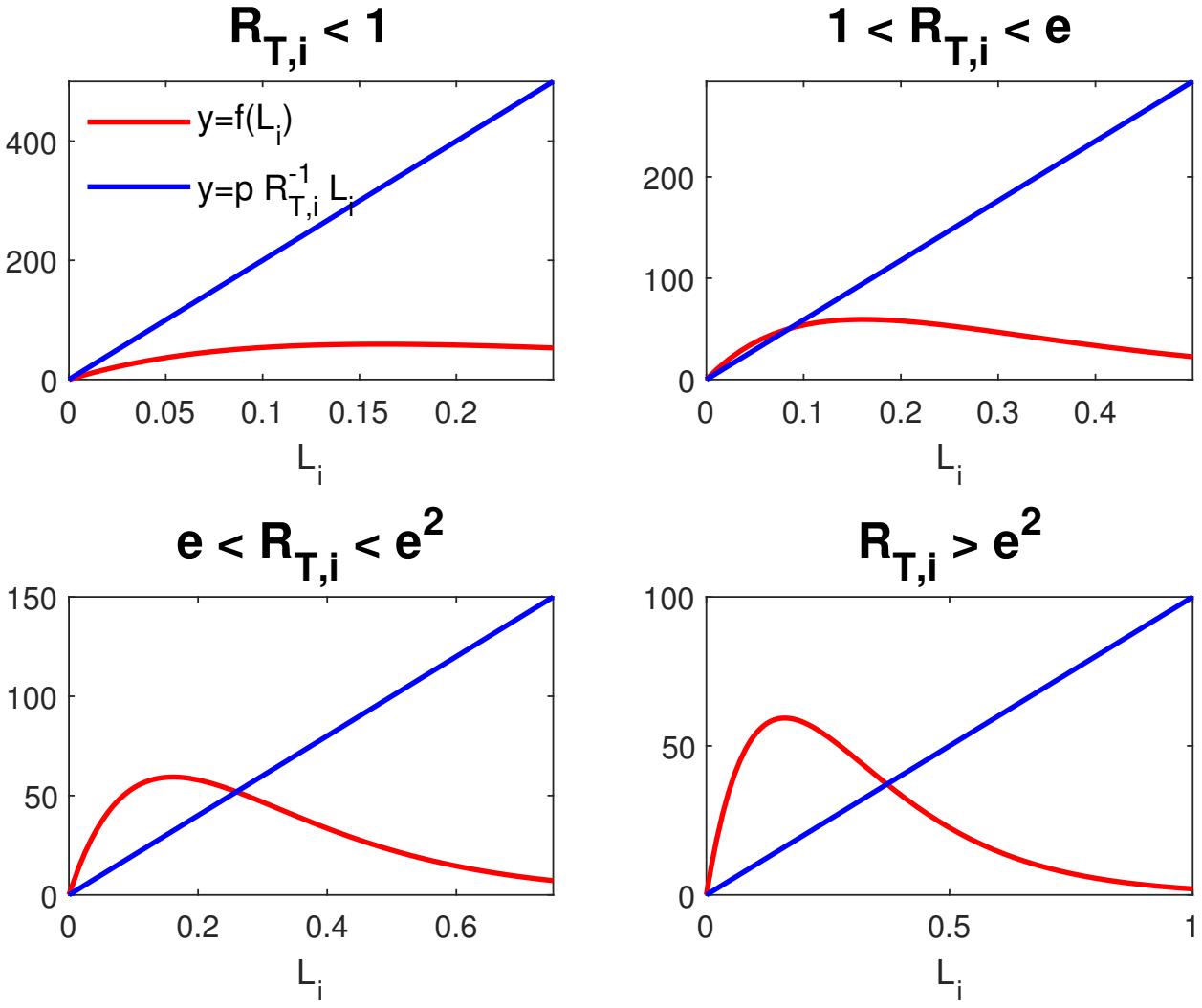

Figure 2.2: Equilibria of the isolated model shown graphically - The x value of the intersection points between the functions drawn in blue and red represent the equilibria for larvae of the isolated system. In the top left panel, there is no non-trivial intersection which corresponds to the case in which $R_{T,i} < 1$ while in the other three panels there is also the non-trivial intersection, where its x value represents L_i^*. The common parameters chosen in the plots are respectively $p = 1000$ and $q = 6.2$. The only parameter that varies throughout the panels is the value of $R_{T,i}$ which is respectively 0.5, 1.7, 5 and 10 in the top-left, top-right, bottom-left and bottom-right panel.

2.5.2 Escalating up

When ticks move only from an unfavourable to a favourable environment (i.e. $\alpha_{12} = 0$), there exists a unique non-trivial equilibrium $(F_1^*, 0, L_1^*, 0)$ where (F_1^*, L_1^*) is identical to the isolated case in the scenario considered ($R_{T,2} < 1 < R_{T,1}$). This is because in patch 1, ticks would already persist in the isolated case and in patch 2, ticks would die out without any inward tick movement.

2.5.3 Cascading down

When ticks move only from a favourable to an unfavourable environment (i.e. $\alpha_{21} = 0$), there are two possible cases. There could be either only a trivial equilibrium or the existence of a coexistence equilibrium as well. In particular,

1. $\alpha_{12} > \frac{R_{T,1}-1}{R_{T,1}}$ guarantees that there exists only the trivial equilibrium $E_0 = (0, 0, 0, 0)$.
2. $\alpha_{12} < \frac{R_{T,1}-1}{R_{T,1}}$ guarantees that there exists also the coexistence equilibrium $E_C = (F_1^*, F_2^*, L_1^*, L_2^*)$.

To show these findings, we start by studying the equations in (2.9) for $\alpha_{12} > 0$ and $\alpha_{21} = 0$:

$$\begin{cases} F_1^* = \dfrac{\rho_1 f(L_1^*)}{\gamma + \mu}, \\ F_2^* = \dfrac{\rho_2 f(L_2^*)}{\gamma + \mu}, \\ L_1^* = \dfrac{(1 - \alpha_{12})\gamma_F F_1^*}{\delta}, \\ L_2^* = \dfrac{\alpha_{12}\gamma_F F_1^* + \gamma_F F_2^*}{\delta}. \end{cases}$$

which yields

$$\begin{cases} L_1^* = \dfrac{\gamma_F(1 - \alpha_{12})\rho_1 f(L_1^*)}{\delta(\gamma + \mu)}, \\ L_2^* = \dfrac{\gamma_F(\alpha_{12}\rho_1 f(L_1^*) + \rho_2 f(L_2^*))}{\delta(\gamma + \mu)}. \end{cases} \tag{2.10}$$

Note that from the first equation of (2.10) and using $\frac{f(x)}{x} = pe^{-qx}$, we find that $L_1^* = q^{-1}\ln((1-\alpha_{12})R_{T,1})$ only if $\alpha_{12} < \frac{R_{T,1}-1}{R_{T,1}}$. In this case we can rewrite the second equation of (2.10) as:

$$L_2^* = \frac{\alpha_{12}}{1-\alpha_{12}}L_1^* + \frac{\gamma_F \rho_2 f(L_2^*)}{\delta(\gamma+\mu)}.$$

By considering the following equality $R_{T,2} = \frac{\rho_2 p}{\gamma+\mu}\frac{\gamma_F}{\delta}$ and defining $\zeta^* := \frac{\alpha_{12}}{1-\alpha_{12}}L_1^*\frac{p}{R_{T,2}}$, we have

$$\frac{p}{R_{T,2}}L_2^* - \zeta^* = f(L_2^*),$$

where $\zeta^* > 0$ guarantees the fact that there is always a nontrivial intersection between the left hand side and right hand side of this equation.

2.5.4 Fully interconnected patches

Analytic Approach

We now consider the fully connected case. First of all, using equations 3 and 4 of (2.9), we find F_1^* and F_2^* as linear combinations of L_1^* and L_2^* whenever $\alpha_{12} \neq 0$, $\alpha_{21} \neq 0$ and $\alpha_{12} + \alpha_{21} < 1$. These are given by

$$\begin{cases} F_1^* = a_{11}L_1^* + a_{12}L_2^*, \\ F_2^* = a_{21}L_1^* + a_{22}L_2^*. \end{cases} \tag{2.11}$$

where

$a_{11} = \frac{\delta(1-\alpha_{21})}{\gamma_F(1-\alpha_{12}-\alpha_{21})}$,
$a_{12} = -\frac{\delta\alpha_{21}}{\gamma_F(1-\alpha_{12}-\alpha_{21})}$,
$a_{21} = -\frac{\delta\alpha_{12}}{\gamma_F(1-\alpha_{12}-\alpha_{21})}$,
$a_{22} = \frac{\delta(1-\alpha_{12})}{\gamma_F(1-\alpha_{12}-\alpha_{21})}$.

Note that

$$\alpha_{12} + \alpha_{21} < 1 \text{ if and only if } a_{11}a_{22} > a_{12}a_{21}.$$

Geometric Approach

We now develop a geometric approach to look at (2.11) as we change α_{12} and α_{21} subject to the constraint $\alpha_{12} + \alpha_{21} < 1$. For notation simplicity, let

$$\xi = \frac{\delta}{\gamma_F(1 - \alpha_{12} - \alpha_{21})}.$$

Then (2.11) becomes

$$\begin{cases} F_1^* = \xi(1 - \alpha_{21})L_1^* - \xi\alpha_{21}L_2^*, \\ F_2^* = -\xi\alpha_{12}L_1^* + \xi(1 - \alpha_{12})L_2^*. \end{cases}$$

So we substitute the feeding adult equilibria in the two patches F_1^* and F_2^* in (2.11) with the first two equations of (2.9) and get

$$\begin{cases} \dfrac{\rho_1 f(L_1^*)}{\gamma + \mu} = \xi(1 - \alpha_{21})L_1^* - \xi\alpha_{21}L_2^*, \\ \dfrac{\rho_2 f(L_2^*)}{\gamma + \mu} = -\xi\alpha_{12}L_1^* + \xi(1 - \alpha_{12})L_2^*. \end{cases}$$

We want to explore graphically the behaviour of L_1^* with respect to L_2^* to study conditions for the presence of a coexistence equilibrium, which would be the intersection of the functions defined below. Taking L_2^* as a function of L_1^* yields

$$L_2^* = F(L_1^*) := \frac{1 - \alpha_{21}}{\alpha_{21}}L_1^* - \frac{\rho_1 f(L_1^*)}{\xi\alpha_{21}(\gamma + \mu)},$$

and L_1^* as a function of L_2^* yields

$$L_1^* = G(L_2^*) := \frac{1 - \alpha_{12}}{\alpha_{12}}L_2^* - \frac{\rho_2 f(L_2^*)}{\xi\alpha_{12}(\gamma + \mu)}.$$

In particular we have

- $F(x) \overset{x\to\infty}{\sim} \frac{1-\alpha_{21}}{\alpha_{21}}x$,
- $G(x) \overset{x\to\infty}{\sim} \frac{1-\alpha_{12}}{\alpha_{12}}x$.

In order for F and G to be plotted on a $x = L_1^*, y = L_2^*$ plot, we need to reflect G about the line $y = x$.

First of all, we study the derivative of both functions:

$$\begin{cases} F'(x) = \dfrac{1-\alpha_{21}}{\alpha_{21}} - \dfrac{\rho_1 f'(x)}{\xi\alpha_{21}(\gamma+\mu)}, \\ G'(x) = \dfrac{1-\alpha_{12}}{\alpha_{12}} - \dfrac{\rho_2 f'(x)}{\xi\alpha_{12}(\gamma+\mu)}. \end{cases}$$

We see that $G'(x)$ is an increasing function for non-negative x in the fully interconnected model using the derivative of the Ricker function $f'(x) = pe^{-qx}(1-qx)$ and the definitions of $R_{T,2}$ and ξ.

$$\begin{aligned} G'(x) &= \frac{1-\alpha_{12}}{\alpha_{12}} - \frac{\rho_2\gamma_F p}{\delta(\gamma+\mu)}\frac{(1-qx)e^{-qx}(1-\alpha_{12}-\alpha_{21})}{\alpha_{12}} \\ &= \frac{1-\alpha_{12}}{\alpha_{12}} - R_{T,2}\frac{(1-qx)e^{-qx}(1-\alpha_{12}-\alpha_{21})}{\alpha_{12}} \\ &> \frac{1-\alpha_{12}}{\alpha_{12}} - \frac{1-\alpha_{12}-\alpha_{21}}{\alpha_{12}} \\ &= \frac{\alpha_{21}}{\alpha_{12}} \\ &> 0. \end{aligned}$$

We also know that

$$\begin{cases} F'(0) = \dfrac{1-\alpha_{21}}{\alpha_{21}} - \dfrac{\rho_1 p}{\xi\alpha_{21}(\gamma+\mu)} &= \dfrac{1}{\alpha_{21}}[(1-\alpha_{21})(1-R_{T,1}) + \alpha_{12}R_{T,1}], \\ G'(0) = \dfrac{1-\alpha_{12}}{\alpha_{12}} - \dfrac{\rho_2 p}{\xi\alpha_{12}(\gamma+\mu)} &= \dfrac{1}{\alpha_{12}}[(1-\alpha_{12})(1-R_{T,2}) + \alpha_{21}R_{T,2}] \end{cases}$$

Since $0 < R_{T,2} < 1$, we see that $G(x)$ is always non-negative for $x \geq 0$, since:

- $G(0) = 0$,
- $G'(0) > 0$,
- $G'(x)$ is an increasing function for $x \geq 0$.

Therefore G^{-1} is well defined for $x \geq 0$ and it is such that:

- $(G^{-1})'(x)$ is a decreasing function for $x \geq 0$.
- $G^{-1}(x) \xrightarrow{x\to\infty} \frac{\alpha_{12}}{1-\alpha_{12}}x$.

We are interested in studying the possible intersections between $F(x)$ and $G^{-1}(x)$. We see that $G^{-1}(x) < F(x)$ for a large x since the following inequality holds for $\alpha_{12} + \alpha_{21} < 1$:

$$\frac{\alpha_{12}}{1-\alpha_{12}} < \frac{1-\alpha_{21}}{\alpha_{21}}.$$

The only case there can be a unique non-trivial intersection between $F(x)$ and $G^{-1}(x)$ (otherwise there is no coexistence equilibrium) occurs if

$$(G^{-1})'(0) = \frac{1}{G'(0)} > F'(0).$$

Therefore we shall study the threshold value $T_{coex} := F'(0)G'(0)$

$$T_{coex} = \frac{1}{\alpha_{21}\alpha_{12}}[(1-\alpha_{21})(1-R_{T,1}) + \alpha_{12}R_{T,1}][(1-\alpha_{12})(1-R_{T,2}) + \alpha_{21}R_{T,2}].$$

In particular, we see that the existence of a non-trivial equilibrium occurs if $T_{coex} < 1$. The graphical representation as intersection of the two curves explained above is represented in Figure 2.3.

Note that we have computed another threshold value which would equivalently determine a possible coexistence equilibrium which is

$$R_{T,c} = \frac{b + \sqrt{b^2 - 4c}}{2},$$

where

$$b = (1-\alpha_{12})R_{T,1} + (1-\alpha_{21})R_{T,2}, \quad c = R_{T,1}R_{T,2}[1-(\alpha_{12}+\alpha_{21})]. \tag{2.12}$$

We prove that these two thresholds have the same role of separating the trivial equilibrium

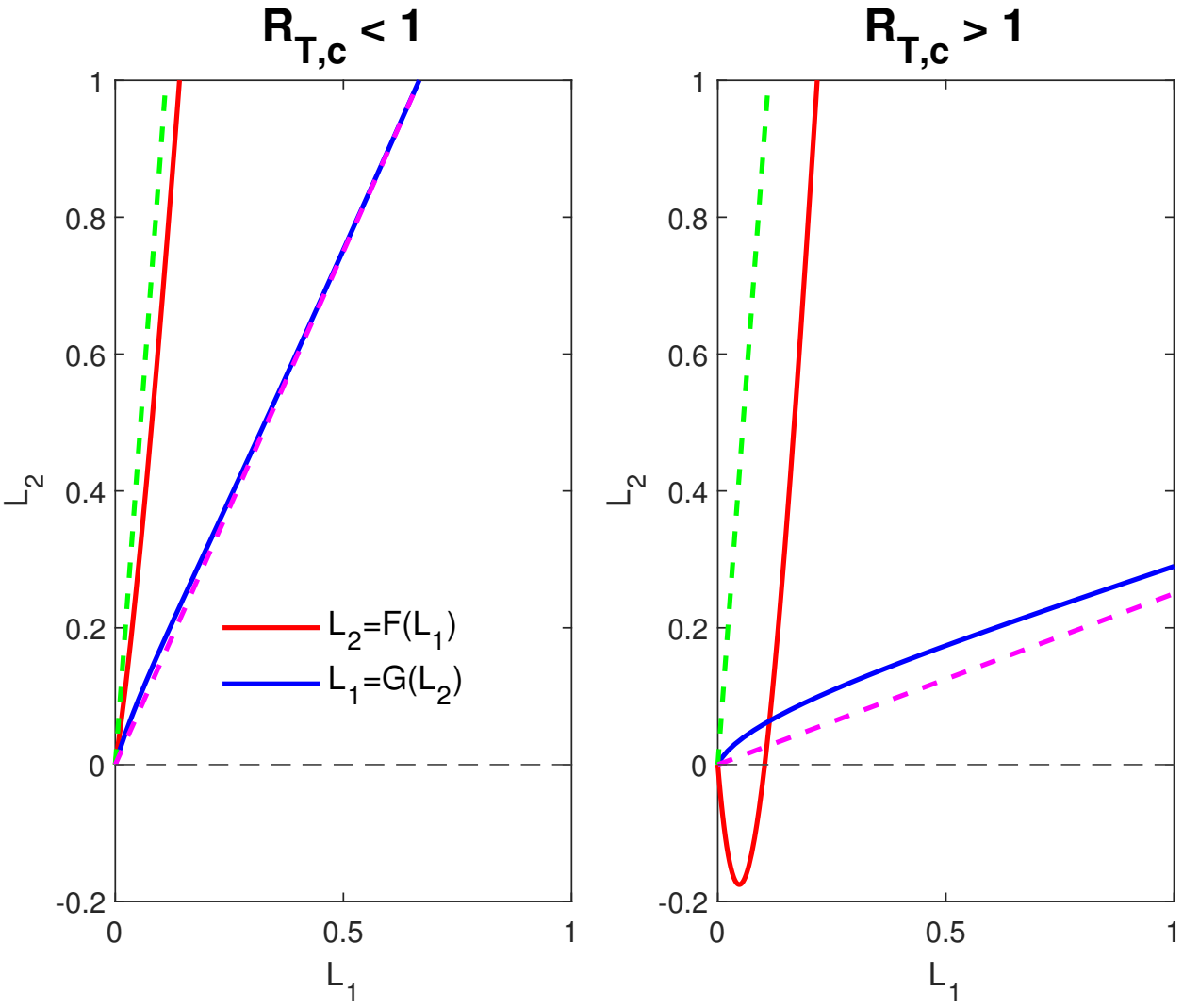

Figure 2.3: Equilibria of the interconnected model shown graphically - The equilibrium values for L_1^* and L_2^* are exactly the intersection of the red and blue curve. In the left panel, there is the case in which $R_{T,c} < 1$ where there is only the trivial intersection. In the right panel, there is also a coexistence equilibrium (L_1^*, L_2^*) since $R_{T,c} > 1$. The dashed green line is $L_2 = \frac{1-\alpha_{21}}{\alpha_{21}} L_1$ which is the limit of the blue curve as $L_1 \to \infty$. In a similar way, the dashed pink line $L_1 = \frac{1-\alpha_{12}}{\alpha_{12}} L_2$ represents the behaviour of the blue curve as $L_2 \to \infty$. The parameters chosen are exactly the same as in the simulations section excluding the survival probabilities and the migration parameters. In the left panel, we have $\rho_1 = 0.002$, $\rho_2 = 0.000625$, $\alpha_{12} = 0.6$ and $\alpha_{21} = 0.1$ while in the right panel we have $\rho_1 = 0.0075$, $\rho_2 = 0.00125$, $\alpha_{12} = 0.2$ and $\alpha_{21} = 0.1$. These parameter choices lead to $R_{T,c} = 0.7417 < 1$ in the left panel and $R_{T,c} = 4.5709 > 1$ in the right panel.

from the non-trivial equilibrium case.

Proposition 3.

$$R_{T,c} > 1 \text{ iff } T_{coex} < 1 \text{ and } R_{T,c} = 1 \text{ iff } T_{coex} = 1.$$

Proof. From the expression of $R_{T,c}$, we note that

$$R_{T,c} > 1 \text{ if and only if } \sqrt{b^2 - 4c} > 2 - b,$$

We consider two cases.

- If $b > 2$, we know $\sqrt{b^2 - 4c} \geq 0$, therefore $R_{T,c} \geq \frac{b}{2} > 1$.
- If $b \leq 2$, then in order for $R_{T,c} > 1$, we need $\sqrt{b^2 - 4c} > 2 - b$. Since $2 - b > 0$ and $b^2 - 4c \geq 0$, we just need to impose $b^2 - 4c > (2 - b)^2$ which occurs if and only if $b > c + 1$.

In a similar way we study when $T_{coex} < 1$, which is equivalent to

$$[(1 - \alpha_{21})(1 - R_{T,1}) + \alpha_{12}R_{T,1}][(1 - \alpha_{12})(1 - R_{T,2}) + \alpha_{21}R_{T,2}] < \alpha_{12}\alpha_{21}.$$

By taking the products and collecting the terms, we can write this inequality equivalently in terms of b and c using (2.12)

$$(1 - \alpha_{12} - \alpha_{21})b > (1 - \alpha_{12} - \alpha_{21})c + (1 - \alpha_{12} - \alpha_{21}).$$

By dividing both sides by $(1 - \alpha_{12} - \alpha_{21}) > 0$, we have that $b > c + 1$. Note that this condition is equivalent to that for $R_{T,c} > 1$ in case $b \leq 2$. It remains to show that $b > 2$ implies $T_{coex} < 1$. We know $R_{T,c} \in \mathbb{R}^+$, therefore $b^2 \geq 4c$. Here $b > 2$ means $4 \geq 4c$, which implies $c \leq 1$; so $b > c + 1$ holds for $b > 2$ and $c \leq 1$. We can use a similar argument to show $R_{T,c} = 1$ if and only if $T_{coex} = 1$. □

So we have the following result

Corollary 4. *If $R_{T,c} < 1$ (i.e. $T_{coex} > 1$), then the model has only the trivial equilibrium $(0,0,0,0)$. If $R_{T,c} > 1$ (i.e. $T_{coex} < 1$), then the model has a nontrivial equilibrium $(F_1^*, F_2^*, L_1^*, L_2^*)$ with each component positive.*

It is relevant to notice that both thresholds are just a function of the basic reproduction number in the isolated patches and of the mobility parameters. Therefore, it is important to study how these thresholds vary by changing its parameters. Here are some results obtained using the geometric threshold.

1. Increasing $R_{T,1}$ helps coexistence since it would decrease the threshold value:

$$\frac{\partial T_{coex}}{\partial R_{T,1}} = \frac{[(1-\alpha_{12})(1-R_{T,2}) + \alpha_{21}R_{T,2}][\alpha_{12}+\alpha_{21}-1]}{\alpha_{21}\alpha_{12}} < 0.$$

2. Increasing $R_{T,2}$ also helps coexistence:

$$\frac{\partial T_{coex}}{\partial R_{T,2}} = \frac{[(1-\alpha_{21})(1-R_{T,1}) + \alpha_{12}R_{T,1}][\alpha_{12}+\alpha_{21}-1]}{\alpha_{21}\alpha_{12}}.$$

   This is because, if the first term of the product in the numerator is negative, coexistence would always be possible, therefore we should consider the positive case, for which the threshold always decreases.

3. Let α_{21} be negligible with respect to α_{12} ($\alpha_{21} = o(1)$). Then

$$\frac{\partial T_{coex}}{\partial \alpha_{12}} \sim \frac{[1-R_{T,2}][R_{T,1}(1-\alpha_{12}^2)-1]}{\alpha_{21}\alpha_{12}^2}.$$

   therefore T_{coex} would be at first increasing for small α_{12} and then undergo a unique change in monotonicity at $\alpha_{12} = \sqrt{\frac{R_{T,1}-1}{R_{T,1}}}$. This implies that in order to help coexistence, it is necessary to have a large movement of ticks from favorable to unfavorable environment. This threshold also depends on $R_{T,1}$ which helps determine when the change of monotonicity would occur.

4. Let α_{12} be negligible with respect to α_{21} ($\alpha_{12} = o(1)$). Then increasing α_{21} does not

help coexistence since

$$\frac{\partial T_{coex}}{\partial \alpha_{21}} \sim \frac{[1-R_{T,1}][R_{T,2}(1-\alpha_{21}^2)-1]}{\alpha_{12}\alpha_{21}^2} > 0.$$

Asymptotic Expansion Analyses

We have seen that in the interconnected case there is no closed form solution for the coexistence equilibrium. In this section, we study the asymptotic coexistence equilibrium when we suppose the migration terms to be small. To do this, let the migration terms be multiplied by ϵ ($\alpha_{12} = \epsilon\alpha_{12}^0$ and $\alpha_{21} = \epsilon\alpha_{21}^0$ for $\epsilon \to 0$). For notation simplicity, we write α_{12} in the following section to indicate α_{12}^0 and consider the following system:

$$\begin{cases} F_1'(t) = \rho_1 f(L_1(t-\tau_1)) - (\gamma+\mu)F_1(t), \\ F_2'(t) = \rho_2 f(L_2(t-\tau_2)) - (\gamma+\mu)F_2(t), \\ L_1'(t) = (1-\epsilon\alpha_{12})\gamma_F F_1(t) + \epsilon\alpha_{21}\gamma_F F_2(t) - \delta L_1(t), \\ L_2'(t) = \epsilon\alpha_{12}\gamma_F F_1(t) + (1-\epsilon\alpha_{21})\gamma_F F_2(t) - \delta L_2(t). \end{cases} \tag{2.13}$$

The equilibria can be computed by solving

$$\begin{cases} 0 = \rho_1 f(L_1^*) - (\gamma+\mu)F_1^*, \\ 0 = \rho_2 f(L_2^*) - (\gamma+\mu)F_2^*, \\ 0 = (1-\epsilon\alpha_{12})\gamma_F F_1^* + \epsilon\alpha_{21}\gamma_F F_2^* - \delta L_1^*, \\ 0 = \epsilon\alpha_{12}\gamma_F F_1^* + (1-\epsilon\alpha_{21})\gamma_F F_2^* - \delta L_2^*. \end{cases} \tag{2.14}$$

Consider the asymptotic expansion of the equilibria as:

$$\begin{aligned} L_1^* &= l_1 + \epsilon l_{1,2} + o(\epsilon), \\ L_2^* &= l_2 + \epsilon l_{2,2} + o(\epsilon), \\ F_1^* &= f_1 + \epsilon f_{1,2} + o(\epsilon), \\ F_2^* &= f_2 + \epsilon f_{2,2} + o(\epsilon). \end{aligned} \tag{2.15}$$

where $(l_1, l_2, f_1, f_2) = (\frac{1}{q}\ln(R_{T,1}), 0, \frac{\delta}{\gamma_F q}\ln(R_{T,1}), 0)$ is the equilibrium in the isolated patches case where $R_{T,1} > 1$ and $R_{T,2} < 1$. Making the appropriate substitutions, (2.15) becomes

$$\begin{aligned}
L_1^* &= \frac{1}{q}\ln(R_{T,1}) + \epsilon l_{1,2} + o(\epsilon),\\
L_2^* &= \epsilon l_{2,2} + o(\epsilon),\\
F_1^* &= \frac{\delta}{\gamma_F q}\ln(R_{T,1}) + \epsilon f_{1,2} + o(\epsilon),\\
F_2^* &= \epsilon f_{2,2} + o(\epsilon).
\end{aligned}$$

By substituting the values in (2.14), we have the following equations:

$$\begin{cases}
0 = \epsilon\left[\dfrac{\rho_1 p}{R_{T,1}}(l_{1,2})(1-\ln(R_{T,1})) - (\gamma+\mu)f_{1,2}\right] + o(\epsilon),\\
0 = \epsilon\left[\rho_2 p l_{2,2} - (\gamma+\mu)f_{2,2}\right] + o(\epsilon),\\
0 = \epsilon\left[f_{1,2}\gamma_F - \alpha_{12}\dfrac{\delta}{q}\ln(R_{T,1}) - \delta l_{1,2}\right] + o(\epsilon),\\
0 = \epsilon\left[f_{2,2}\gamma_F + \alpha_{12}\dfrac{\delta}{q}\ln(R_{T,1}) - \delta l_{2,2}\right] + o(\epsilon).
\end{cases}$$

This is a linear system of four equations and four unknowns $l_{1,2}$, $l_{2,2}$, $f_{1,2}$, $f_{2,2}$ which yields the solution

$$\begin{aligned}
l_{1,2} &= -\frac{\alpha_{12}}{q},\\
l_{2,2} &= \frac{\alpha_{12}}{q}\frac{\ln(R_{T,1})}{1-R_{T,2}},\\
f_{1,2} &= \frac{\alpha_{12}\delta}{q\gamma_F}[\ln(R_{T,1}) - 1],\\
f_{2,2} &= \frac{\alpha_{12}\delta}{q\gamma_F}\frac{\ln(R_{T,1})}{1-R_{T,2}},
\end{aligned}$$

and therefore the final asymptotic solution of the coexistence equilibrium is

$$\begin{aligned} L_1^* &= \frac{\ln(R_{T,1}) - \alpha_{12}\epsilon}{q}, \\ L_2^* &= \frac{\alpha_{12}}{q}\frac{\ln(R_{T,1})}{1 - R_{T,2}}\epsilon, \\ F_1^* &= \frac{\delta}{q\gamma_F}\{\ln(R_{T,1}) + \alpha_{12}\epsilon[\ln(R_{T,1}) - 1]\}, \\ F_2^* &= \frac{\alpha_{12}\delta}{q\gamma_F}\frac{\ln(R_{T,1})}{1 - R_{T,2}}\epsilon. \end{aligned} \tag{2.16}$$

We observe that, first of all, the solution $(L_1^*, L_2^*, F_1^*, F_2^*)$ is always positive since $R_{T,1} > 1 > R_{T,2}$ and $\epsilon << 1$. Secondly, a small host mobility causes the decrease of egg-laying adults in the favorable environment and an increase in the unfavorable patch. Also, the feeding adult equilibrium in the favorable environment can increase or decrease, depending on the size of $R_{T,1}$. If $R_{T,1} > e$, then F_1^* increases, otherwise if $R_{T,1} < e$, then F_1^* decreases. Finally, the fact that F_1^* increases with mobility of the host if $R_{T,1} > e$ is interesting: although mobility of the host decreases L_1^*, a large basic reproduction number in the favorable patch amplifies the number of ticks in the stage from eggs to feeding adults to compensate for the loss of L_1^*.

2.6 Stability analyses

2.6.1 Initial considerations

It is necessary to analyse $f'(L_1^*)$ and $f'(L_2^*)$ for stability purposes and study first of all their sign. For this purpose, we analyse the system in (2.9) which yields

$$L_1^* + L_2^* = \frac{\gamma_F}{\delta}(F_1^* + F_2^*).$$

Therefore the total amount of egg-laying adults with respect to feeding adults at equilibrium is proportional to the development rate from feeding to egg-laying adult divided by the death

rate for egg-laying adults. By studying (2.11), we have the following equations for L_1^* and L_2^*

$$\begin{cases} L_1^* = \dfrac{\gamma_F}{\delta(\gamma+\mu)}[(1-\alpha_{12})\rho_1 f(L_1^*) + \alpha_{21}\rho_2 f(L_2^*)], \\ L_2^* = \dfrac{\gamma_F}{\delta(\gamma+\mu)}[\alpha_{12}\rho_1 f(L_1^*) + (1-\alpha_{21})\rho_2 f(L_2^*)], \end{cases} \tag{2.17}$$

and we can directly derive the following using (2.7):

$$\begin{cases} L_1^* + L_2^* = R_{T,1} f(L_1^*) + R_{T,2} f(L_2^*)), \\ L_1^* - L_2^* = [(1-2\alpha_{12})R_{T,1} f(L_1^*) - (1-2\alpha_{21})R_{T,2} f(L_2^*)]. \end{cases}$$

The maximum of the Ricker function $f(x)$ occurs for $x = q^{-1}$ and is equal to $p(qe)^{-1}$, therefore

$$L_1^* + L_2^* \leq \frac{R_{T,1} + R_{T,2}}{qe}.$$

So if $L_1^* + L_2^* < q^{-1}$, we have that $f'(L_1^*) > 0$ and $f'(L_2^*) > 0$.

2.6.2 Linearization

We study the local stability of the two equilibria by studying whether the eigenvalues of the characteristic equation at their linearized system are all negative (stability) or there exists at least a positive eigenvalue (instability).

Linearization around the trivial equilibrium $(0, 0, 0, 0)$ yields:

$$\begin{cases} F_1'(t) = \rho_1 p L_1(t-\tau_1) - (\gamma+\mu)F_1(t), \\ F_2'(t) = \rho_2 p L_2(t-\tau_2) - (\gamma+\mu)F_2(t), \\ L_1'(t) = (1-\alpha_{12})\gamma_F F_1(t) + \alpha_{21}\gamma_F F_2(t) - \delta L_1(t), \\ L_2'(t) = \alpha_{12}\gamma_F F_1(t) + (1-\alpha_{21}\gamma_F F_2(t) - \delta L_2(t). \end{cases} \tag{2.18}$$

We look for possible $\lambda \in \mathbb{C}$ that satisfy

$$\det\Big(B_0 + B_1 e^{-\lambda\tau_1} + B_2 e^{-\lambda\tau_2} - \lambda I\Big) = 0,$$

where

$$B_0 = \begin{pmatrix} -(\gamma+\mu) & 0 & 0 & 0 \\ 0 & -(\gamma+\mu) & 0 & 0 \\ (1-\alpha_{12})\gamma_F & \alpha_{21}\gamma_F & -\delta & 0 \\ \alpha_{12}\gamma_F & (1-\alpha_{21})\gamma_F & 0 & -\delta \end{pmatrix},$$

$$B_1 = \begin{pmatrix} 0 & 0 & \rho_1 p & 0 \\ 0 & 0 & 0 & 0 \\ 0 & 0 & 0 & 0 \\ 0 & 0 & 0 & 0 \end{pmatrix},$$

and

$$B_2 = \begin{pmatrix} 0 & 0 & 0 & 0 \\ 0 & 0 & 0 & \rho_2 p \\ 0 & 0 & 0 & 0 \\ 0 & 0 & 0 & 0 \end{pmatrix}.$$

Let $B := B_0 + B_1 e^{-\lambda\tau_1} + B_2 e^{-\lambda\tau_2} - \lambda I$, then

$$B = \begin{pmatrix} -(\gamma+\mu)-\lambda & 0 & \rho_1 p e^{-\lambda\tau_1} & 0 \\ 0 & -(\gamma+\mu)-\lambda & 0 & \rho_2 p e^{-\lambda\tau_2} \\ (1-\alpha_{12})\gamma_F & \alpha_{21}\gamma_F & -\delta-\lambda & 0 \\ \alpha_{12}\gamma_F & (1-\alpha_{21})\gamma_F & 0 & -\delta-\lambda \end{pmatrix}.$$

Defining $\psi := (\gamma+\mu+\lambda)(\delta+\lambda)$, we write the previous condition as

$$\det(B) = \psi^2 - b_0\psi + b_1 = 0, \tag{2.19}$$

where

$$b_0 = (1-\alpha_{12})\gamma_F\rho_1 p e^{-\lambda\tau_1} + (1-\alpha_{21})\gamma_F\rho_2 p e^{-\lambda\tau_2},$$

and

$$b_1 = \gamma_F\rho_1 p e^{-\lambda\tau_1}\gamma_F\rho_2 p e^{-\lambda\tau_2}[1-(\alpha_{12}+\alpha_{21})].$$

In a similar way, linearization around the non-trivial equilibrium $(F_1^*, F_2^*, L_1^*, L_2^*)$ yields:

$$\begin{cases} F_1'(t) = \rho_1 f'(L_1^*)L_1(t-\tau_1) - (\gamma+\mu)F_1(t), \\ F_2'(t) = \rho_2 f'(L_2^*)L_2(t-\tau_2) - (\gamma+\mu)F_2(t), \\ L_1'(t) = (1-\alpha_{12})\gamma_F F_1(t) + \alpha_{21}\gamma_F F_2(t) - \delta L_1(t), \\ L_2'(t) = \alpha_{12}\gamma_F F_1(t) + (1-\alpha_{21}\gamma_F F_2(t) - \delta L_2(t). \end{cases} \tag{2.20}$$

The characteristic equation can be computed in a similar way as above by finding $\lambda \in \mathbb{C}$ such that $\det(C) = 0$ where

$$C = \begin{pmatrix} -(\gamma+\mu)-\lambda & 0 & \rho_1 f'(L_1^*)e^{-\lambda\tau_1} & 0 \\ 0 & -(\gamma+\mu)-\lambda & 0 & \rho_2 f'(L_2^*)e^{-\lambda\tau_2} \\ (1-\alpha_{12})\gamma_F & \alpha_{21}\gamma_F & -\delta-\lambda & 0 \\ \alpha_{12}\gamma_F & (1-\alpha_{21})\gamma_F & 0 & -\delta-\lambda \end{pmatrix}.$$

Using the ψ just defined, we can write the determinant of C in this form:

$$\det(C) = \psi^2 - c_0\psi + c_1,$$

where

$$c_0 = (1-\alpha_{12})\gamma_F\rho_1 f'(L_1^*)e^{-\lambda\tau_1} + (1-\alpha_{21})\gamma_F\rho_2 f'(L_2^*)e^{-\lambda\tau_2},$$

and

$$c_1 = \gamma_F\rho_1 f'(L_1^*)e^{-\lambda\tau_1}\gamma_F\rho_2 f'(L_2^*)e^{-\lambda\tau_2}[1-(\alpha_{12}+\alpha_{21})].$$

2.6.3 Isolated patches

In case there is no movement between patches, the problem simplifies a lot since we can treat the two patches independently.

By imposing $\alpha_{12} = \alpha_{21} = 0$, we can break the product of the determinant in this way:

$$\det(B) = \psi^2 - \psi(\gamma_F \rho_1 p e^{-\lambda\tau_1} + \gamma_F \rho_2 p e^{-\lambda\tau_2}) + \gamma_F \rho_1 p e^{-\lambda\tau_1} \gamma_F \rho_2 p e^{-\lambda\tau_2}.$$

Imposing $\det(B) = 0$ yields:

$$(\psi - \gamma_F \rho_1 p e^{-\lambda\tau_1})(\psi - \gamma_F \rho_2 p e^{-\lambda\tau_2}) = 0.$$

Note that the left (resp. right) member of the product is the characteristic equation of isolated patch 1 (resp. 2) linearised at the trivial equilibrium.

Similarly, imposing $\det(C) = 0$ yields:

$$(\psi - \gamma_F \rho_1 f'(L_1^*) e^{-\lambda\tau_1})(\psi - \gamma_F \rho_2 f'(L_2^*) e^{-\lambda\tau_2}) = 0.$$

Therefore, in the same way we can study independently stability in the isolated patches 1 and 2. We study first the stability of the trivial equilibrium by linearising around $(0, 0)$ (we know $f'(0) = p$):

$$\begin{cases} F_i'(t) = \rho_i p L_i(t - \tau_i) - (\gamma + \mu) F_i(t), \\ L_i'(t) = \gamma_F F_i(t) - \delta L_i(t). \end{cases}$$

The characteristic equation is obtained by solving $\det(B) = 0$ where

$$B = \begin{pmatrix} -(\gamma + \mu + \lambda) & \rho_i p e^{-\lambda\tau_i} \\ \gamma_F & -(\delta + \lambda) \end{pmatrix},$$

which yields

$$(\gamma + \mu + \lambda)(\delta + \lambda) = \gamma_F \rho_i p e^{-\lambda\tau_i}, \tag{2.21}$$

and can be rewritten as

$$\frac{(\gamma+\mu+\lambda)(\delta+\lambda)}{\gamma_F\rho_i p} = e^{-\lambda\tau_i}. \tag{2.22}$$

Proposition 5. *The trivial equilibrium* $(0,0)$ *of* (2.6) *is locally asymptotically stable if* $R_{T,i} < 1$ *and unstable if* $R_{T,i} > 1$.

Proof. We first prove the case where $R_{T,i} < 1$, when the only equilibrium is the trivial one. In order to show this, we want to prove that there are no solutions to the characteristic equation (2.21) with positive real part.

Suppose by contradiction there exists a root of (2.21) $\lambda = x + iy$ with $x \geq 0$. So the following equality holds:

$$|(\gamma+\mu+x+iy)(\delta+x+iy)| = |\gamma_F\rho_i p e^{-(x+iy)\tau_i}|,$$

We also know

$$\begin{aligned}
|(\gamma+\mu+x+iy)(\delta+x+iy)| &= |(\gamma+\mu+x+iy)||(\delta+x+iy)| \\
&= \sqrt{(\gamma+\mu+x)^2+y^2}\sqrt{(\delta+x)^2+y^2} \\
&\geq \sqrt{(\gamma+\mu)^2}\sqrt{\delta^2} \\
&= (\gamma+\mu)\delta,
\end{aligned}$$

while the right hand side follows the inequality

$$|\gamma_F\rho_i p e^{-(x+iy)\tau_1}| \leq \gamma_F\rho_i p.$$

But since $R_{T,i} < 1$, we have

$$\gamma_F\rho_i p < (\gamma+\mu)\delta,$$

which leads to contradiction. Therefore all the roots of the characteristic equation have negative real part and $(0,0)$ is locally asymptotically stable.

Then we determine the instability of the trivial equilibrium whenever $R_{T,i} > 1$. The left hand side of (2.22) as a function of real λ is a parabola facing upwards ($g(\lambda) = a\lambda^2 + b\lambda + c$) with

$$c = \frac{\delta(\gamma + \mu)}{\gamma_f \rho_i p} = \frac{1}{R_{T,i}}.$$

Moreover $b > 0$ and $a > 0$, therefore the vertex of the concave up parabola will be on the left side of the y axis. Also $g(0) = c$ with $c < 1$ (since $R_{T,i} > 1$) and $g(\lambda)$ is increasing for positive λ. If we consider the right hand side of (2.22) to be $h(\lambda) = e^{-\lambda\tau_i}$. We see that $h(0) = 1$ and it is always decreasing. This means that there is an intersection between the left and right hand side of (2.22) for $\lambda > 0$, therefore there is a root with positive real part and the trivial equilibrium will be unstable. □

Proposition 6. *The trivial equilibrium* $(0, 0)$ *is a global attractor of* (2.6) *if* $R_{T,1} < 1$.

Proof. We have described in section 2.4.1 that it is possible to study the stability of the trivial equilibrium of (2.6) by setting $\tau_i = 0$ [76],

$$\begin{cases} F_i'(t) = \rho_i f(L_i(t)) - (\gamma + \mu)F_i(t), \\ L_i'(t) = \gamma_F F_i(t) - \delta L_i(t), \end{cases} \tag{2.23}$$

We then use the principle of linearized stability and study the properties of the trivial equilibrium in the following linearized system:

$$\begin{cases} \bar{F_i}'(t) = \rho_i p \bar{L}_i(t) - (\gamma + \mu)\bar{F}_i(t), \\ \bar{L_i}'(t) = \gamma_F \bar{F}_i(t) - \delta \bar{L}_i(t). \end{cases} \tag{2.24}$$

In the proof to Proposition 2, we have shown that Γ (2.2) is a positively invariant set of (2.1) and the ω-limit of the solutions is in Γ. Let

$$\Gamma_{iso} := \{(F_i, L_i) \in \mathbb{R}^2_+ : F_i \leq F_i^\infty, L_i \leq L_i^\infty\}, \tag{2.25}$$

where

$$F_i^\infty = \frac{\rho_i p}{qe(\gamma+\mu)},$$
$$L_i^\infty = \frac{\gamma_F p \rho_i}{qe\delta(\gamma+\mu)}.$$

From (2.24) we see that the Jacobian matrix is

$$J = \begin{pmatrix} -(\gamma+\mu) & \rho_i p \\ \gamma_F & -\delta \end{pmatrix}.$$

We note that

1. Γ_{iso} is a positively invariant set of (2.6) containing the trivial solution and the ω-limit of its solutions is contained in Γ_{iso}. Its derivation is analogous to Proposition 2.

2. (2.24) is a cooperative system since $j_{1,2}$, $j_{2,1} \geq 0$ if $R_{T,i} < 1$.

3. J is irreducible since $j_{1,2}$, $j_{2,1} \neq 0$.

Using monotone dynamical theory [76], we deduce that (2.6) does not contain any periodic solution for $R_{T,i} < 1$, therefore $(0,0)$ is attractive and $(\bar{F}_i(t), \bar{L}_i(t)) \to (0,0)$ as $t \to \infty$ for any initial condition. □

Then we consider the stability of the non-trivial equilibrium, when it exists, by linearising around $(F_i^*, L_i^*) = \left(\frac{\delta \ln(R_{T,i})}{\gamma_F q}, \frac{\ln(R_{T,i})}{q}\right)$,

$$\begin{cases} F_i'(t) = \rho_i f'(L_i^*) L_i(t-\tau_i) - (\gamma+\mu) F_i(t), \\ L_i'(t) = \gamma_F F_i(t) - \delta L_i(t). \end{cases} \tag{2.26}$$

where

$$f'(L_i^*) = p\,\frac{1-\ln(R_{T,i})}{R_{T,i}}. \tag{2.27}$$

Therefore

1. $1 < R_{T,i} < e \Rightarrow f'(L_i^*) > 0$,

2. $R_{T,i} > e \Rightarrow f'(L_i^*) < 0$.

The characteristic equation is obtained by imposing the determinant of the following matrix equal to 0,

$$B = \begin{pmatrix} -(\gamma + \mu + \lambda) & \rho_i f'(L_i^*) e^{-\lambda \tau_i} \\ \gamma_F & -(\delta + \lambda) \end{pmatrix},$$

which is

$$(\gamma + \mu + \lambda)(\delta + \lambda) = \gamma_F \rho_i f'(L_i^*) e^{-\lambda \tau_i}, \tag{2.28}$$

and can be rewritten as

$$\frac{(\gamma + \mu + \lambda)(\delta + \lambda)}{\gamma_F \rho_i f'(L_i^*)} = e^{-\lambda \tau_i}. \tag{2.29}$$

Note that if $1 < R_{T,1} < e$, the system is cooperative and the stability of the non-trivial equilibrium of (2.26) is same for all τ_i so we can impose $\tau_i = 0$ and study its stability for the ODE instead [76].

Proposition 7. *The non-trivial equilibrium (F_i^*, L_i^*) is locally asymptotically stable for all $\tau_i \geq 0$ if $1 < R_{T,i} < e^2$.*

Proof. Similarly to the previous proof, we want to show that there are no solutions to the characteristic equation (2.29) with positive real part. Suppose by contradiction there exists a root of (2.29) $\lambda = x + iy$ with $x \geq 0$. So the following equality holds:

$$|(\gamma + \mu + x + iy)(\delta + x + iy)| = |\gamma_F \rho_i f'(L_i^*) e^{-(x+iy)\tau_i}|,$$

We also know

$$\begin{aligned} |(\gamma + \mu + x + iy)(\delta + x + iy)| &= |(\gamma + \mu + x + iy)||(\delta + x + iy)|, \\ &= \sqrt{(\gamma + \mu + x)^2 + y^2}\sqrt{(\delta + x)^2 + y^2}, \\ &\geq \sqrt{(\gamma + \mu)^2}\sqrt{\delta^2}, \end{aligned}$$

$$= (\gamma + \mu)\delta,$$

while the right hand side with $1 < R_{T,i} < e^2$ satisfies

$$\begin{aligned} |\gamma_F \rho_i f'(L_i^*) e^{-(x+iy)\tau_i}| &\leq \gamma_F \rho_i |f'(L_i^*)|, \\ &= \gamma_F \rho_i p \left| \frac{1 - \ln(R_{T,i})}{R_{T,i}} \right|, \\ &= (\gamma + \mu)\delta |1 - \ln(R_{T,i})|, \\ &< (\gamma + \mu)\delta. \end{aligned}$$

We thus reach a contradiction, therefore all the roots of the characteristic equation have negative real part and (F_i^*, L_i^*) is locally asymptotically stable for $1 < R_{T,i} < e^2$. □

Proposition 8. *Every non-trivial solution of* (2.6) *converges to* (F_i^*, L_i^*) *as* $t \to \infty$ *if* $1 < R_{T,i} < e$.

Proof. Consider the Jacobian of (2.26) for $\tau_i = 0$:

$$J = \begin{pmatrix} -(\gamma + \mu) & \rho_i f'(L_i^*) \\ \gamma_F & -\delta \end{pmatrix},$$

and Γ_{iso} defined in (2.25). We see that

1. Γ_{iso} is a positively invariant set of (2.6) containing (F_i^*, L_i^*) and the ω-limit of its solutions is contained in Γ_{iso}.

2. (2.26) is a cooperative system (for $\tau_i = 0$) - $j_{1,2},\ j_{2,1} \geq 0$ since $f'(L_i^*) > 0$ if $1 < R_{T,i} < e$.

3. J is irreducible - $j_{1,2},\ j_{2,1} \neq 0$.

Using monotone dynamical theory [76], we deduce that (2.6) does not contain any periodic solution for $1 < R_{T,i} < e$, therefore (F_i^*, L_i^*) is attractive. □

It is possible to extend global attractivity of the non-trivial equilibrium also for $e \leq R_{T,i} < e^2$ using exponential ordering [76].

Proposition 9. *If $R_{T,i} > e^2$, there exists a Hopf bifurcation point at a specific threshold $\tau = \tau^*$. The non-trivial equilibrium (F_i^*, L_i^*) is asymptotically stable for $0 \leq \tau_i < \tau^*$ and is unstable for $\tau_i > \tau^*$.*

Proof. We consider the asymptotic stability of the non-trivial equilibrium when $\tau_i = 0$. The characteristic equation becomes

$$(\gamma + \mu + \lambda)(\delta + \lambda) = \rho_i \gamma_F f'(L_i^*),$$

which can be rewritten as

$$\lambda^2 + (\gamma + \mu + \delta)\lambda + \delta(\gamma + \mu) + \rho_i \gamma_F p \left(\frac{\ln(R_{T,i}) - 1}{R_{T,i}} \right) = 0.$$

Since it is a second degree polynomial and all coefficients of this polynomial are greater than 0, we have that $\lambda_1 + \lambda_2 < 0$ and $\lambda_1 \lambda_2 > 0$, therefore both eigenvalues are strictly negative and (F_i^*, L_i^*) is asymptotically stable in the absence of delay. We expect the presence of a Hopf bifurcation as the delay grows.

In order to apply the Hopf bifurcation theorem for DDE systems [79], we have to show

1. Simplicity condition: there is a pair of simple roots $\lambda^* = \pm i\omega$ for some $\tau_i = \tau_i^*$ of (2.28).
2. Transversality condition: $\frac{d(\mathrm{Re}\lambda)}{d\tau_i}|_{\tau_i = \tau_i^*} \neq 0$.

1. Suppose there exists a purely imaginary root $\lambda^* = \pm i\omega$. Then

$$(\gamma + \mu + i\omega)(\delta + i\omega) = \rho_i \gamma_F f'(L_i^*) e^{-i\omega\tau_i^*}.$$

We separate the real and imaginary parts of this system and yield

$$\begin{cases} \delta(\gamma+\mu) - \omega^2 = \rho_i \gamma_F f'(L_i^*)\cos(\omega\tau_i^*), \\ \omega(\delta+\gamma+\mu) \ = -\rho_i \gamma_F f'(L_i^*)\sin(\omega\tau_i^*). \end{cases} \tag{2.30}$$

The Hopf bifurcation point τ_i^* is the smallest τ_i that satisfies (2.30). Summing up the square of first line to the square of the second line yields the value of ω which affects the period of the periodic solution - the larger the ω, the smaller the period. We have

$$\omega^4 + \omega^2[\delta+\gamma+\mu-2\delta(\gamma+\mu)] + \delta^2(\gamma+\mu)^2 - (\rho_i\gamma_F f'(L_i^*))^2 = 0.$$

Let $\zeta = \omega^2$ and search for a positive real solution of ζ in the following equation:

$$\zeta^2 + \zeta[\delta+\gamma+\mu-2\delta(\gamma+\mu)] + \delta^2(\gamma+\mu)^2 - (\rho_i\gamma_F f'(L_i^*))^2 = 0.$$

We can rewrite the last term using (2.27)

$$\zeta^2 + \zeta[\delta+\gamma+\mu-2\delta(\gamma+\mu)] + \delta^2(\gamma+\mu)^2(1-(1-\ln(R_{T,i}))^2) = 0.$$

Note that if $R_{T,i} > e^2$, there will always be a unique positive solution since

$$\begin{aligned} \Delta_{i1} &= (\delta+\gamma+\mu-2\delta(\gamma+\mu))^2 - 4[\delta^2(\gamma+\mu)^2][1-(1-\ln(R_{T,i}))^2] \\ &> (\delta+\gamma+\mu-2\delta(\gamma+\mu))^2 \geq 0. \end{aligned} \tag{2.31}$$

The two real solutions of ζ are:

$$\zeta_{1,2} = \frac{1}{2}(2\delta(\gamma+\mu) - (\delta+\gamma+\mu) \pm \sqrt{\Delta_{i1}}),$$

and the only positive solution is

$$\zeta_1 = \frac{1}{2}(2\delta(\gamma+\mu) - (\delta+\gamma+\mu) + \sqrt{\Delta_{i1}}). \tag{2.32}$$

Therefore $\omega = \pm\sqrt{\zeta_1}$. To find τ_i^*, we divide equation 2 with equation 1 in (2.30) which yields

$$\tan(\omega\tau_i^*) = \frac{\omega(\delta+\gamma+\mu)}{\omega^2 - \delta(\gamma+\mu)}, \tag{2.33}$$

therefore

$$\tau_i^* = \omega^{-1}\arctan\left(\frac{\omega(\delta+\gamma+\mu)}{\omega^2-\delta(\gamma+\mu)}\right).$$

2. Consider

$$h(\lambda,\xi) = (\gamma+\mu+\lambda)(\delta+\lambda) - \gamma_F\rho_i f'(L_i^*)e^{-\lambda(\tau_i^*+\xi)}.$$

Since λ^* is a root of 2.28 for $\tau_i = \tau_i^*$, $h(\lambda^*, 0) = 0$. Using the simplicity condition just proved, we also have that $h_\lambda(\lambda^*, 0) \neq 0$.

We apply Implicit Function Theorem which states that there exists $\lambda(\xi) \in C^1$ such that $\lambda(0) = \lambda^* = i\omega$. So proving transversality condition reduces to showing that $\mathrm{Re}(\lambda'(0)) \neq 0$. Using implicit differentiation and the fact that $h(\lambda(\xi),\xi) = 0$, we have

$$0 = \frac{d}{d\xi}h(\lambda(\xi),\xi) = \frac{\partial h}{\partial\lambda}\lambda'(\xi) + \frac{\partial h}{\partial\xi},$$

and

$$\lambda'(0) = -\frac{\frac{\partial h}{\partial\xi}|_{(\lambda^*,0)}}{\frac{\partial h}{\partial\lambda}|_{(\lambda^*,0)}}.$$

The computation of the partial derivatives of h at $(\lambda^*, 0)$ yields

$$\lambda'(0) = \frac{\gamma_F\rho_i f'(L_i^*)\lambda^* e^{-\lambda^*\tau_i^*}}{2\lambda^* + \gamma + \mu + \delta + \gamma_F\rho_i f'(L_i^*)\tau_i^* e^{-\lambda^*\tau_i^*}}.$$

We replace $\lambda^* = i\omega$ and using the fact that $\mathrm{Re}(z) = \frac{ac+bd}{c^2-d^2}$ for a complex number $z = \frac{a+ib}{c+id}$ where $(c,d) \neq (0,0)$ and Euler's formula, after a series of computations, we have

$$\mathrm{Re}(\lambda'(0)) \neq 0 \iff \sin(\omega\tau_i^*)(\gamma+\mu+\delta) + 2\omega\cos(\omega\tau_i^*) \neq 0.$$

We have already computed the tangent from (2.33) so we divide both sides by $\cos(\omega\tau_i^*)$

so we need to show

$$\tan(\omega\tau_i^*)(\gamma+\mu+\delta)+2\omega\neq 0,$$

or equivalently

$$(\delta+\gamma+\mu)^2+2[\omega^2-\delta(\gamma+\mu)]\neq 0,$$

which isolating ω^2 yields

$$\omega^2\neq\frac{1}{2}(2\delta(\gamma+\mu)-(\delta+\gamma+\mu)^2).$$

But $\omega^2=\zeta_1$ in (2.32) so we want to compare the two quantities and check if

$$\sqrt{\Delta_{i1}}\neq(\delta+\gamma+\mu)-(\delta+\gamma+\mu)^2.$$

Using (2.31) for $R_{T,i}>e^2$ and the fact that $(\delta+\gamma+\mu)^2\geq 2\delta(\gamma+\mu)$,

$$\begin{aligned}\sqrt{\Delta_{i1}}&>\delta+\gamma+\mu-2\delta(\gamma+\mu),\\&\geq\delta+\gamma+\mu-(\delta+\gamma+\mu)^2,\end{aligned}$$

which proves the transversality condition.

□

The critical value τ_i^* decreases when $p\rho_i\gamma_F$ increase, therefore survival probabilities and maximal amount of eggs produced influence the Hopf bifurcation. Also ω^2 depends directly on $b:=\delta+\gamma+\mu-2\delta(\gamma+\mu)$. In this case as b decreases, also τ_i^* decreases.

In our case, we know that $R_{T,1}>1$ and $R_{T,2}<1$ so we use the propositions just proved to study the stability of the different equilibria. In patch 2, the only existing equilibrium is the trivial one. In patch 1, we have also a non-trivial equilibrium (F_1^*,L_1^*). In particular

1. $(0,0,0,0)$ is unstable since $R_{T,1}>1$ (Proposition 5).

2. $(F_1^*,0,L_1^*,0)$ is:

- Asymptotically stable if $1 < R_{T,1} < e^2$ for all $\tau_1 > 0$ (Proposition 7).
- Asymptotically stable when $R_{T,1} > e^2$ if $\tau_1 < \tau^*$, and unstable if $\tau_1 > \tau^*$ (Proposition 9).

2.6.4 Escalating up

In this case, we have both the trivial equilibria and a non-trivial equilibrium $(F_1^*, 0, L_1^*, 0)$. Studying the characteristic equation at the equilibria yields:

$$\det(B) = x^2 - c_0 x + c_1 = 0$$

where

$$c_0 = \gamma_F \rho_1 f'(L_1^*) e^{-\lambda \tau_1} + (1 - \alpha_{21}) \gamma_F \rho_2 f'(L_2^*) e^{-\lambda \tau_2},$$

and

$$c_1 = \gamma_F \rho_1 f'(L_1^*) e^{-\lambda \tau_1} \gamma_F \rho_2 f'(L_2^*) e^{-\lambda \tau_2} [1 - \alpha_{21}].$$

We can break the condition $\det(B) = 0$ this way:

$$(x - a)(x - b) = 0,$$

where

$$a = \gamma_F \rho_1 f'(L_1^*) e^{-\lambda \tau_1},$$

and

$$b = (1 - \alpha_{21}) \gamma_F \rho_2 f'(L_2^*) e^{-\lambda \tau_2}.$$

Patch two only admits the equilibrium $(0, 0)$ which is asymptotically stable and it can be easily proved by contradiction as in Proposition 5. The stability of the equilibria in patch 1 instead will be exactly the same as that of the isolated case, therefore the combined equilibria will be such that:

1. Trivial equilibrium $(0, 0, 0, 0)$ is unstable since $R_{T,1} > 1$ (Proposition 5);

2. Non-trivial equilibrium $(F_1^*, 0, L_1^*, 0)$ is:

   - Asymptotically stable if $1 < R_{T,1} < e^2$ for all τ_1 (Proposition 7),
   - Asymptotically stable if $R_{T,1} > e^2$ for $\tau_1 < \tau^*$ and unstable otherwise since it undergoes a Hopf bifurcation at a certain τ^* derived by (2.30) (Proposition 9).

2.6.5 Cascading down

In the cascading down case (i.e. $\alpha_{21} = 0$), there is either only the trivial equilibrium if $\alpha_{12} > \frac{R_{T,1}-1}{R_{T,1}}$, or there is also a coexistence equilibrium $(F_1^*, F_2^*, L_1^*, L_2^*)$. Studying the characteristic equation at the trivial equilibrium yields:

$$\det(B) = x^2 - c_0 x + c_1,$$

where

$$c_0 = (1 - \alpha_{12})\gamma_F \rho_1 f'(L_1^*) e^{-\lambda\tau_1} + \gamma_F \rho_2 f'(L_2^*) e^{-\lambda\tau_2},$$

and

$$c_1 = \gamma_F \rho_1 f'(L_1^*) e^{-\lambda\tau_1} \gamma_F \rho_2 f'(L_2^*) e^{-\lambda\tau_2} [1 - \alpha_{12}].$$

We can similarly break the condition $\det(B) = 0$ this way:

$$(x - a)(x - b) = 0,$$

where

$$a = (1 - \alpha_{12})\gamma_F \rho_1 f'(L_1^*) e^{-\lambda\tau_1},$$

and

$$b = \gamma_F \rho_2 f'(L_2^*) e^{-\lambda\tau_2}.$$

Note that $x - b = 0$ will result only in eigenvalues with negative real part since $f'(L_2^*) \leq p$ and $R_{T,2} < 1$ by arguments related to Proposition 5, so it will not influence the stability of the coexistence equilibrium. Therefore, we analyse $x - a = 0$ using arguments similar to the computations above and we have our conclusive equilibrium analysis:

1. Trivial equilibrium $(0, 0, 0, 0)$ is:
   - Asymptotically stable if $(1 - \alpha_{12})R_{T,1} < 1$
   - Unstable if $(1 - \alpha_{12})R_{T,1} < 1$
2. Coexistence equilibrium $(F_1^*, F_2^*, L_1^*, L_2^*)$ exists if $(1 - \alpha_{12})R_{T,1} < 1$ and is:
   - Asymptotically stable if $1 < (1 - \alpha_{12})R_{T,1} < e^2$ for all τ_1,
   - Asymptotically stable if $(1 - \alpha_{12})R_{T,1} > e^2$ for $\tau_1 < \tilde{\tau}$ and unstable otherwise since it undergoes a Hopf bifurcation at $\tau_1 = \tilde{\tau}$ derived below.

Hopf bifurcation occurs when there exists a purely imaginary root $\lambda = i\omega$ to $x - a = 0$, which is found by solving the following system:

$$\begin{cases} \delta(\gamma + \mu) - \omega^2 = (1 - \alpha_{12})\rho_1\gamma_F f'(L_1^*)\cos(\omega\tilde{\tau}), \\ \omega(\delta + \gamma + \mu) \ = -(1 - \alpha_{12})\rho_1\gamma_F f'(L_1^*)\sin(\omega\tilde{\tau}). \end{cases}$$

Using calculations similar to the isolated patch case in Proposition 9 yields

$$\Delta_{cd} = (\delta + \gamma + \mu - 2\delta(\gamma + \mu))^2 - 4[\delta^2(\gamma + \mu)^2][1 - (1 - \alpha_{12})(1 - \ln(R_{T,1}))^2],$$

$$\omega = \pm\sqrt{\frac{1}{2}\left(2\delta(\gamma + \mu) - (\delta + \gamma + \mu) + \sqrt{\Delta_{cd}}\right)},$$

and

$$\tilde{\tau} = \omega^{-1}\arctan\left(\frac{\omega(\delta + \gamma + \mu)}{\omega^2 - \delta(\gamma + \mu)}\right).$$

2.6.6 Interconnected patches

Stability in the interconnected case presents several complications due to the fact that the equilibrium is not in a closed form and that the characteristic equation cannot be factored out like in the previous cases. We analyse the solutions of the characteristic equation shown in Section 2.6.2

$$\psi^2 - b_0\psi + b_1 = 0,$$

where

$$\psi := (\gamma + \mu + \lambda)(\delta + \lambda),$$

and

$$\begin{aligned} b_0 &= (1-\alpha_{12})\gamma_F\rho_1 p e^{-\lambda\tau_1} + (1-\alpha_{21})\gamma_F\rho_2 p e^{-\lambda\tau_2} \\ &= \delta(\gamma+\mu)[(1-\alpha_{12})R_{T,1}e^{-\lambda\tau_1} + (1-\alpha_{21})R_{T,2}e^{-\lambda\tau_2}], \\ b_1 &= \gamma_F\rho_1 p e^{-\lambda\tau_1}\gamma_F\rho_2 p e^{-\lambda\tau_2}[1-(\alpha_{12}+\alpha_{21})] \\ &= \delta^2(\gamma+\mu)^2[R_{T,1}R_{T,2}e^{-\lambda\tau_1}e^{-\lambda\tau_2}(1-\alpha_{12}-\alpha_{21})], \end{aligned}$$

in terms of the basic reproduction numbers $R_{T,1}$ and $R_{T,2}$.

First, we study the solution of this second order equation with respect to ψ, therefore we compute

$$\begin{aligned} \Delta_{c1} = \delta^2(\gamma+\mu)^2\{&[(1-\alpha_{12})R_{T,1}e^{-\lambda\tau_1} + (1-\alpha_{21})R_{T,2}e^{-\lambda\tau_2}]^2 \\ &- 4R_{T,1}R_{T,2}e^{-\lambda\tau_1}e^{-\lambda\tau_2}(1-\alpha_{12}-\alpha_{21})\}. \end{aligned}$$

So the two solutions are

$$\psi_{1,2} = \frac{\delta(\gamma+\mu)[(1-\alpha_{12})R_{T,1}e^{-\lambda\tau_1} + (1-\alpha_{21})R_{T,2}e^{-\lambda\tau_2} \pm \sqrt{\xi}]}{2}, \tag{2.34}$$

where

$$\xi = [(1-\alpha_{12})R_{T,1}e^{-\lambda\tau_1} + (1-\alpha_{21})R_{T,2}e^{-\lambda\tau_2}]^2 - 4R_{T,1}R_{T,2}e^{-\lambda\tau_1}e^{-\lambda\tau_2}(1-\alpha_{12}-\alpha_{21}),$$

and we can rewrite the characteristic equation as

$$(\psi - \psi_1)(\psi - \psi_2) = 0.$$

Therefore, by rewriting ψ, we have

$$[(\gamma+\mu+\lambda)(\delta+\lambda) - \psi_1][(\gamma+\mu+\lambda)(\delta+\lambda) - \psi_2] = 0,$$

and the two different terms can be rewritten separately for $i = 1, 2$ as

$$\lambda^2 + \lambda(\delta+\gamma+\mu) + \delta(\gamma+\mu)\left[1 - \frac{\psi_i}{\delta(\gamma+\mu)}\right] = 0.$$

Therefore the solutions of the characteristic equation (i.e. the eigenvalues of linearised matrix at trivial equilibrium) have to satisfy one of the following 4 equations for $i = 1, 2$:

$$\lambda = \frac{-(\delta+\gamma+\mu) \pm \sqrt{\Delta_{i2}}}{2}, \tag{2.35}$$

where

$$\begin{aligned}\Delta_{i2} &= (\delta+\gamma+\mu)^2 - 4\delta(\gamma+\mu)\left[1 - \frac{\psi_i}{\delta(\gamma+\mu)}\right], \\ &= [\delta - (\gamma+\mu)]^2 + 4\psi_i.\end{aligned}$$

Note that ψ_i is a function of λ. At this point we can prove a similar result as in the isolated case.

Proposition 10. *The trivial equilibrium* $(0,0,0,0)$ *of* (2.1) *is locally asymptotically stable if* $R_{T,c} < 1$ *and unstable if* $R_{T,c} > 1$.

Proof. We know there is a positive feedback in the linearised system (2.18) since $f'(0) = p > 0$. Therefore we apply the monotone dynamical theory [76] that states that in a positive feedback system, stability of the trivial equilibrium of (2.18) is equivalent to that of the corresponding ODE system (where $\tau_1 = \tau_2 = 0$). Suppose that there exists a solution λ with positive real part. From (2.35), we see that if $|\Delta_{i2}| \leq (\delta + \gamma + \mu)^2$, then there would be a contradiction since the real part of the eigenvalues would always be negative. Note that

$$\Delta_{i2} = \delta^2 + (\gamma + \mu)^2 - 2\delta(\gamma + \mu) + 4\psi_i$$

and

$$(\delta + \gamma + \mu)^2 = \delta^2 + (\gamma + \mu)^2 + 2\delta(\gamma + \mu).$$

Therefore, in order to prove asymptotic stability, we just need to prove that

$$|\psi_i| < \delta(\gamma + \mu).$$

where ψ_i derives from the equation (2.34) in case of no delay:

$$\psi_i = \frac{\delta(\gamma + \mu)[(1 - \alpha_{12})R_{T,1} + (1 - \alpha_{21})R_{T,2} \pm \sqrt{\zeta}]}{2},$$

and $\zeta = [(1 - \alpha_{12})R_{T,1} + (1 - \alpha_{21})R_{T,2}]^2 - 4R_{T,1}R_{T,2}(1 - \alpha_{12} - \alpha_{21})$. We know

$$R_{T,c} = \frac{(1 - \alpha_{12})R_{T,1} + (1 - \alpha_{21})R_{T,2} \pm \sqrt{\zeta}}{2},$$

thus

$$\psi_i \leq \delta(\gamma + \mu)R_{T,c}.$$

If $R_{T,c} < 1$, it follows directly that

$$\psi_i < \delta(\gamma + \mu),$$

which proves stability of the trivial equilibrium.

Then we determine the instability of the trivial equilibrium when $R_{T,c} > 1$.
Let $g(\lambda)$ be the right hand side of (2.35) when $i = 1$ and we consider the positive value of the square root. Note that if $\lambda = 0$, then (2.34) shows that $\psi_i = \delta(\gamma + \mu)R_{T,c}$. It follows that

$$\begin{aligned} g(0) &= \frac{-(\delta+\gamma+\mu) + \sqrt{[\delta-(\gamma+\mu)]^2 + 4\delta(\gamma+\mu)R_{T,c}}}{2}, \\ &> \frac{-(\delta+\gamma+\mu) + \sqrt{[\delta-(\gamma+\mu)]^2 + 4\delta(\gamma+\mu)}}{2}, \\ &= 0, \end{aligned}$$

which means that $g(0) > 0$ if $R_{T,c} > 1$. Now consider the limit of $g(\lambda)$ as $\lambda \to \infty$. Note that $\psi_i \to 0$ in this case since (2.34) holds and $e^{-\lambda\tau_i} \to 0$.

$$\begin{aligned} \lim_{\lambda\to\infty} g(\lambda) &= \frac{-(\delta+\gamma+\mu) + \sqrt{[\delta-(\gamma+\mu)]^2}}{2}, \\ &= \frac{-(\delta+\gamma+\mu) + |\delta-(\gamma+\mu)|}{2}, \\ &< 0. \end{aligned}$$

Since $g(\lambda)$ is continuous with respect to λ, there is at least a positive real intersection with $f(\lambda) = \lambda$ (see equation (2.35)). This concludes the proof of the instability of the trivial equilibrium if $R_{T,c} > 1$. □

Proposition 11. *The trivial equilibrium* $(0, 0, 0, 0)$ *is a global attractor of* (2.1) *if* $R_{T,c} < 1$.

Proof. We study stability of the trivial equilibrium of (2.6) by setting $\tau_1 = \tau_2 = 0$ as described in section 2.4.1,

$$\begin{cases} F_1'(t) = \rho_1 f(L_1(t)) - (\gamma+\mu)F_1(t), \\ F_2'(t) = \rho_2 f(L_2(t)) - (\gamma+\mu)F_2(t), \\ L_1'(t) = (1-\alpha_{12})\gamma_F F_1(t) + \alpha_{21}\gamma_F F_2(t) - \delta L_1(t), \\ L_2'(t) = \alpha_{12}\gamma_F F_1(t) + (1-\alpha_{21})\gamma_F F_2(t) - \delta L_2(t). \end{cases} \tag{2.36}$$

We then use the principle of linearized stability and study the properties of the trivial equilibrium for the linearized system

$$\begin{cases} \bar{F_1}'(t) = \rho_1 p L_1(t) - (\gamma+\mu)F_1(t), \\ \bar{F_2}'(t) = \rho_2 p L_2(t) - (\gamma+\mu)F_2(t), \\ \bar{L_1}'(t) = (1-\alpha_{12})\gamma_F F_1(t) + \alpha_{21}\gamma_F F_2(t) - \delta L_1(t), \\ \bar{L_2}'(t) = \alpha_{12}\gamma_F F_1(t) + (1-\alpha_{21})\gamma_F F_2(t) - \delta L_2(t). \end{cases} \tag{2.37}$$

Its Jacobian is

$$J = \begin{pmatrix} -(\gamma+\mu)-\lambda & 0 & \rho_1 p & 0 \\ 0 & -(\gamma+\mu)-\lambda & 0 & \rho_2 p \\ (1-\alpha_{12})\gamma_F & \alpha_{21}\gamma_F & -\delta-\lambda & 0 \\ \alpha_{12}\gamma_F & (1-\alpha_{21})\gamma_F & 0 & -\delta-\lambda \end{pmatrix}.$$

In the proof to Proposition 2, we have shown that Γ defined by (2.2) is a positively invariant set of (2.1) and the ω-limit of the solutions is in Γ. To sum up, we observe that

1. Γ is a positively invariant set of (2.37) containing the trivial equilibrium and the ω-limit of its solutions is contained in Γ_{asy} - check Proposition 2 for derivation.

2. (2.37) is a cooperative system since $j_{kl} \geq 0$ for $k \neq l$.

3. J is irreducible since for every nonempty proper set I of $N = \{1,2,3,4\}$, there is a $k \in I,\ j \in N \setminus I$ such that $j_{kl} \neq 0$ and the digraph is strongly connected.

Therefore, using monotone dynamical theory [76], we deduce that (2.13) does not contain any periodic solution for $R_{T,c} < 1$, therefore $(\bar{F_1}(t), \bar{F_2}(t), \bar{L_1}(t)\bar{L_2}(t)) \to (0,0,0,0)$ as $t \to \infty$ for any initial condition and $(0,0,0,0)$ is a global attractor for (2.37) and (2.1) □

Analytical considerations on the coexistence equilibrium cannot be made since there is no closed-form solution. We can study though the stability of the coexistence equilibrium in (2.13) and show that the stability properties of (2.6) are preserved.

Proposition 12. *The non-trivial equilibrium* $(F_1^*, F_2^*, L_1^*, L_2^*)$ *in* (2.16) *is locally asymptotically stable in* (2.13) *for all* $(\tau_1, \tau_2) \geq 0$ *if* $1 < R_{T,c} + o(\epsilon) < e^2$.

Proof. We calculate $R_{T,c}$ for (2.13)

$$R_{T,c} = \frac{b + \sqrt{b^2 - 4c}}{2},$$

where

$$b = (1 - \epsilon\alpha_{12})R_{T,1} + (1 - \epsilon\alpha_{21})R_{T,2}, \quad c = R_{T,1}R_{T,2}[1 - \epsilon(\alpha_{12} + \alpha_{21})].$$

Through a series of algebraic computations we have that

$$b^2 - 4c = (R_{T,1} - R_{T,2})^2 + 2\epsilon(\alpha_{12}R_{T,1} - \alpha_{21}R_{T,2})(R_{T,2} - R_{T,1}).$$

We consider the asymptotic expansion for $x \to 0$ and $a > 0$,

$$\sqrt{a^2 + x} \sim a + \frac{x}{2a} + o(x),$$

and observe that

$$\begin{aligned}\sqrt{b^2 - 4c} &= (R_{T,1} - R_{T,2}) + \frac{\epsilon(\alpha_{12}R_{T,1} - \alpha_{21}R_{T,2})(R_{T,2} - R_{T,1})}{2(R_{T,1} - R_{T,2})} + o(\epsilon), \\ &= (R_{T,1} - R_{T,2}) - \epsilon(\alpha_{12}R_{T,1} - \alpha_{21}R_{T,2}) + o(\epsilon).\end{aligned}$$

So the asymptotic form of $R_{T,c}$ is

$$R_{T,c} = R_{T,1}(1 - \epsilon\alpha_{12}) + o(\epsilon). \tag{2.38}$$

We study the characteristic equation

$$x^2 - c_0 x + c_1 = 0,$$

where

$$x = (\gamma + \mu + \lambda)(\delta + \lambda),$$

the parameters

$$c_0 = (1 - \epsilon\alpha_{12})\gamma_F\rho_1 f'(L_1^*)e^{-\lambda\tau_1} + (1 - \epsilon\alpha_{21})\gamma_F\rho_2 f'(L_2^*)e^{-\lambda\tau_2},$$

and

$$c_1 = \gamma_F\rho_1 f'(L_1^*)e^{-\lambda\tau_1}\gamma_F\rho_2 f'(L_2^*)e^{-\lambda\tau_2}[1 - \epsilon(\alpha_{12} + \alpha_{21})].$$

As in the isolated case, we can rewrite the equation as

$$[x - (1 - \epsilon\alpha_{12})\gamma_F\rho_1 f'(L_1^*)e^{-\lambda\tau_1}][x - (1 - \epsilon\alpha_{21})\gamma_F\rho_2 f'(L_2^*)e^{-\lambda\tau_2}] + o(\epsilon) = 0.$$

Therefore the solutions with respect to x are

$$x_1 = (1 - \epsilon\alpha_{12})\gamma_F\rho_1 f'(L_1^*)e^{-\lambda\tau_1},$$
$$x_2 = (1 - \epsilon\alpha_{21})\gamma_F\rho_2 f'(L_2^*)e^{-\lambda\tau_2}.$$

We want to show that there are no solutions to the characteristic equation with positive real part

$$(\gamma + \mu + \lambda)(\delta + \lambda) = x_i \text{ for } i = 1, 2. \tag{2.39}$$

Suppose by contradiction there exists a root of (2.39) $\lambda = x + iy$ with $x \geq 0$. So the following equality holds for $j = 1, 2$:

$$|(\gamma + \mu + x + iy)(\delta + x + iy)| = |(1 - \epsilon\alpha_{12})\gamma_F\rho_i f'(L_j^*)e^{-(x+iy)\tau_j}|.$$

We also know

$$|(\gamma + \mu + x + iy)(\delta + x + iy)| = |(\gamma + \mu + x + iy)||(\delta + x + iy)|$$

$$
\begin{aligned}
&= \sqrt{(\gamma+\mu+x)^2+y^2}\sqrt{(\delta+x)^2+y^2} \\
&\geq \sqrt{(\gamma+\mu)^2}\sqrt{\delta^2} \\
&= (\gamma+\mu)\delta.
\end{aligned}
$$

Taking the asymptotic solution from (2.16) and using the fact that $f(x) = pxe^{-qx}$, we see that

$$
\begin{aligned}
f'(L_1^*) &= \frac{p}{R_{T,1}}\{1-\ln(R_{T,1})+\epsilon\alpha_{12}[2-\ln(R_{T,1})]\}+o(\epsilon), \\
f'(L_2^*) &= p - 2p\alpha_{12}\epsilon\frac{\ln(R_{T,1})}{1-R_{T,2}}.
\end{aligned}
\tag{2.40}
$$

For $j=1$, the right hand side with $1+\epsilon\alpha_{12} < R_{T,i} < e^2(1+\epsilon\alpha_{12})$ satisfies

$$
\begin{aligned}
|(1-\epsilon\alpha_{12})\gamma_F\rho_1 f'(L_1^*)e^{-(x+iy)\tau_2}| &\leq (1-\epsilon\alpha_{12})\gamma_F\rho_1|f'(L_1^*)|, \\
&= \frac{\gamma_F\rho_1 p}{R_{T,1}}\,|1-\ln(R_{T,i})+\epsilon\alpha_{12}|+o(\epsilon), \\
&< (\gamma+\mu)\delta+o(\epsilon).
\end{aligned}
$$

Note that the condition $1+\epsilon\alpha_{12} < R_{T,i} < e^2(1+\epsilon\alpha_{12})$ is satisfied if $1 < R_{T,c} < e^2$ using (2.38).

A similar conclusion can be inferred for $j=2$ when $R_{T,2} < 1$

$$
\begin{aligned}
|(1-\epsilon\alpha_{21})\gamma_F\rho_2 f'(L_2^*)e^{-(x+iy)\tau_1}| &\leq (1-\epsilon\alpha_{21})\gamma_F\rho_2|f'(L_2^*)|, \\
&\leq (1-\epsilon\alpha_{21})\gamma_F\rho_2 p, \\
&= (1-\epsilon\alpha_{21})R_{T,2}(\gamma+\mu)\delta, \\
&\leq R_{T,2}(\gamma+\mu)\delta, \\
&< (\gamma+\mu)\delta.
\end{aligned}
$$

We thus reach a contradiction, therefore all the roots of the characteristic equation have negative real part and (F_i^*, L_i^*) is locally asymptotically stable for $1 < R_{T,i} < e^2$. □

Proposition 13. *Every non-trivial solution of* (2.13) *converges to the equilibrium* $(F_1^*, F_2^*, L_1^*, L_2^*)$ *in* (2.16) *for all* $(\tau_1, \tau_2) \geq 0$ *if* $1 < R_{T,c} + o(\epsilon) < e$.

Proof. Consider the linearized system of the asymptotic model with $\tau_1 = \tau_2 = 0$:

$$\begin{cases} \bar{F_1}'(t) = \rho_1 f'(L_1^*) L_1(t) - (\gamma + \mu) F_1(t), \\ \bar{F_2}'(t) = \rho_2 f'(L_2^*) L_2(t) - (\gamma + \mu) F_2(t), \\ \bar{L_1}'(t) = (1 - \epsilon\alpha_{12})\gamma_F F_1(t) + \epsilon\alpha_{21}\gamma_F F_2(t) - \delta L_1(t), \\ \bar{L_2}'(t) = \epsilon\alpha_{12}\gamma_F F_1(t) + (1 - \epsilon\alpha_{21})\gamma_F F_2(t) - \delta L_2(t), \end{cases} \tag{2.41}$$

In the proof to Proposition 2, we have shown that Γ defined by (2.2) is a positively invariant set of (2.1) and the ω-limit of the solutions is in Γ. In a similar way, by multiplying both migration terms by ϵ, we find a set Γ_{asy} preserving the same properties for (2.13). Let

$$\Gamma_{asy} := \{(F_1, F_2, L_1, L_2) \in \mathbb{R}_+^4 : F_1 \leq F_1^\infty,\ F_2 \leq F_2^\infty,\ L_1 \leq L_1^\infty,\ L_2 \leq L_2^\infty\}, \tag{2.42}$$

where

$$\begin{aligned} F_1^\infty &= \frac{\rho_1 p}{qe(\gamma + \mu)}, \\ F_2^\infty &= \frac{\rho_2 p}{qe(\gamma + \mu)}, \\ L_1^\infty &= \frac{\gamma_F p}{qe\delta(\gamma + \mu)}[(1 - \epsilon\alpha_{12})\rho_1 + \epsilon\alpha_{21}\rho_2], \\ L_2^\infty &= \frac{\gamma_F p}{qe\delta(\gamma + \mu)}[\rho_1\epsilon\alpha_{12} + \rho_2(1 - \epsilon\alpha_{21})]. \end{aligned}$$

Consider the Jacobian of (2.41)

$$J = \begin{pmatrix} -(\gamma + \mu) - \lambda & 0 & \rho_1 p & 0 \\ 0 & -(\gamma + \mu) - \lambda & 0 & \rho_2 p \\ (1 - \epsilon\alpha_{12})\gamma_F & \epsilon\alpha_{21}\gamma_F & -\delta - \lambda & 0 \\ \epsilon\alpha_{12}\gamma_F & (1 - \epsilon\alpha_{21})\gamma_F & 0 & -\delta - \lambda \end{pmatrix}.$$

We see from (2.40) that for small ϵ, $f'(L_2^*) > 0$. We want to understand how $f'(L_1^*)$ is related to $R_{T,c}$ using (2.16). We study the case in which $f'(L_1^*) > 0$, which corresponds to the case in which $L_1^* < \frac{1}{q}$.

$$\begin{aligned} \ln(R_{T,1}) &< 1 + \alpha_{12}\epsilon, \\ R_{T,1} &< e^{1+\alpha_{12}\epsilon}, \\ R_{T,1} &< e(1 + \alpha_{12}\epsilon) + o(\epsilon). \end{aligned}$$

From (2.38) we see that $f'(L_1^*) > 0 \iff R_{T,c} + o(\epsilon) < e$. So we have that

1. Γ_{asy} is a positively invariant set of (2.41) containing $(F_1^*, F_2^*, L_1^*, L_2^*)$ in (2.16) and the ω-limit of its solutions is contained in Γ_{asy}.

2. (2.41) is a cooperative system (for $\tau_1 = \tau_2 = 0$) since $j_{kl} \geq 0$ for $k \neq l$. This is true since $f'(L_1^*), f'(L_2^*) > 0$ if $1 < R_{T,c} + o(\epsilon) < e$

3. J is irreducible since for every nonempty proper set I of $N = \{1, 2, 3, 4\}$, there is a $k \in I,\ j \in N \setminus I$ such that $j_{kl} \neq 0$ and the digraph is strongly connected.

Therefore, using monotone dynamical theory [76], we deduce that (2.13) does not contain any periodic solution for $1 < R_{T,c} < e$, therefore $(F_1^*, F_2^*, L_1^*, L_2^*)$ is attractive. □

It is possible to extend global attractivity of the coexistence equilibrium also for $e \leq R_{T,c} < e^2$ using exponential ordering [76]. We are also able to study Hopf bifurcations of (2.13).

Proposition 14. *If $R_{T,c} + o(\epsilon) > e^2$, there exists a Hopf bifurcation point at a specific threshold $\tau_1 = \tau_c$. The non-trivial equilibrium $(F_1^*, F_2^*, L_1^*, L_2^*)$ of (2.13) is asymptotically stable for $0 \leq \tau_1 < \tau_c$ and is unstable for $\tau_1 > \tau_c$.*

Proof. Suppose there exists a purely imaginary root $\lambda^* = \pm i\omega$. It needs to satisfy (2.39), therefore we need to solve the following equation

$$(\gamma + \mu + i\omega)(\delta + i\omega) = (1 - \epsilon\alpha_{12})\gamma_F \rho_1 f'(L_1)^* e^{-\lambda\tau_1}.$$

Note that we do not consider the second equation $x - x_2 = 0$ in (2.39) since we have proved that all roots for $R_{T,2} < 1$ have negative real part. We separate the real and imaginary parts of this system and yield

$$\begin{cases} \delta(\gamma+\mu) - \omega^2 = (1-\epsilon\alpha_{12})\rho_1\gamma_F f'(L_1^*)\cos(\omega\tau_1^*), \\ \omega(\delta+\gamma+\mu) \ = -(1-\epsilon\alpha_{12})\rho_1\gamma_F f'(L_1^*)\sin(\omega\tau_1^*). \end{cases} \tag{2.43}$$

The Hopf bifurcation point τ_c is the smallest τ_1 that satisfies (2.43). Summing up the square of first line to the square of the second line yields the value of ω. We have

$$\omega^4 + \omega^2[\delta+\gamma+\mu-2\delta(\gamma+\mu)] + \delta^2(\gamma+\mu)^2 - [(1-\epsilon\alpha_{12})\rho_1\gamma_F f'(L_1^*)]^2 = 0.$$

Let $\zeta = \omega^2$ and search for a positive real solution of ζ in the following equation:

$$\zeta^2 + \zeta[\delta+\gamma+\mu-2\delta(\gamma+\mu)] + \delta^2(\gamma+\mu)^2 - ((1-\epsilon\alpha_{12})\rho_i\gamma_F f'(L_1^*))^2 = 0. \tag{2.44}$$

We want to write $f'(L_1^*)$ in terms of $R_{T,c}$ by using (2.40) and (2.38).

$$f'(L_1^*) = \frac{p(1-\epsilon\alpha_{12})}{R_{T,c}}\left\{1 - \ln\Big(\frac{R_{T,c}}{1-\epsilon\alpha_{12}}\Big) + \epsilon\alpha_{12}\left[2 - \ln\Big(\frac{R_{T,c}}{1-\epsilon\alpha_{12}}\Big)\right]\right\} + o(\epsilon).$$

Since $\epsilon \to 0$, we use Taylor expansion $\ln\Big(\frac{a}{1-\epsilon}\Big) = \ln(a) + \epsilon + o(\epsilon)$ and find that

$$\begin{aligned} f'(L_1^*) &= \frac{p(1-\epsilon\alpha_{12})}{R_{T,c}}\{1 - (\ln(R_{T,c}) + \epsilon\alpha_{12}) + \epsilon\alpha_{12}[2 - (\ln(R_{T,c}) + \epsilon\alpha_{12})]\} + o(\epsilon), \\ &= \frac{p}{R_{T,c}}\{[1 - \ln(R_{T,c})] + \epsilon[\alpha_{12}(1 - \ln(R_{T,c})) - \alpha_{12} + 2\alpha_{12} - \alpha_{12}\ln(R_{T,c})]\} + o(\epsilon), \\ &= \frac{p}{R_{T,c}}[1 - \ln(R_{T,c})] + o(\epsilon). \end{aligned}$$

Using this result and (2.38), (2.44) becomes (by omitting $o(\epsilon)$)

$$\zeta^2 + \zeta[\delta+\gamma+\mu-2\delta(\gamma+\mu)] + \delta^2(\gamma+\mu)^2 - (1-\epsilon\alpha_{12})\frac{\rho_1\gamma_F p}{R_{T,1}(1-\epsilon\alpha_{12})}[1 - \ln(R_{T,c})])^2 = 0.$$

From the definition of $R_{T,1}$, it can be rewritten as

$$\zeta^2 + \zeta[\delta + \gamma + \mu - 2\delta(\gamma + \mu)] + \delta^2(\gamma + \mu)^2 - \delta^2(\gamma + \mu)^2[1 - \ln(R_{T,c})]^2 = 0.$$

Note that if $R_{T,c} > e^2$, there will always be a unique positive solution since

$$\begin{aligned} \Delta_{c2} &= (\delta + \gamma + \mu - 2\delta(\gamma + \mu))^2 - 4[\delta^2(\gamma + \mu)^2][1 - (1 - \ln(R_{T,c}))^2]. \\ &> (\delta + \gamma + \mu - 2\delta(\gamma + \mu))^2 \geq 0. \end{aligned} \tag{2.45}$$

The two real solutions of ζ are similar to the isolated case:

$$\zeta_{1,2} = \frac{1}{2}(2\delta(\gamma + \mu) - (\delta + \gamma + \mu) \pm \sqrt{\Delta_{c2}}),$$

and the only positive solution is

$$\zeta_1 = \frac{1}{2}(2\delta(\gamma + \mu) - (\delta + \gamma + \mu) + \sqrt{\Delta_{c2}}). \tag{2.46}$$

Therefore $\omega = \pm\sqrt{\zeta_1}$. To find τ_c, we divide equation 2 with equation 1 in (2.43) which yields

$$\tan(\omega\tau_c) = \frac{\omega(\delta + \gamma + \mu)}{\omega^2 - \delta(\gamma + \mu)}, \tag{2.47}$$

therefore

$$\tau_c = \omega^{-1} \arctan\left(\frac{\omega(\delta + \gamma + \mu)}{\omega^2 - \delta(\gamma + \mu)}\right).$$

Note that the proof for the transversality condition can be acquired similarly to Proposition 9 and has not been included in this chapter. □

For the general interconnected case (2.1), we observe through simulations that $R_{T,c}$ has a similar behaviour to $R_{T,i}$ and the properties that have been proved by studying the isolated model and asymptotic expansion can be extended to the general model. In particular we observe that:

- $1 < R_{T,c} < e^2$ - the coexistence equilibrium is a global attractor of (2.1).
- $R_{T,c} > e^2$ - the coexistence equilibrium is conditionally asymptotically stable on the choices of the delays.

2.7 Simulations - tick dynamics

Parameter	**Value**
ρ_1	Variable (days^{-1})
ρ_2	Variable (days^{-1})
τ_1	730 (days)
τ_2	1095 (days)
γ	[1/28,1/10] (days^{-1}) [5]
μ	[0.005,0.011] (days^{-1}) [6, 80]
θ	0.81 [15]
α_{12}	Variable
α_{21}	Variable
p	1000 (day^{-1}) [81, 15]
q	6.2 [15]
δ	1 (day^{-1}) [5]

Table 2.2: Table including parameter values and ranges described in other references together with the measurement units.

The parameters considered in the following simulations are deriving from literature and we assume them to be fixed (see Table 2.2). The normal development delay τ_1 is set to 2 years (730 days) while the diapause development delay τ_2 is set to 3 years (1095 days). The development time from feeding adult to egg-laying is between 10 and 28 days [5] so we choose it to be on average two weeks (i.e. $\gamma = 1/14$). The death rate of feeding adults is set to $\mu = 0.005$ [6, 80], the survival probability of ticks from feeding to egg-laying stage is $\theta = 0.81$ [15] and the exit rate δ for feeding adults is set to 1 [5]. The final fixed parameters

are $p = 1000$ and $q = 6.2$ which appear in the Ricker function [81, 15]. We choose this value for the rate p since we consider only the female population and the maximal number of eggs is considered to be 2000 (average time in feeding adult stage is 1 day), so we assume that the male and female tick populations are similar. We use Matlab to provide the simulations using the dde23 algorithm with initial conditions $F_1 = L_1 = 1$ and $F_2 = L_2 = 0.1$ and the biftool package. We have seen numerically that the choice of initial conditions does not have an impact on the plots in the long run.

Since the aim of this paper is to study how environment and movement affect tick dynamics, survival probabilities and migration coefficients between both patches will be the only parameters that vary throughout the experiments. Note that ρ_1 and ρ_2 are always chosen such that patch 1 has a favourable environment for ticks while patch 2 has unfavourable environment for ticks ($R_{T,1} > 1$ and $R_{T,2} < 1$). In addition to that, both the survival probabilities and migration parameters are chosen to satisfy different conditions in each case to show the possible tick population dynamics generated by the model.

2.7.1 Isolated patches

In the absence of host migration, ticks always die out in patch 2, while in patch 1 they converge to a non-trivial equilibrium in the left plot or to a periodic solution in the right plot of Figure 2.4. The difference in these two plots is the choice of the survival probability which is larger in the right plot ($\rho_1 = 0.015$) with respect to the former ($\rho_1 = 0.0065$). We have previously shown that the threshold $R_{T,i} = e^2$ is key to study global dynamics of the model. In the right plot, periodic solutions occur since $R_{T,1} = 11.36 > e^2$ and the 3-year delay is larger than the threshold delay τ_1^* which can be computed using Hopf bifurcation theory to be $\tau_1^* \sim 28$ days in this specific case. In the left plot instead $R_{T,1} < e^2$ which means the coexistence equilibrium is attractive.

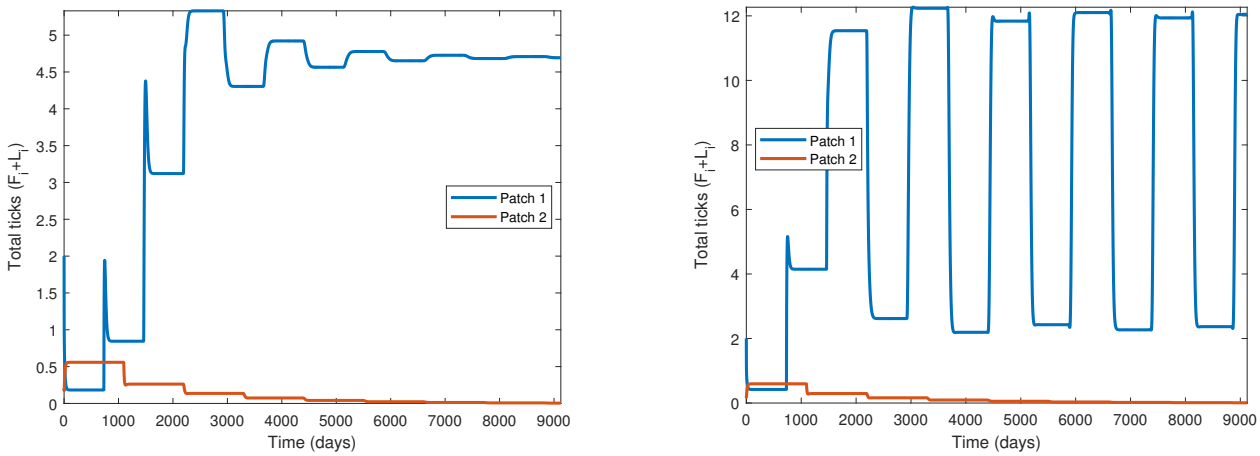

Figure 2.4: **Isolated model** - In both plots patch 2 dies out since $\rho_2 = 0.0008$ which yields $R_{T,2} = 0.57$. The plot on the left represents the non-trivial equilibrium case where $\rho_1 = 0.0065$ and $R_{T,1} = 4.92$, while the plot on the right represents the periodic solution when $\rho_1 = 0.015$ and $R_{T,1} = 11.36$.

2.7.2 Escalating up

The escalating up case ($\alpha_{12} = 0$) is similar to the isolated case since patch two always dies out while patch 1 either reaches a coexistence equilibrium in the left plot or converges to a periodic solution in the right plot of Figure 2.5. Note that most of the parameters in the left (resp. right) plot for patch 1 of Figure 2.5 are identical to the left (resp. right) plot of Figure 2.4. The only differences are a larger ρ_2 in the left plot of Figure 2.5 with respect to its correspondent plot in Figure 2.4 and the possibility of ticks to move from the unfavourable to the favourable patch. Since we have shown that $R_{T,eu} = R_{T,1}$, the global dynamics is not heavily impacted by the addition of uni-lateral host migration.

2.7.3 Cascading down

The cascading down model ($\alpha_{21} = 0$) presents three possible dynamics which depend on the value of $R_{T,cd} = \max(R_{T,1}(1 - \alpha_{12}), R_{T,2})$, as we have shown in Section 2.4.4. The first case leads to extinction as it is shown in the left plot of Figure 2.6 where $R_{T,cd} = 0.75 < 1$. The second case leads to convergence to a coexistence equilibrium in the central plot of Figure 2.6 where $1 < R_{T,cd} = 3.41 < e^2$. The third case leads to convergence to a periodic solution as in

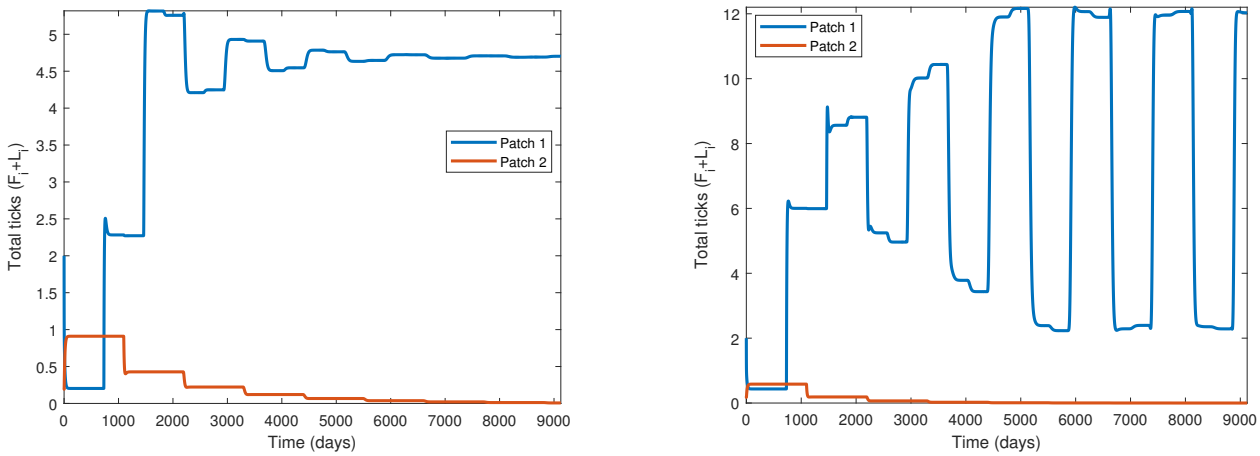

Figure 2.5: **Escalating up model** - In both plots patch 2 dies out since $\rho_2 = 0.00125$ in the left plot and $\rho_2 = 0.0008$ in the right plot which yields in the left plot $R_{T,2} = 0.95 < 1$ and in the right plot $R_{T,2} = 0.61 < 1$. The host migration probability from patch 2 to patch 1 is 40% in both plots. The plot on the left represents the non-trivial equilibrium case where $\rho_1 = 0.0065$ and $R_{T,1} = 4.92$, while the plot on the right represents the periodic solution when $\rho_1 = 0.015$ and $R_{T,1} = 11.36$.

the right plot of Figure 2.6 we have a large delay and $R_{T,cd} = 8.18 > e^2$ for large delays.

2.7.4 Interconnected patches

The interconnected case dynamics is similar to the cascading down model since the ticks would either persist in both patches or die out. Though we have not shown full stability of this model, we observe similar behaviours as in the other cases. In particular, the threshold $R_{T,c}$ is key to determine the global stability of the model and can be computed using its definition. In the left plot of Figure 2.7, $R_{T,c} = 0.74 < 1$ guarantees tick extinction; in the central plot of Figure 2.7, dynamics lead to a coexistence equilibrium since $1 < R_{T,c} = 4.57 < e^2$ while in the right plot of Figure 2.7, tick dynamics converges to a periodic solution for $R_{T,c} = 8.02 > e^2$ and delay larger than a specific threshold.

We also included bifurcation diagrams to show how the survival probability ρ_1, the migration rate α_{12} and the delay τ_1 affect tick dynamics. In Figure 2.8, we see the effect of survival probability in patch 1 with respect to the model dynamics. In the left, we see how it affects the tick reproduction number $R_{T,c}$ and we see that for this parameter choice

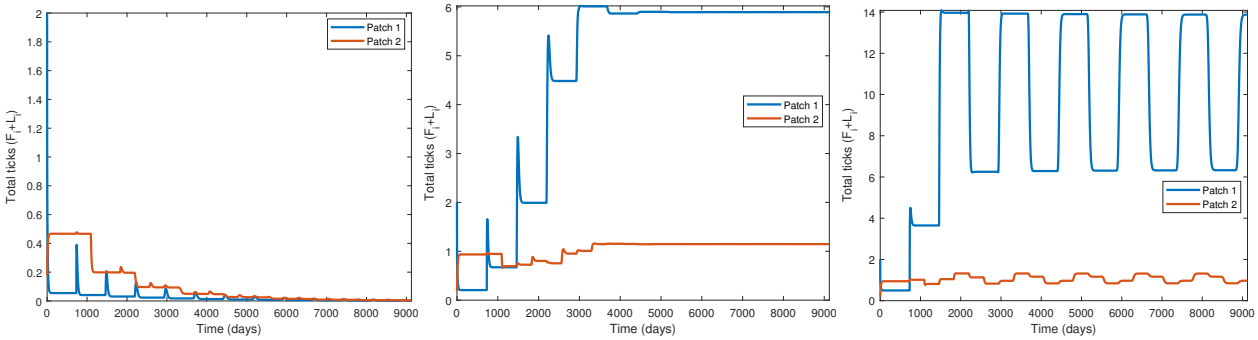

Figure 2.6: **Cascading down model** - In the left plot ticks die out ($\rho_1 = 0.002$, $\rho_2 = 0.000625$, $R_{T,1} = 1.51$, $R_{T,2} = 0.47$, $\alpha_{12} = 0.5$), in the central plot a coexistence equilibrium is reached ($\rho_1 = 0.0075$, $\rho_2 = 0.00125$, $R_{T,1} = 5.68$, $R_{T,2} = 0.95$, $\alpha_{12} = 0.4$), while in the right plot convergence to a periodic solution occurs ($\rho_1 = 0.018$, $\rho_2 = 0.00125$, $R_{T,1} = 13.63$, $R_{T,2} = 0.95$, $\alpha_{12} = 0.4$).

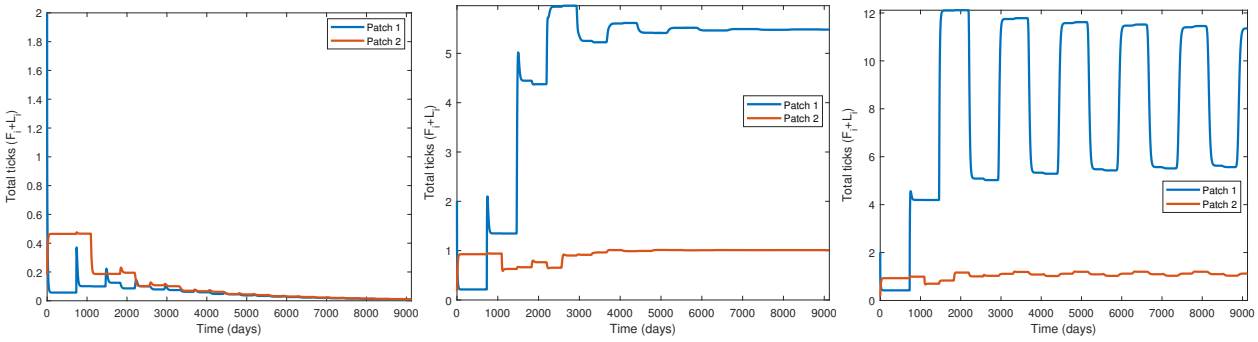

Figure 2.7: **Interconnected model** - In the left plot ticks die out ($\rho_1 = 0.002$, $\rho_2 = 0.000625$, $R_{T,1} = 1.51$, $R_{T,2} = 0.47$, $\alpha_{12} = 0.6$, $\alpha_{21} = 0.1$), in the central plot a coexistence equilibrium is reached ($\rho_1 = 0.0075$, $\rho_2 = 0.00125$, $R_{T,1} = 5.68$, $R_{T,2} = 0.95$, $\alpha_{12} = 0.2$, $\alpha_{21} = 0.1$), while in the right plot there is convergence to a periodic solution ($\rho_1 = 0.015$, $\rho_2 = 0.00125$, $R_{T,1} = 11.36$, $R_{T,2} = 0.95$, $\alpha_{12} = 0.3$, $\alpha_{21} = 0.15$).

there seems to be an approximately linear relationship. In the right plot, we see how this affects the model dynamics through a bifurcation diagram. Note that decreasing the survival probability below 0.0014 would lead to tick extinction. In Figure 2.9, we see the effect of host migration from favourable to unfavourable environment impacts the model dynamics. In particular, increasing the mobility parameter α_{12} would lead to a decrease in $R_{T,c}$ and it still seems to follow an approximately linear relationship but with a negative correlation as shown in the left plot. As migration grows, the dynamics of the model might change possibly from convergence to a periodic solution to convergence to an attractive coexistence

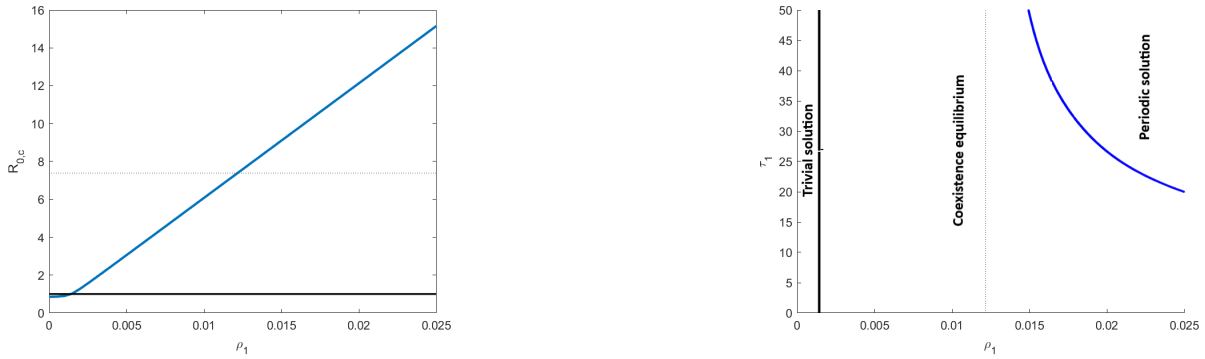

Figure 2.8: Effect of survival probability ρ_1 on the tick reproduction number and bifurcation diagram including ρ_1 and τ_1 as bifurcation parameters. The parameters (excluding ρ_1 and τ_1) are chosen as in the central plot of Figure 2.7. In the left plot, it is shown how the tick reproduction number $R_{T,c}$ is affected by the survival probability ρ_1. In the right plot, the solution behaviour for different choices of ρ_1 and τ_1 (bifurcation parameters) is analysed. The solid blue line is the Hopf bifurcation curve and separates the convergence to an equilibrium (on the left) and the convergence to a periodic solution (on the right). The dotted black line represents the threshold $R_{T,c} = e$ under which there is always a convergence to an equilibrium for every delay τ_1. The solid black line indicates the value of ρ_1 for which $R_{T,c} = 1$ and separates convergence to the trivial equilibrium (on the left) and convergence to a non-trivial solution (on the right).

equilibrium, depending also on the value of τ_1 as shown in the right plot. We also observe that τ_2 does not significantly impact tick dynamics since survival of ticks mainly depends on the dynamics in patch 1.

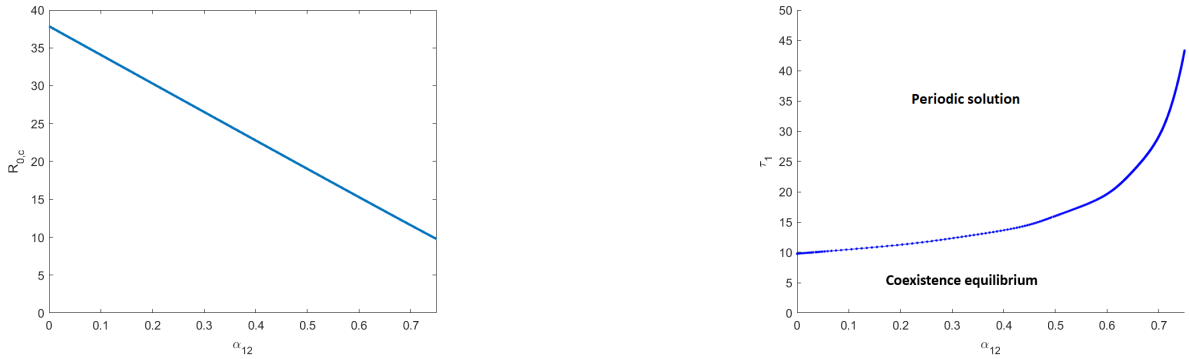

Figure 2.9: Effect of mobility parameter α_{12} on the tick reproduction number and bifurcation diagram including α_{12} and τ_1 as bifurcation parameters. The parameters (excluding α_{12} and τ_1) are chosen as in the central plot of Figure 2.7. In the left plot, it is shown how the tick reproduction number $R_{T,c}$ is affected by the mobility parameter α_{12}. In the right plot, the solution behaviour for different choices of α_{12} and τ_1 (bifurcation parameters) is analysed. The solid blue line is the Hopf bifurcation curve and separates the convergence to a coexistence equilibrium and the convergence to a periodic solution.

2.8 Final considerations for the patchy model

We have introduced a spatial DDE model for tick demographics in a two-patch environment and shown how changes in environment favourability and tick movement on large mammals could affect the dynamics. Depending on the key parameter $R_{T,c}$, we have shown three possible long-term behaviours of tick population including extinction, convergence to a coexistent solution and convergence to a periodic solution.

It is important to note that tick control intervention plays a key role in some of the parameters of the model. Firstly, patch-specific survival probabilities and development delays can be heavily influenced by habitat modification strategies including controlled burns. Secondly, the mobility of mammal hosts between patches can be modified by strategies such as deer fencing which would restrict the tick movement. The plots in Figures 2.8 and 2.9 show how the effect of these parameter change can change the dynamics of the model.

Regarding the specific model studied, there are also several topics that need further analysis. For example, the global stability of the coexistence equilibrium has not been resolved, though we suspect this is true and our numerical simulations also support this

conjecture, in the case in which $e < R_{T,c} < e^2$. We suggest the idea that exponential ordering [76] coupled with the monotone dynamical systems theory can be used to establish the global convergence. We have not done much stability analysis for the bifurcated periodic solutions for (2.13), and the global continuation of these local Hopf branches also deserves additional attention [67]. Finally, in the real world setting, the environmental conditions are subject to seasonal temperature variations so we could analyse a more realistic model considering these by making the model non-autonomous, maybe starting with the time-periodic case [82].

Chapter 3

Multi-cycle periodic solutions of a differential equation with periodically switching delays

We describe the behaviour of solutions of a scalar Delay Differential Equation (DDE) with delay that periodically switches between two constant values. Such an equation arises naturally from structured vector populations involved in a range of vector-borne diseases spreading in a periodically varying environment. We examine if and how the two different time lags and the switching time influence the existence and patterns of periodic solutions. We pay particular attention to the patterns involving multi-cycles within the prime period of the periodic solutions.

3.1 Introduction of the switching delay model

Our focus here is to study the effect of diapause and periodicity in tick population dynamics. In this case, we work with a scalar delay differential equation with periodically switching delays. Such an equation arises naturally from structured vector populations involved in a range of vector-borne diseases spreading in a periodically varying environment. In particular,

we consider two fixed delays which represent either a normal or a diapause development delay. The diapause is a hormone controlled state which occurs in certain ticks where ticks are not actively developing therefore it would lead to a longer development time for ticks as described in the introduction. The work is inspired by the paper by Zhang and Wu [62] where a similar model for tick dynamics was proposed and examined with two fixed time lags involved, which indicated respectively as in this model, the normal and the diapause development delay. The main difference is that in [62] there is the assumption that just a fixed portion of population would undergo diapause. In this paper instead, we consider that this depends periodically on the birth time for ticks. This means that ticks born in a certain period of the year would all undergo diapause while others would not. Our focus here is to see if this format of simplified model can generate complicated patterns of oscillations in the tick population.

In this chapter, we first introduce the initial model. We then normalize it at the equilibrium and study the behaviour of the solutions. We consider how crossing times (times when solution intersect the x-axis) affect the final outcome of the solutions and generate different oscillatory behaviours according to specific parameter choices. We then analyse the conditions related to the existence of multi-cycle periodic solutions (where m-cycle indicates that in one period there are 2*m crossing times) and describe simulations showing some examples of these.

3.2 Model overview

We consider the following scalar differential equation

$$a'(t) = -da(t) + \rho b(a(t - \tau(t))), \tag{3.1}$$

where $a(t)$ represents the female adult tick population, d is the death rate, ρ is the survival probability for a tick from the egg to the adult stage and b is the birth rate. The delay derives from the fact that we are considering only adult ticks so the new feeding adults are the eggs that survive the development time $\tau(t)$ which we will consider to be switching between two different values.

We see that the nontrivial equilibrium satisfies

$$da^* = \rho b(a^*), \tag{3.2}$$

so we normalize the system by considering $a(t) = a^* + x(t)$. In terms of $x(t)$, (3.1) becomes

$$x'(t) = -da^* - dx(t) + \rho b(a^* + x(t - \tau(t))). \tag{3.3}$$

Let

$$f(x(t)) = \rho b(a^* + x(t)) + \rho b(a^*),$$

then we can rewrite (3.3) using (3.2), and this yields

$$x'(t) = -dx(t) + f(x(t - \tau(t))). \tag{3.4}$$

f naturally is a decreasing function since we consider the birth-rate b to be density-dependent. In our simplified case, we suppose it is the piecewise function

$$f(x) = -\text{sgn}(x) = \begin{cases} 1, & \text{if } x < 0 \\ 0, & \text{if } x = 0 \\ -1, & \text{if } x > 0. \end{cases}$$

We also consider a temporally varying delay that periodically switches between two values τ_1 and τ_2 which is described by

$$\tau(t) = \begin{cases} \tau_2, & \text{if mod(t,T)} \geq \gamma \\ \tau_1 = \beta\tau_2, & \text{if mod(t,T)} < \gamma. \end{cases} \tag{3.5}$$

Here d, τ_2, $\beta > 0$; $T > \gamma > 0$ are given constants. We denote by $\tau_{\max} := \max(\beta\tau_2, \tau_2)$ and

$\tau_{\min} := \min(\beta\tau_2, \tau_2)$. We consider model (3.4) subject to the initial condition

$$\begin{cases} x(t) > 0,\ t \in [-\tau_{\max}, 0] \\ x(0) = k_0 \geq 0. \end{cases} \tag{3.6}$$

Due to the nonlinearity of f, this initial value problem (IVP) (3.4) and (3.6) can be solved iteratively by connecting solutions of the linear ordinary differential equations (ODEs)

$$y^{-'}(t) = -dy^{-}(t) - 1,$$

and

$$y^{+'}(t) = -dy^{+}(t) + 1,$$

along the time sequences when the solution of the ODEs changes their signs.

For the sake of reference, the general IVP

$$\begin{cases} y'(t) = -dy(t) + c \\ y(t_0) = y_0, \end{cases}$$

admits the unique solution

$$y(t) = e^{-d(t-t_0)}\left(y_0 - \frac{c}{d}\right) + \frac{c}{d}.$$

Note also that the solution of (3.4) satisfies

$$-dx(t) - 1 \leq x'(t) \leq -dx(t) + 1.$$

Note that

- If $x(t^*) > \frac{1}{d}$, then $x'(t) < 0$;
- If $x(t^*) < -\frac{1}{d}$, then $x'(t) > 0$.

This guarantees that the solution of (3.4) is bounded ($\limsup_{t\to\infty} |x(t)| \leq 1/d$). In addition, we see that it is also unique since it is calculated connecting solutions of linear ODEs (which are unique).

We also note that due to the symmetry of f, if we let $x^{\pm}(t)$ be the solutions for (3.4) with the initial conditions

$$\begin{cases} x^{+}(t) > 0, & \forall t \in [-\tau_{\max}, 0) \\ x(0) = k, \end{cases}$$

and

$$\begin{cases} x^{-}(t) < 0, & \forall t \in [-\tau_{\max}, 0) \\ x(0) = -k, \end{cases}$$

then $x^{+}(t) = -x^{-}(t)$ for $t \geq 0$.

Note the nature of the negative feedback:

$$x(t-s) > 0,\ \forall s \in (0, \tau_{\max}] \Longrightarrow x'(t) < 0,$$

$$x(t-s) < 0,\ \forall s \in (0, \tau_{\max}] \Longrightarrow x'(t) > 0.$$

This means that the solution will start decreasing at $t = 0$ at least until it reaches the x-axis faster than the line $y = -x$ as shown below:

$$x(t) > 0,\ x(t-\tau(t)) > 0 \Longrightarrow x'(t) < f(x(t-\tau(t))) = -1,$$

$$x(t) < 0,\ x(t-\tau(t)) < 0 \Longrightarrow x'(t) > f(x(t-\tau(t))) = 1.$$

These properties, together with non-zero initial conditions, guarantee that the solution $x(t)$ of (3.4) will oscillate around the only normalized equilibrium $x = 0$ of the model.

3.3 Behaviours of solutions

We start by introducing relevant notations to be used in this chapter. For a given solution $x(t)$ of (3.4), we consider the set S containing the non-negative times when the solution crosses the x-axis:

$$S := \{t \geq 0 \mid x(t) = 0\},$$

We introduce the following notations:

(i) t_i^* represents the i-th ordered element of S (i.e. the i-th time in which the solution intersects the t-axis).

(ii) $\hat{t_i}$: for a given t_i^* so that $x(t_i^*) = 0$, the IVP of ODE

$$\begin{cases} x'(t) = -dx(t) \mp 1 \\ x(t_i^*) = 0, \end{cases} \tag{3.7}$$

has the solution $x(t) = \frac{1}{d}(\pm e^{-d(t-t_i^*)} \mp 1)$. We define $\hat{t_i} \in (t_i^*, t_{i+1}^*)$, when it exists, such that the IVP

$$\begin{cases} x'(t) = -dx(t) \pm 1 \\ x(\hat{t_i}) = \frac{1}{d}(\pm e^{-d(\hat{t_i}-t_i^*)} \mp 1), \end{cases} \tag{3.8}$$

satisfies $x(t_{i+1}^*) = 0$. We see that for i odd, the signs of the two equations would be respectively - in (3.7) and + in (3.8) while they would be reversed for even i. In the special case of a single monotonicity change in the solution $x(t)$ to ODE (3.4) in (t_i^*, t_{i+1}^*), $\hat{t_i}$ is the time corresponding to the local maximum or minimum.

(iii) $\mathring{t_i} := \hat{t_i} - t_i^*$.

(iv) the cycle and cycle length: we call the restriction of $x(t)$ on $[t_{2i-1}^*, t_{2i+1}^*]$ the i-th cycle, the length of the i-th cycle is denoted by $T_i := t_{2i+1}^* - t_{2i-1}^*$.

In order to study how the solution $x(t)$ to (3.4) starts oscillating around $x = 0$, we search

for the possible values of t_i^* and $\mathring{t}_i$ in a simplified case in which the parameters satisfy these three conditions:

(C1) $\beta < 1$;

(C2) $(1-\beta)\tau_2 < \min(\gamma, T-\gamma)$;

(C3) $\beta > \frac{\left[\ln\left(1+e^{d\tau_2}\right)-\ln(2)\right]}{d\tau_2}$.

(C1) implies $\tau_{\min} = \beta\tau_2$ and $\tau_{\max} = \tau_2$. (C2) is necessary to avoid multiple switchings of delay in $[t_i^* + \beta\tau_2, t_i^* + \tau_2]$ and (C3) is used to guarantee that $t_i^* + \tau_2 < t_{i+1}^*$. Note that (C1) and (C2) are satisfied in case $\tau_{\max} - \tau_{\min} < \min(\gamma, T-\gamma)$ and (C3) is satisfied if $d\tau_{\max} = d\tau_2$ is sufficiently large. These conditions can be equivalently rewritten in terms of τ_1 and τ_2 since $\beta = \tau_1/\tau_2$ as:

(C1*) $\tau_1 < \tau_2$;

(C2*) $\tau_1 > \tau_2 - \min(\gamma, T-\gamma)$;

(C3*) $\tau_1 > \frac{1}{d}[\ln\left(1+e^{d\tau_2}\right) - \ln(2)]$.

In Figure 3.1, we show the region where the delays chosen satisfy the three conditions we would like to analyse according to the specific chosen parameters. In general, we expect the two delays not to differ substantially.

We have shown that the value of function f determines the monotonicity of the solution $x(t)$ of (3.4). In this case, the positive initial conditions of (3.6) guarantee that $f(x(t-\tau(t)))$ would be negative and solution will be decreasing in $[0, \tilde{t_1}]$ with

$$\tilde{t_1} = \min\{t : f(x(t-\tau(t))) \geq 0\},$$

which is equivalent to asking

$$\tilde{t_1} = \min\{t : x(t-\tau(t)) \leq 0\}.$$

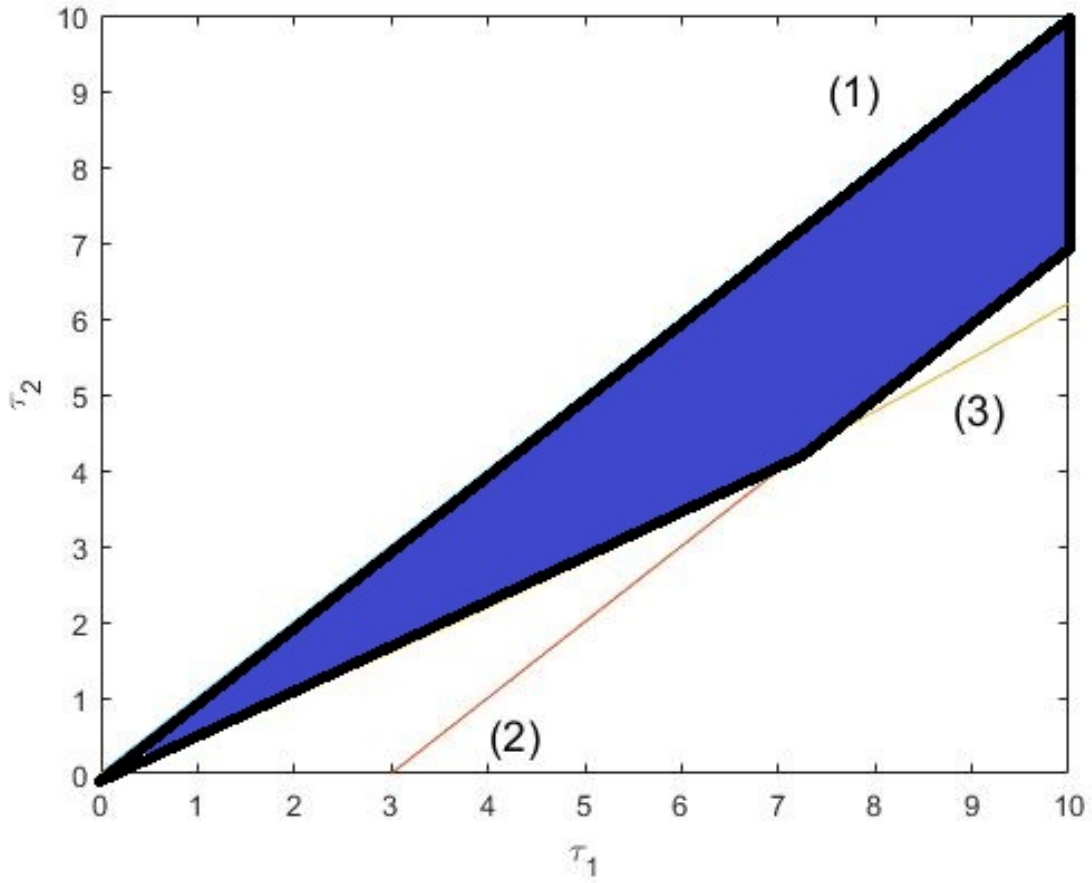

Figure 3.1: This figure shows a $\tau_1 - \tau_2$ plot where the blue section represents the choices of τ_1 and τ_2 that satisfy (C1)-(C3), where (1) is the line $\tau_2 = \tau_1$ of (C1), (2) represents the line $\tau_1 = \tau_2 - \min(\gamma, T-\gamma)$ of (C2) and (3) is the solution of $\tau_1 = \frac{1}{d}[\ln\left(1+e^{d\tau_2}\right) - \ln(2)]$ of (C3). The parameter values are chosen to be constant: $\beta = 0.6$, $\gamma = 3$, $d = 0.1$, $T = 8.6295$.

Therefore $\tilde{t_1} \in [t_1^* + \beta\tau_2, t_1^* + \tau_2]$. Adopting the method of steps, we note that solving (3.4) in $[0, \tilde{t_1}]$ is equivalent to solving the following IVP of the ODE

$$\begin{cases} x'(t) = -dx(t) - 1 \\ x(0) = k_0. \end{cases} \tag{3.9}$$

We know that the unique solution of (3.9) is given by

$$y^{-}(t) = e^{-dt}\left(k_0 + \frac{1}{d}\right) - \frac{1}{d}. \tag{3.10}$$

It is possible to extract the value of t_1^* by considering $y^{-}(t_1^*) = 0$ in equation (3.10). Therefore,

$$t_1^* = \frac{1}{d}\ln(k_0 d + 1).$$

We note that t_1^* is independent from the parameters T, τ_2, α, β and consider $t_1^* = 0$ whenever $k_0 = 0$.

At this point, we would like to analyse $\hat{t_1} \in [t_1^*, t_2^*]$. We know the solution continues decreasing after t_1^* and from the definition of t_i^* and the fact that the solution is continuous, we know that

$$x(t) < 0, \quad t \in [t_1^*, t_2^*],$$

and $x(\hat{t_1}) < 0$.

Lemma 15. *If $(1-\beta)\tau_2 < \min(\gamma, T-\gamma)$, then for every i we have that $\tau(t)$ defined in (3.5) cannot change value more than once in $[t_i^* + \beta\tau_2, t_i^* + \tau_2]$.*

Proof. We prove this by way of contradiction. Suppose that $\tau(t)$ changes value at least twice in $[t_i^* + \beta\tau_2, t_i^* + \tau_2]$ and we want to reach a contradiction by using (C2). The length of the interval aforementioned is $t_1 = (1-\beta)\tau_2$. We know from (3.5) that $\tau(t)$ changes value periodically and alternately after γ and $T-\gamma$. This means that both time intervals above have to be smaller than or equal to t_1. In other words,

$$\min(\gamma, T-\gamma) \leq (1-\beta)\tau_2.$$

This completes the proof since it contradicts with the hypothesis. □

Lemma 16. *If $\beta > \frac{\left[\ln\left(1+e^{d\tau_2}\right)-\ln(2)\right]}{d\tau_2}$, then for every i we have $t_i^* + \tau_2 < t_{i+1}^*$.*

Proof. We prove this statement by induction. We start by proving the base step and showing that it is true for $i = 1$. The basic idea is to consider the case in which solution changes monotonicity at the earliest moment possible $\hat{t_1} = t_1^* + \beta\tau_2$ and impose the condition $x(t_1^* + \tau_2) < 0$. Using the method of steps, we consider the IVP of ODE (3.9) in $[t_1^*, t_1^* + \beta\tau_2]$ and we compute $x(t_1^* + \beta\tau_2)$ by substituting $\hat{t_1} = t_1^* + \beta\tau_2$, which yields

$$x(t_1^* + \beta\tau_2) = \frac{1}{d}(e^{-d\beta\tau_2} - 1).$$

Then we compute the solution to (3.8) to obtain

$$x(t) = \frac{1}{d}\left[e^{-d(t-(t_1^*+\beta\tau_2))}\left(e^{-d\beta\tau_2} - 2\right) + 1\right].$$

Imposing $x(t_1^* + \tau_2) < 0$, we have

$$x(t_1^* + \tau_2) = \frac{1}{d}\left[e^{-d(1-\beta)\tau_2}\left(e^{-d\beta\tau_2} - 2\right) + 1\right] < 0.$$

By solving the inequality, we have

$$\beta > \frac{\left[\ln\left(1 + e^{d\tau_2}\right) - \ln(2)\right]}{d\tau_2},$$

which is exactly what we need in order for $t_1^* + \tau_2 < t_2^*$.

Now let $t_i^* + \tau_2 < t_{i+1}^*$ be true for $i \in \mathbb{N}$. We aim to prove it holds also for $i+1$ or in other words that

$$t_{i+1}^* + \tau_2 < t_{i+2}^*. \tag{3.11}$$

Since $t_i^* + \tau_2 < t_{i+1}^*$ holds, $x(t)$ has the same monotonicity for t in $[t_{i+1}^*, t_{i+1}^* + \beta\tau_2)$. This leads to two possible cases:

Case 1 - $x(t)$ is decreasing in the aforementioned interval, therefore

$$x(s) < 0, \quad \forall s \in [t^*_{i+1}, t^*_{i+1} + \beta\tau_2).$$

Case 2 - $x(t)$ is increasing in the aforementioned interval, therefore

$$x(s) > 0, \quad \forall s \in [t^*_{i+1}, t^*_{i+1} + \beta\tau_2).$$

We consider the case in which the solution changes monotonicity at the earliest moment possible $t = t^*_i + \beta\tau_2$.

Case 1 : (3.11) holds if $x(t^*_i + \tau_2) < 0$, when the solution increases in $[t^*_i + \beta\tau_2, t^*_i + \tau_2]$. This is analogous as the case for $i = 1$. Therefore

$$x(t^*_i + \tau_2) = \frac{1}{d}\left[e^{-d(1-\beta)\tau_2}\left(e^{-d\beta\tau_2} - 2\right) + 1\right] < 0.$$

Case 2 : (3.11) holds if $x(t^*_i + \tau_2) > 0$, when solution decreases in $[t^*_i + \beta\tau_2, t^*_i + \tau_2]$.
Let $y(t) = -x(t)$ and note that conditions on $y(t)$ are equivalent as in the case above. □

Note that Lemma 16 guarantees that for all $t \in (0, \tau_2]$

$$x(t^*_i - t) \begin{cases} > 0 & \text{if } i \text{ is odd,} \\ < 0 & \text{if } i \text{ is even.} \end{cases} \tag{3.12}$$

This is a really important property since it guarantees that the changes of monotonicity can be confined to the interval $[t^*_i + \beta\tau_2, t^*_i + \tau_2]$ and

$$\hat{t}_i \in [t^*_i + \beta\tau_2, t^*_i + \tau_2].$$

Now we start computing $\mathring{t}_i$ for (3.4) with parameters satisfying (C1), (C2) and (C3). Using (3.12) and the symmetry of the system we can consider, without loss of generality, i to be odd which yields:

$$x(t) < 0, \quad t \in (t_i^*, t_{i+1}^*).$$

Lemma 16 guarantees that the solution $x(t)$ of (3.4), and therefore $\mathring{t}_i$, depend on the value of $\tau(t)$ for $t \in [t_i^* + \beta\tau_2, t_i^* + \tau_2]$. In addition, Lemma 15 shows that $\tau(t)$ can change value maximum once in the aforementioned interval.

This leads to four possible different scenarios which can be separated according to the value of $\tau(t_i^* + \beta\tau_2)$:

(S1) $\tau(t_i^* + \beta\tau_2) = \tau_2$ (i.e. $\mathrm{mod}(t_i^* + \beta\tau_2, T) \geq \gamma$).

(S1a) $\tau(t_i^* + t) = \tau_2, \quad \forall t \in [\beta\tau_2, \tau_2]$.

(S1b) $\exists \breve{t}_i \in (\beta\tau_2, \tau_2)$ such that
$\tau(t_i^* + t) = \tau_2, \quad \forall t \in [\beta\tau_2, \breve{t}_i)$,
$\tau(t_i^* + t) = \beta\tau_2, \quad \forall t \in (\breve{t}_i, \tau_2]$.

(S2) $\tau(t_i^* + \beta\tau_2) = \beta\tau_2$ (i.e. $\mathrm{mod}(t_i^* + \beta\tau_2, T) < \gamma$).

(S2a) $\tau(t_i^* + t) = \beta\tau_2, \quad \forall t \in [\beta\tau_2, \tau_2]$.

(S2b) $\exists \breve{t}_i \in (\beta\tau_2, \tau_2)$ such that
$\tau(t_i^* + t) = \beta\tau_2, \quad \forall t \in [\beta\tau_2, \breve{t}_i)$,
$\tau(t_i^* + t) = \tau_2, \quad \forall t \in (\breve{t}_i, \tau_2]$.

We study the monotonicity of $x(t)$ for $t \in [t_i^* + \beta\tau_2, t_i^* + \tau_2]$ which depends on the sign of $f(x(t-\tau(t))) = -\text{sgn}(x(t-\tau(t)))$.

In case (S1a),

$$x(t-\tau_2) > 0, \quad \forall t \in [t_i^* + \beta\tau_2, t_i^* + \tau_2),$$

$x(t)$ is thus decreasing in $[t_i^*, t_i^* + \tau_2)$ and then increasing in $(t_i^* + \tau_2, t_{i+1}^*]$. There is a unique change of monotonicity so $\hat{t}_i = t_i^* + \tau_2$ and $\mathring{t}_i = \tau_2$.

In case (S1b), $x(t)$ decreases in $[t_i^* + \beta\tau_2, t_i^* + \breve{t}_i]$ and in the delay changing point, it starts increasing since

$$x(t-\beta\tau_2) < 0, \quad \forall t \in [t_i^* + \breve{t}_i, t_i^* + \tau_2).$$

Moreover $\mathring{t}_i = \breve{t}_i$, since it is the time when the unique monotonicity change occurs and $\hat{t}_i = t_i^* + \breve{t}_i = cT$ for some natural number c.

In case (S2a),

$$x(t-\beta\tau_2) < 0, \quad \forall t \in [t_i^* + \beta\tau_2, t_i^* + \tau_2).$$

$x(t)$ is thus increasing in $[t_i^* + \beta\tau_2, t_{i+1}^*)$. The change of monotonicity occurs in $\hat{t}_i = t_i^* + \beta\tau_2$ and $\mathring{t}_i = \beta\tau_2$.

In these three cases, we use the method of steps and consider the IVP of the ODE (3.7) in $[t_i^*, t_i^* + \mathring{t}_i]$. Here we substitute $\hat{t}_i = t_i^* + \mathring{t}_i$ to yield:

$$x(\hat{t}_i) = \frac{1}{d}(e^{-d\mathring{t}_i} - 1).$$

In case (S2b), there is a triple change of monotonicity since

$$\begin{aligned} x(t-\beta\tau_2) < 0, &\quad \forall t \in [t_i^* + \beta\tau_2, t_i^* + \breve{t}_i), \\ x(t-\tau_2) > 0, &\quad \forall t \in [t_i^* + \breve{t}_i, t_i^* + \tau_2), \\ x(t-\tau(t)) < 0, &\quad \forall t \in [t_i^* + \tau_2, t_{i+1}^*). \end{aligned}$$

As in case (S2a), considering an odd i, the first monotonicity change of $x(t)$ occurs at $t = t_i^* + \beta\tau_2$ where the solution increases until it reaches $t_i^* + \breve{t}_i$. At this point, $\tau(t_i^* + \breve{t}_i) = \tau_2$

and this change in delay forces the solution to decrease again until time $t_i^* + \tau_2$ and then finally increases in $[t_i^* + \tau_2, t_{i+1}^*]$.

We aim to calculate $\hat{t_i}$ in this scenario. The first step consists of calculating t_{i+1}^*. We note that, similarly as in case (S2a), we have $x(t_i^* + \beta\tau_2) = \frac{1}{d}\left(e^{-d\beta\tau_2} - 1\right)$. Then we consider the IVP below in $[t_i^* + \beta\tau_2, t_i^* + \breve{t_i}]$:

$$\begin{cases} x'(t) = -dx(t) + 1 \\ x(t_i^* + \beta\tau_2) = \frac{1}{d}\left(e^{-d\beta\tau_2} - 1\right), \end{cases}$$

which yields the solution

$$x(t) = \frac{1}{d}\left[e^{-d(t-(t_i^*+\beta\tau_2))}\left(e^{-d\beta\tau_2} - 2\right) + 1\right].$$

So

$$x(t_i^* + \breve{t_i}) = \frac{1}{d}\left[e^{-d(\breve{t_i}-\beta\tau_2)}\left(e^{-d\beta\tau_2} - 2\right) + 1\right].$$

Now consider the following system in $[t_i^* + \breve{t_i}, t_i^* + \tau_2]$:

$$\begin{cases} x'(t) = -dx(t) - 1, \\ x(t_i^* + \breve{t_i}) = \frac{1}{d}\left[e^{-d(\breve{t_i}-\beta\tau_2)}\left(e^{-d\beta\tau_2} - 2\right) + 1\right]. \end{cases}$$

Its solution is given by

$$x(t) = \frac{1}{d}\left[e^{-d(t-(t_i^*+\breve{t_i}))}\left[e^{-d(\breve{t_i}-\beta\tau_2))}\left(e^{-d\beta\tau_2} - 2\right) + 2\right] - 1\right],$$

and

$$x(t_i^* + \tau_2) = \frac{1}{d}\left(e^{-d\tau_2} - 1 - 2e^{-d(1-\beta)\tau_2} + 2e^{-d(\tau_2-\breve{t_i})}\right).$$

Finally, we consider the increasing system in $[t_i^* + \tau_2, t_{i+1}^*]$:

$$\begin{cases} x'(t) = -dx(t) + 1, \\ x(t_i^* + \tau_2) = \frac{1}{d}\left(e^{-d\tau_2} - 1 - 2e^{-d(1-\beta)\tau_2} + 2e^{-d(\tau_2 - \breve{t}_i)}\right), \end{cases}$$

with its solution given by

$$x(t) = \frac{1}{d}\left[e^{-d(t-(t_i^*+\tau_2))}\left(e^{-d\tau_2} - 2 - 2e^{-d(1-\beta)\tau_2} + 2e^{-d(\tau_2-\breve{t}_1)}\right) + 1\right].$$

By imposing $x(t_{i+1}^*) = 0$ in the above equation, we get

$$t_{i+1}^* = t_i^* + \tau_2 + \frac{1}{d}\ln\left(-e^{-d\tau_2} + 2 + 2e^{-d(1-\beta)\tau_2} - 2e^{-d(\tau_2-\breve{t}_i)}\right).$$

At this point, we solve for $\hat{t}_i$ by considering the increasing system for t in $[\hat{t}_i, t_{i+1}^*]$ described in (3.8). The solution of

$$\begin{cases} x'(t) = -dx(t) + 1 \\ x(t_1^* + \mathring{t}_i) = \frac{1}{d}\left(e^{-d\mathring{t}_i} - 1\right), \end{cases}$$

is given by

$$x(t) = \frac{1}{d}\left[e^{-d(t-(t_i^*+\mathring{t}_i))}\left(e^{-d\mathring{t}_i} - 2\right) + 1\right].$$

In the same way, we impose $x(t_{i+1}^*) = 0$ to yield

$$t_{i+1}^* = t_i^* + \mathring{t}_i + \frac{1}{d}\ln\left(2 - e^{-d\mathring{t}_i}\right). \tag{3.13}$$

Now we can find $\mathring{t}_i$ by equating the two quantities derived for t_{i+1}^*.

$$\mathring{t}_i + \frac{1}{d}\ln\left(2 - e^{-d\mathring{t}_i}\right) = \tau_2 + \frac{1}{d}\ln\left(-e^{-d\tau_2} + 2 + 2e^{-d(1-\beta)\tau_2} - 2e^{-d(\tau_2-\breve{t}_i)}\right). \tag{3.14}$$

Note that the equation above (3.14) includes scenarios (S1a) when $\breve{t}_i = \beta\tau_2$, and (S2a) when $\breve{t}_i = \tau_2$.

At this point, we drop condition (C1) and we are able to find the length of a cycle as a function of $\mathring{t}_k$.

Proposition 17. *Let $x(t)$ be the solution to (3.4) where the parameters satisfy the following assumption:*

$$\frac{\left[\ln\left(1+e^{d\tau_2}\right)-\ln(2)\right]}{d\tau_2} < \beta < \frac{\left[\ln\left(2e^{d\tau_2}-1\right)\right]}{d\tau_2}. \tag{3.15}$$

Then for $i > j$

$$t_i^* - t_j^* = \sum_{k=j}^{i-1}\left[\mathring{t}_k + \frac{1}{d}\ln\left(2-e^{-d\mathring{t}_k}\right)\right]. \tag{3.16}$$

Moreover,

1) *If $\beta < 1$, $\mathring{t}_k$ can be calculated exactly if and only if $cT+\gamma$ is not in the interval $[t_k^*+\beta\tau_2, t_k^*+\tau_2]$, for all natural c.*

2) *If $\beta > 1$, $\mathring{t}_k$ can be calculated exactly if and only if dT is not in the interval $[t_k^*+\tau_2, t_k^*+\beta\tau_2]$, for all natural d.*

Proof. Condition (3.15) guarantees that $\hat{t}_i < t_{i+1}^*$ for all i. The first inequality derives directly from Lemma 16 when $\beta < 1$ since

$$\hat{t}_i \leq t_i^* + \tau_2 < t_{i+1}^*, \tag{3.17}$$

while the second part of the inequality occurs when $\beta > 1$ and is computed in a similar way. Condition (3.17) is enough to guarantee equality (3.13); therefore we apply (3.13) iteratively $i-j$ times and end up with (3.16).

Moreover, there is a single change of monotonicity in $[t_k^*, t_{k+1}^*]$ when the delay $\tau(t)$ defined in (3.5) does not change from $\tau_{\min}$ to $\tau_{\max}$ in the interval $[t_k^*+\tau_{\min}, t_k^*+\tau_{\max}]$. Only when this happens, we can calculate $\mathring{t}_k$ analytically (i.e. this corresponds to scenarios (S1) or (S2a) in case $\beta < 1$), otherwise we should adopt a procedure similar to scenario (S2b) to calculate it numerically. □

3.4 Periodic Solutions

In this section, we use the method of steps to solve (3.4) with initial condition (3.6) where $k_0 = 0$ without loss of generality, and find its periodic solutions.

We define an m-cycle periodic solution of period P of (3.4) to be a periodic solution of period $P = t^*_{j+2m+1} - t^*_{j+1}$ for all natural j. We are searching for the periodic solutions that complete m cycles in one period.

Theorem 18. *Consider the following delay differential equation:*

$$\begin{cases} x'(t) = -dx(t) + f(x(t - \tau(t))) \\ x(t) > 0 \quad \forall t \in [-\tau_{\max}, 0) \\ x(0) = 0, \end{cases} \tag{3.18}$$

where

$$\tau(t) = \begin{cases} \tau_2, & \text{if} \mod (t,T) \geq \gamma \\ \tau_1 = \beta\tau_2, & \text{if} \mod (t,T) < \gamma \end{cases}$$

and

$$f(x) = -sgn(x) = \begin{cases} 1, & \text{if } x < 0 \\ 0, & \text{if } x = 0 \\ -1, & \text{if } x > 0, \end{cases}$$

for d, τ_2, $\beta > 0$; $\gamma > 0$ where $\tau_{\max} := \max(\beta\tau_2, \tau_2)$ and $\tau_{\min} := \min(\beta\tau_2, \tau_2)$.

Moreover, let τ_2, β, d, γ satisfy inequality (3.15) and let $l \in \mathbb{Q}$ be such that $l = \frac{m}{n}$ and $gcd(m,n) = 1$ for $m, n \in \mathbb{N}$ and suppose the parameters satisfy

$$\gamma < 2l\,[\beta\tau_2 + \frac{1}{d}\ln\Big(2 - e^{-d\beta\tau_2}\Big)]. \tag{3.19}$$

Then there exists a T such that (3.18) yields an m-cycle periodic solution of period nT.

Before proving the theorem, we analyse the two conditions assumed and explain why they

are relevant. As seen in Proposition 17, the first condition (3.15) guarantees that $\hat{t}_i < t^*_{i+1}$ for all i. Note that this condition limits the values of β which should be "close enough" to one; this can be translated into requiring the two switching delays to be similar. The following lemma describes instead why condition (3.19) is relevant.

Lemma 19. *If condition* (3.19) *is not satisfied, then there is no m-cycle periodic solution of period nT for the system* (3.18).

Proof. Suppose that condition (3.19) does not hold or equivalently

$$\gamma \geq 2l\,[\beta\tau_2 + \frac{1}{d}\ln\Big(2 - e^{-d\beta\tau_2}\Big)].$$

In this case $\tau(t) = \beta\tau_2$ for all $t \in [0, 2l\,(\beta\tau_2 + \frac{1}{d}\ln\Big(2 - e^{-d\beta\tau_2}\Big))]$ which yields:

$$T = 2l(\beta\tau_2 + \frac{1}{d}\ln\Big(2 - e^{-d\beta\tau_2}\Big)) \leq \gamma.$$

This choice of T contradicts with the assumption ($\gamma < T$), thus there is no m-cycle periodic solution of period nT for the system (3.18). □

Proof. of Theorem 18 - Since condition (3.15) holds, we can apply Proposition 17 to obtain

$$nT = t^*_{2m+1} - t^*_1 = \sum_{k=1}^{2m}\left[\mathring{t}_k(T) + \frac{1}{d}\ln\left(2 - e^{-d\mathring{t}_k(T)}\right)\right]. \tag{3.20}$$

If there exists a T that satisfies (3.20), we know that $\tau(t^*_{2m+1} + t) = \tau(t^*_1 + t)$ for all $t \geq 0$ so it is an m-cycle periodic solution of period $t^*_{2m+1} - t^*_1 = nT$.
This is equivalent to showing that the function

$$g(T) = nT - \sum_{k=1}^{2m}\left[\mathring{t}_k(T) + \frac{1}{d}\ln\left(2 - e^{-d\mathring{t}_k(T)}\right)\right], \tag{3.21}$$

contains at least one root. We analyse the periodic solutions separately if $l = \frac{m}{n}$ is natural or not.

a) Periodic solutions for $l \in \mathbb{N}$ (i.e. $n = 1$). It is important to note that $\mathring{t}_k$ does not depend on T for $k \leq 2m$, thus we can study the different $\mathring{t}_k$ separately. This leads to the possibility of simplifying (3.20) into

$$T = \sum_{k=1}^{2m} \left[\mathring{t}_k + \frac{1}{d} \ln \left(2 - e^{-d\mathring{t}_k} \right) \right].$$

The choice of T is unique since the right hand side is a constant given all the other parameters, so we just need to consider the value of each $\mathring{t}_k$.
The calculation of $\mathring{t}_k$ depends on the choice of γ:

1) If $\gamma \geq \tau_2 + (k-1)\beta\tau_2 + \frac{k-1}{d} \ln\left(2 - e^{-d\beta\tau_2}\right)$, then $\mathring{t}_k = \beta\tau_2$.

2) If $\gamma \leq k\beta\tau_2 + \frac{k-1}{d} \ln\left(2 - e^{-d\beta\tau_2}\right)$, then $\mathring{t}_k = \tau_2$.

3) Otherwise $\mathring{t}_k \in (\tau_{\min}, \tau_{\max})$ and this can be branched into two further cases:

   (a) If $\beta > 1$, then $\mathring{t}_k = \gamma - t_k^*$.

   (b) If $\beta < 1$, then $\mathring{t}_k$ is calculated numerically using (3.14).

We are able to predict in this case all the other $\mathring{t}_k$ without further calculations since:

- If $j < k$, then $\mathring{t}_j = \beta\tau_2$;
- If $k < j < 2m + 1$, then $\mathring{t}_j = \tau_2$.

b) Periodic solutions in all other cases ($l \in \mathbb{Q} \setminus \mathbb{N}$). In this case we have $n > 1$. This means that $\mathring{t}_k$ are functions of T which complicates the problem of searching for a root of (3.21). We first consider the continuity of $\mathring{t}_1(T)$ with respect to T and want to prove that given $T > 0$ and for $\epsilon > 0$,

$$\lim_{\epsilon \to 0} \mathring{t}_1(T - \epsilon) = \lim_{\epsilon \to 0} \mathring{t}_1(T + \epsilon) = \mathring{t}_1(T).$$

If no change of delay occurs in $[\beta\tau_2, \tau_2]$, there always exists a small enough ϵ such that

$$\mathring{t}_1(T - \epsilon) = \mathring{t}_1(T + \epsilon) = \mathring{t}_1(T),$$

and continuity is verified.

We now study the subcase in which $\beta < 1$ and there is exactly one change in delay in $[\beta\tau_2, \tau_2]$, given T. This can be further subdivided into scenarios (S1b) and (S2b) of Section 3.3:

(S1b) occurs when $\mathring{t}_1(T) = \mu T$ for some $\mu \in \mathbb{N}$. We can always find a small enough ϵ such that $\mathring{t}_1(T-\epsilon) = \mu(T-\epsilon)$ and $\mathring{t}_1(T+\epsilon) = \mu(T+\epsilon)$. So the continuity holds as $\epsilon \to 0$. (S2b) occurs when there is a change of monotonicity at $\mu T + \gamma$ for some $\mu \in \mathbb{N}$. In a similar way, we can always find a small enough ϵ such that $\tilde{t}_1(T-\epsilon) = \mu(T-\epsilon) + \gamma$ and $\tilde{t}_1(T+\epsilon) = \mu(T+\epsilon) + \gamma$. Let

$$h_1(x) := x + \frac{1}{d}\ln\left(2 - e^{-dx}\right)$$

and

$$h_2(\tilde{t}) := \tau_2 + \frac{1}{d}\ln\left(-e^{-d\tau_2} + 2 + 2e^{-d(1-\beta)\tau_2} - 2e^{-d(\tau_2-\tilde{t})}\right).$$

Note that $h_1(x)$ and $h_2(\tilde{t})$ are continuous functions with respect to x and $\tilde{t}$ respectively. But μ is finite, therefore if $\epsilon \to 0$,

$$h_2(\mu(T+\epsilon)+\gamma) \to h_2(\mu T + \gamma),$$
$$h_2(\mu(T-\epsilon)+\gamma) \to h_2(\mu T + \gamma).$$

Using (3.14), we get the following three equations:

$$h_1(\mathring{t}_1(T)) = h_2(\mu T + \gamma),$$
$$h_1(\mathring{t}_1(T+\epsilon)) = h_2(\mu(T+\epsilon)+\gamma),$$
$$h_1(\mathring{t}_1(T-\epsilon)) = h_2(\mu(T-\epsilon)+\gamma).$$

Since the right hand side of all equations converges to the same quantity as $\epsilon \to 0$ and $h_1(x)$ is continuous, then $\mathring{t}_1(T)$ is also a continuous function. At this point, it is clear that the continuity can be generalized for multiple delay changes, for cases where $\beta > 1$ and for $\mathring{t}_k(T)$

with $k \in \{1, ..., 2m\}$.

In particular, $g(T)$ defined in (3.21) is a continuous function with respect to T since it is a composition of continuous functions. Moreover, condition (3.15) guarantees that $\tau_{\min} \leq \mathring{t}_k(T) \leq \tau_{\max}$ so we can consider the following:

1) $T_{\min} = 2l\left[\tau_{\min} + \frac{1}{d}\ln\left(2 - e^{-d\tau_{\min}}\right)\right]$,

2) $T_{\max} = 2l\left[\tau_{\max} + \frac{1}{d}\ln\left(2 - e^{-d\tau_{\max}}\right)\right]$.

Note that the continuous function g satisfies $g(T_{\min}) \leq 0$ and $g(T_{\max}) \geq 0$. Therefore we can apply the Intermediate Value Theorem which states that there exists at least one $\hat{T} \in [T_{\min}, T_{\max}]$ such that $g(\hat{T}) = 0$. This $\hat{T}$ will yield an m-cycle periodic solution of period nT we are searching for and this proves the Theorem. □

The delay-change period T can be approximated numerically by considering a grid of values for $I = [T_{\min}, T_{\max}]$ and choosing the value that minimizes $|g(T)|$. We have produced a code using Matlab to find a period under conditions (3.15) and (3.19).

We can also adopt a similar procedure to find γ that leads to a m-cycle periodic solution of period nT, given T and the other parameters.

Theorem 20. *Consider equation* (3.18) *with known parameters* τ_2, β, d *and* T *satisfying condition* (3.15) *of Theorem 18 and the following condition:*

$$2l[\tau_{\min} + \frac{1}{d}\ln\left(2 - e^{-d\tau_{\min}}\right)] \leq T \leq 2l[\tau_{\max} + \frac{1}{d}\ln\left(2 - e^{-d\tau_{\max}}\right)].$$

Then there exists a γ *such that* (3.18) *yields an* m*-cycle periodic solution of period* nT*.*

The proof is similar to Theorem 18 where the main step is to show that $\mathring{t}_k(\gamma)$ is a continuous function for $k \in \{1, ..., 2m\}$. Theorems 18 and 20 show that under certain conditions, it is possible to find coexisting periodic solutions with different periods and cycles by varying just one of the switching-delay related parameters.

3.5 Simulations - Multi-cycle periodic solutions

In this section, we provide some simulations using Matlab to obtain different multi-cycle periodic solutions using Theorem 18 as explained above. First, we study how the parameters impact T and the period of the periodic solution nT, by using the code from the previous section. Then, we input the same parameters with the computed T to the model and plot our results.

We assume that in all the plots three of the parameters are always fixed: $\beta = 0.6$, $\tau_2 = 3$, $d = 0.1$. Then we choose γ satisfying condition (3.19). In Figures 3.2 and 3.3, we take $\gamma = 3$, in Figures 3.4 and 3.5 we take a larger $\gamma = 8$ to demonstrate different possible periodic dynamics. We also introduce dashed lines at $y = nT$ for natural n to separate the behaviour of the solution according to the period. The other parameters that vary throughout these plots are m and n which regulate the behaviour of solutions since we aim to search for an m-cycle periodic solution of period nT.

The two plots in Figure 3.2 show two of the possible 1-cycle periodic solutions of (3.18) which are obtained by choosing $n = 1$ and $n = 2$ respectively. Important to notice is that the two solutions present different behaviours since the solution in the right panel presents two extrema (maximum and minimum) in every period with the same absolute value but this does not occur in the left panel because the maxima presents a higher absolute value.

The two plots in Figure 3.3 show examples of 2-cycle periodic solutions of (3.18). In this case, it is interesting to note how the two solutions present similar behaviour and their period is just slightly different.

The two plots in Figure 3.4 represent different 3-cycle periodic solutions of (3.18) where $\gamma = 8$. Note that the global maxima and minima of the solutions are the same since all parameters coincide except m; this small difference modifies the peak patterns in the plots since the former presents two global maxima and minima in every period while the latter just one of both.

The two plots in Figure 3.5 represent different 5-cycle periodic solutions of (3.18). In this case, we see additional oscillations on the right panel since one of the local peaks undergoes

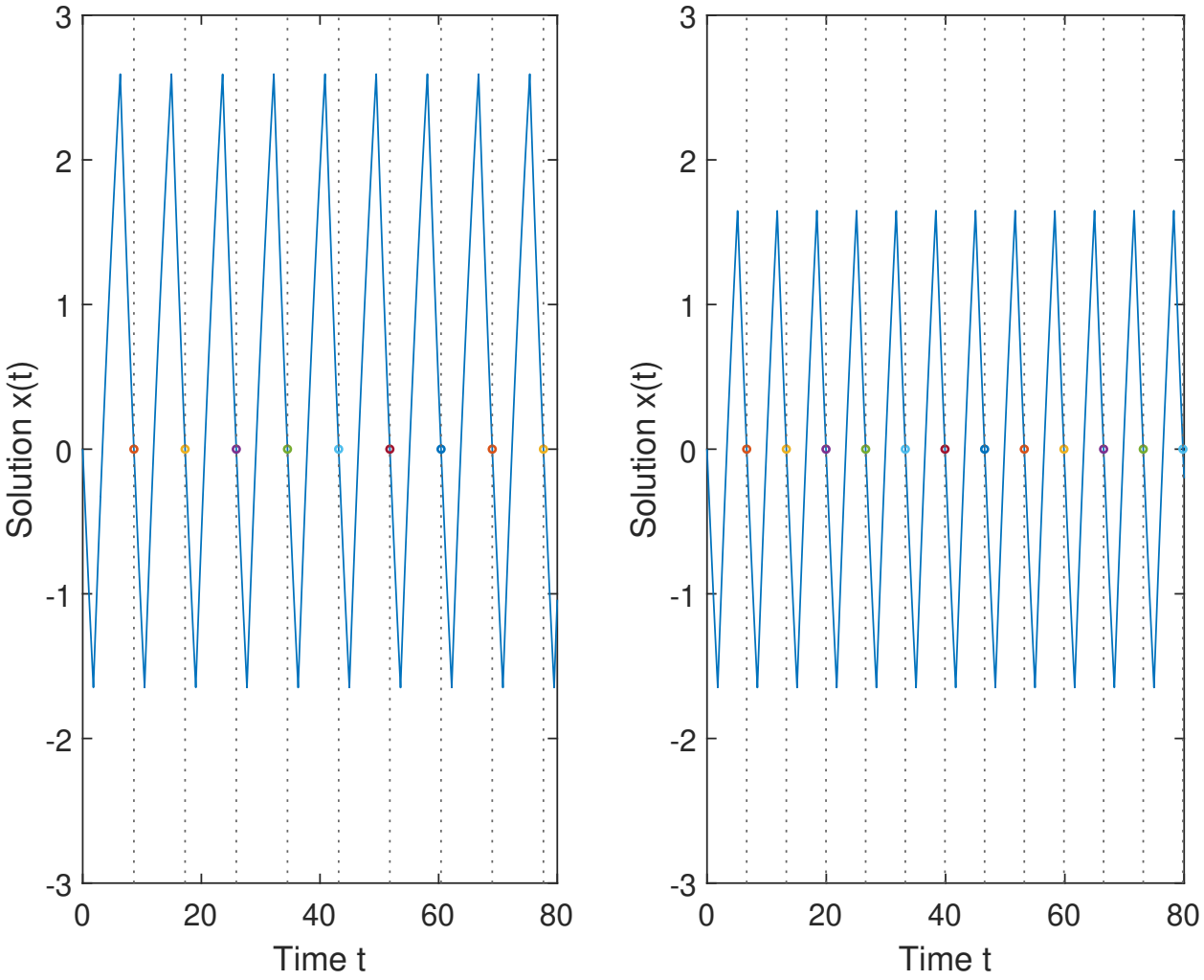

Figure 3.2: In the left panel, we see a 1-cycle periodic solution of period $T = 8.6295$ is described; in the right panel we see a 1-cycle periodic solution of period $2T = 6.6498$.

periodically through a triple change of monotonicity. This happens since that special case identifies with scenario (S2b) of Chapter 3.3.

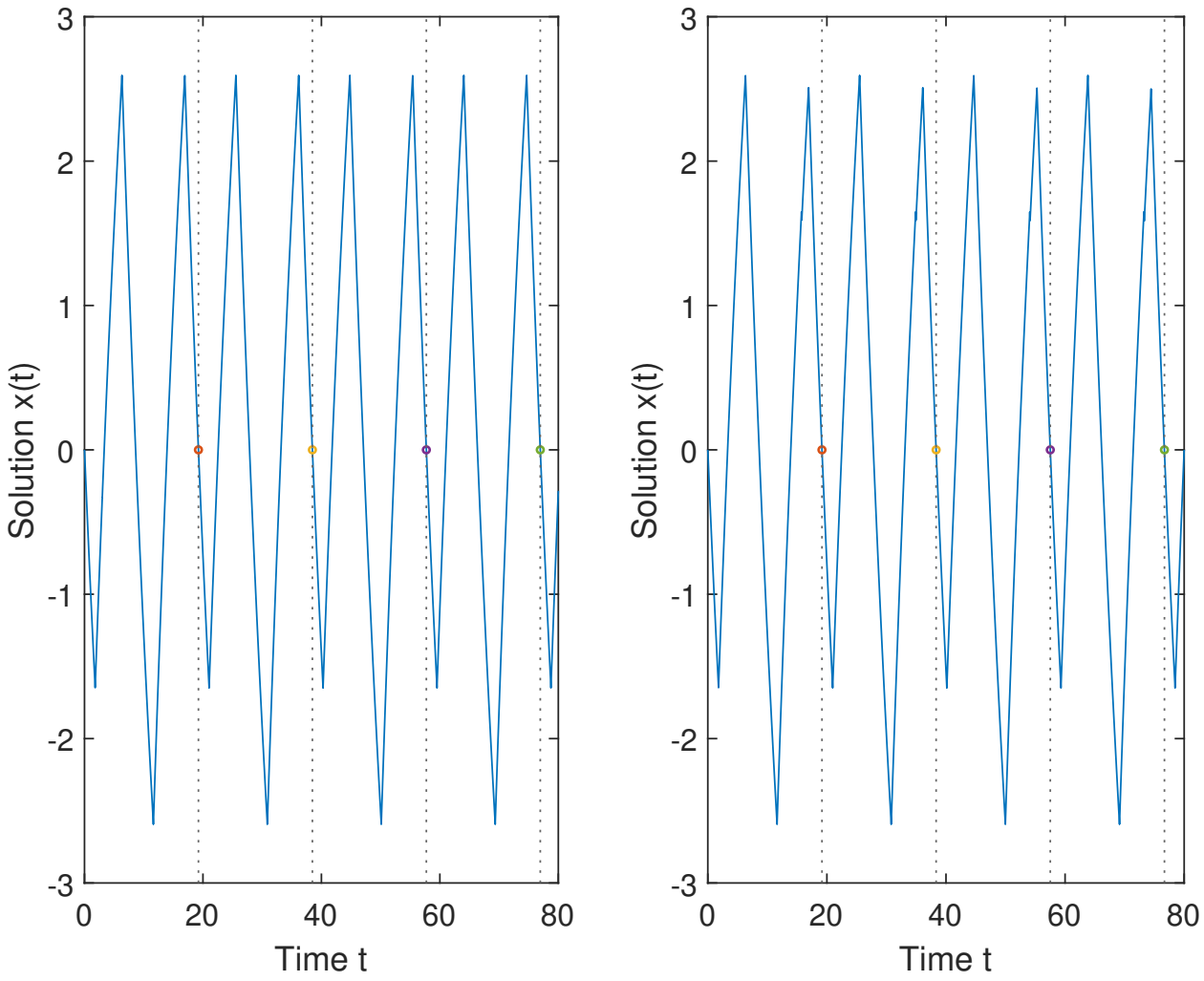

Figure 3.3: In the left panel, we see a 2-cycle periodic solution of period $T = 19.2388$; in the right panel, we see a 2-cycle periodic solution of period $3T = 19.1721$.

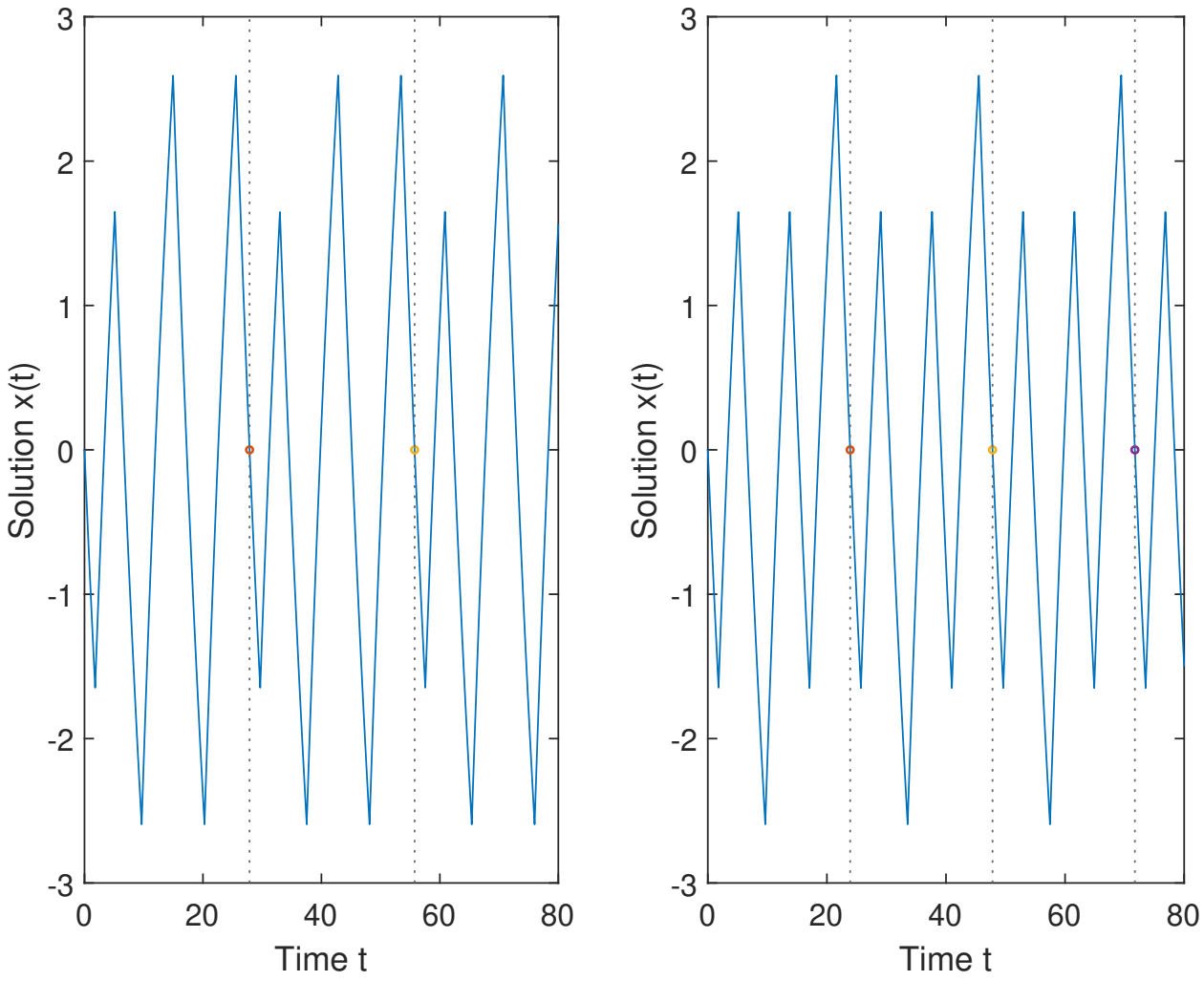

Figure 3.4: In the left panel, we see a 3-cycle periodic solution of period $T = 27.8687$; in the right panel, we see a 3-cycle periodic solution of period $2T = 23.9084$.

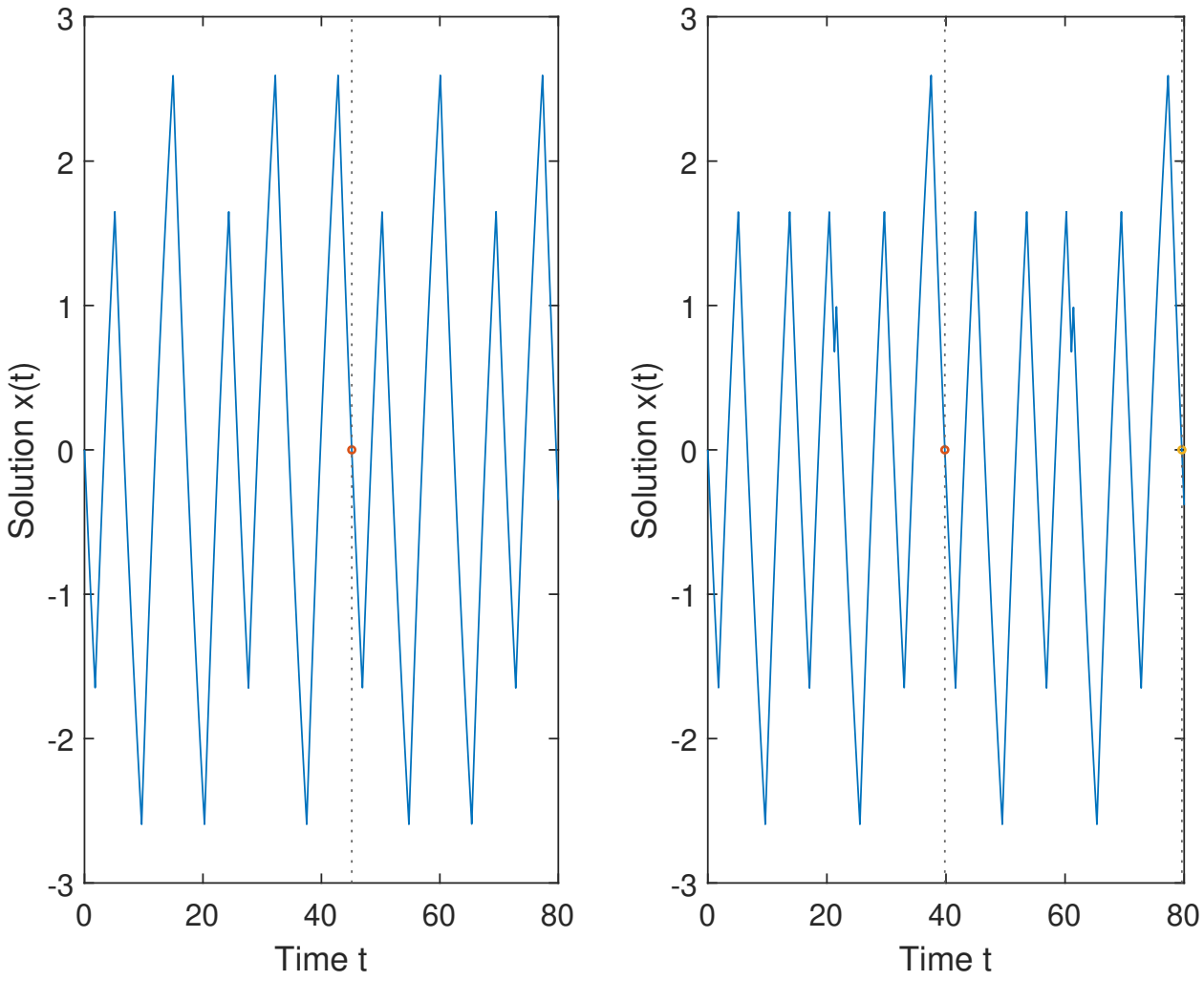

Figure 3.5: In the left panel, we see a 5-cycle periodic solution of period $2T = 45.1272$; in the right panel, we see a 5-cycle periodic solution of period $3T = 39.8079$.

3.6 Final considerations for the switching delay model

We have introduced a DDE model with periodic switching delays and described the behaviour of solutions induced by its negative feedback. In particular, we know that the solutions are always bounded and we rigorously proved the conditions that would allow oscillations of different frequencies given by the two different delays to cause multi-cycle periodic solutions. The main condition requires that the two switching delays, which can be considered for example in the tick population dynamics in [62] as the normal and diapause delay, should be close enough to each other. This guarantees that the model dynamics can be studied analytically and in the case where the two delays are similar, we can approximate their dynamics to a single-delay population model which is described in [83].

The model studied in this paper can be used for single-species model affected periodically by different factors [84] but it is not limited to the ecological field. In [85] for example, the model produced to study cell production in the body has a very similar structure to our model since it also includes an oscillatory delay and a discontinuous f. In that paper though, the aim was to study how a periodic stimulus would modify the model. In this direction, we would like to further analyse our model by considering the effects of perturbation on these periodic solutions and dropping some of the simplifying assumptions on the model (for example considering f to be continuous). We would like to observe if a slight change in the initial conditions of the model can have a significant impact on the model dynamics.

Chapter 4

Effectiveness of control strategies to eradicate tick borne diseases

Ticks are responsible for spreading harmful diseases including Lyme disease and tick-borne encephalitis. Understanding tick population dynamics and predicting risk of tick-borne disease insurgence helps to design preventive actions against the disease spread. Using a compartmental model describing the pathogen transmission among ticks and hosts, we study the influence of host-targeted tick control strategies with chemical insecticides on tick population and disease transmission dynamics. Our analysis shows that in areas with rapid-growing population of ticks, host-targeted controls using chemical insecticides may enhance disease persistence and even turn a disease-free area to a disease endemic area. Therefore, the complex dynamics of pathogen spread among ticks and hosts should be carefully examined when designing tick control strategies.

4.1 Introduction to the host-tick epidemiological model including control strategies

Our focus here is to study the effect of host-targeted tick control strategies in tick-borne disease prevention. As we have described in the introduction, there is a wide range of control

strategies that have been applied to reduce tick-borne disease risk. In this chapter, we study the effect of acaricide host-targeting control strategies for rodents such as bait boxes and tick tubes. Two acaricides will be utilised for our study: "Fipronil" which has been proved to be highly effective in killing ticks that are exposed to it and "Permethrin" which has a repellent effect to ticks since ticks can detect its smell and avoid to feed on those hosts [35, 86]. For this purpose, we construct a host-tick transmission dynamics model with acaricide and repellent control on the host population and study how the variation of these control parameters would affect tick dynamics and disease transmission.

In this chapter, we first introduce the dynamics of tick population growth and the dynamics of tick-host disease transmission including the control parameters. Then, we derive the two basic reproduction numbers for tick growth and disease spread [77, 78]. In the results section, we show the impact of host-targeted controls on tick population and on the tick and disease reproduction numbers and include plots to corroborate the theoretical work. Finally, we discuss the implication of these results for tick and tick-borne disease control.

4.2 Overview of the transmission model

The model describes the transmission dynamics of tick borne diseases under the host-targeting control strategies using a compartmental model including female ticks and rodent host population. Two main transmission routes of tick borne diseases are considered: the systemic transmission of pathogens between ticks and hosts and the non-systemic transmission of the pathogen between co-feeding ticks. Three stages of ticks' life cycle are included in the model: larvae (L), nymphs (N) and adults (A). Note that the egg stage is not included therefore we include only the eggs that manage to reach the larval stage. Nymph population is further stratified according to the state of the infection (susceptible with subscript S, infected with subscript I). Hosts in the model represent the rodent population which is assumed to be constant in time (H), and can be infested by larvae and nymphs.

The birth rate of larvae is modeled as the Ricker function $\beta A e^{-\gamma A}$, considering the density-

dependent negative feedback which is induced in the feeding stages of the adult population [87]. The choice of β and γ is slightly different than respectively p and q in Chapter 2 since we are considering β and γ to be parameters relative to larvae and not to eggs, but the idea is the same. We consider the stage-dependent mortality rates for larvae, nymphs and adults, μ_L, μ_N, and μ_H, respectively. Larval and nymphal ticks attach to a host with the rate b_L and b_N, respectively. Ticks develop into the next stage upon feeding a host. After feeding, larvae remain susceptible if both systemic transmission and co-feeding do not take place, otherwise they become infected nymphs. If a larva is attached to infected hosts, systemic transmission may occur with probability p_{HL}. If systemic transmission does not occur, the larva may still be infected with probability c by co-feeding with infected nymphs. Note that co-feeding transmission can also occur when ticks feed on immunized hosts [16]. The probability of co-feeding transmission c depends on the number of infected nymphs and on the proportion of hosts that assumed repellent (r) as shown in Nah et al. [15]

$$c = 1 - (1 - \delta)^{\frac{N_I}{(1-r)H}}.$$

Host population is then divided into susceptibles (H_S), infected (H_I) and immune or recovered (H_R). Systemic transmission for hosts occurs with probability p_{NH} when infected nymphs are feeding on susceptible hosts. We consider also a mortality rate for hosts (μ_H) and assume that every dead individual is replaced by a new susceptible individual to keep the population constant.

As for tick-control methods, we consider the application of acaricides and repellent on rodents, the main host for larvae and nymphs. Parameter r which is present also in the cofeeding probability represents the fraction of the effectively repelled host population, therefore tick host attachment rates are reduced by a factor $1-r$. The non-repellent acaricide is applied to a fraction a of rodents and we assume that questing ticks immediately die when they attach to rodents with insecticide. In the end, we consider the combined effect of both repellent and non-repellent insecticide applied on rodents. In case a rodent undergoes both treatments, we assume that the repellent effect dominates since ticks avoid biting the host.

We consider the effective acaricide coverage to be constant in time.

In summary, we describe the transmission dynamics of pathogens among ticks and hosts under repellent and acaricide control strategies using the following system of ordinary differential equations.

$$\begin{cases} H_S' = \mu_H H - b_N p_{NH}(1-r)N_I \dfrac{H_S}{H} - \mu_H H_S, \\ H_I' = b_N p_{NH}(1-r)N_I \dfrac{H_S}{H} - \gamma_H H_I - \mu_H H_I, \\ H_R' = \gamma_H H_I - \mu_H H_R, \\ L' = \beta A e^{-\gamma A} - b_L L(1-r) - \mu_L L, \\ N_S' = b_L L(1-r)(1-a)(1-c)\dfrac{[H_S + (1-p_{HL})H_I + H_R]}{H} - b_N N_S(1-r) - \mu_N N_S, \\ N_I' = b_L L(1-r)(1-a)p_{HL}\dfrac{H_I}{H} + b_L L(1-r)(1-a)c\dfrac{[H_S + (1-p_{HL})H_I + H_R]}{H}, \\ \quad - b_N N_I(1-r) - \mu_N N_I, \\ A' = b_N(N_S + N_I)(1-r)(1-a) - \mu_A A. \end{cases} \tag{4.1}$$

We normalize the system by introducing variables

$$\bar{H}_S = \frac{H_S}{H}, \quad \bar{H}_I = \frac{H_I}{H}, \quad \bar{L} = \frac{L}{H}, \quad \bar{N}_S = \frac{N_S}{H}, \quad \bar{N}_I = \frac{N_I}{H}, \quad \bar{A} = \frac{A}{H},$$

and substitute $H_R = H - H_S - H_I$, where H represents the total number of hosts which is considered to be constant in time. Then, the system becomes

$$\begin{cases} \bar{H}_S' = \mu_H - b_N p_{NH}(1-r)\bar{N}_I \bar{H}_S - \mu_H \bar{H}_S, \\ \bar{H}_I' = b_N p_{NH}(1-r)\bar{N}_I \bar{H}_S - \gamma_H \bar{H}_I - \mu_H \bar{H}_I, \\ \bar{L}' = \beta \bar{A} e^{-\bar{\gamma}\bar{A}} - b_L \bar{L}(1-r) - \mu_L \bar{L}, \\ \bar{N}_S' = b_L \bar{L}(1-r)(1-a)(1-\bar{c})(1-p_{HL}\bar{H}_I) - b_N \bar{N}_S(1-r) - \mu_N \bar{N}_S, \\ \bar{N}_I' = b_L \bar{L}(1-r)(1-a)\left[p_{HL}\bar{H}_I + \bar{c}(1-p_{HL}\bar{H}_I)\right] - b_N \bar{N}_I(1-r) - \mu_N \bar{N}_I, \\ \bar{A}' = b_N(\bar{N}_S + \bar{N}_I)(1-r)(1-a) - \mu_A \bar{A}, \end{cases} \tag{4.2}$$

where

$$\bar{\gamma} = \gamma H,$$

and

$$\bar{c} = 1 - (1-\delta)^{\frac{\bar{N}_I}{1-r}}.$$

From now on, we analyse the normalized model. For notational simplicity, we omit the bar on top of the variables and parameters.

A summary of the parameters and their explanation can be found in Table 4.1.

List of parameters	
Parameter	**Explanation**
b_L	Biting rate for larvae
b_N	Biting rate for nymphs
β	Maximum birth rate for larvae per unit time
γ	Intensity of the density-dependence in birth rate of larvae
μ_L	Mortality rate of larvae
μ_N	Mortality rate of nymphs
μ_A	Mortality rate of adults
μ_H	Mortality rate of hosts
p_{NH}	Nymph-to-host systemic infection probability
p_{HL}	Probability of systemic infection from hosts to larvae
p_{HN}	Probability of systemic infection from hosts to nymphs
γ_H	Recovery rate of hosts
c	Probability of non-systemic transmission (co-feeding)
δ	Probability of cofeeding transmission for larvae with a single infected nymph
r	Proportion of hosts assuming effective repellent insecticide
a	Proportion of hosts assuming effective non-repellent insecticide

Table 4.1: Table including parameters and their explanation used in the model.

4.3 Equilibria of the transmission model

The equilibria of the system are obtained from solving the following system of equations:

$$0 = \mu_H - b_N p_{NH}(1-r)N_I H_S - \mu_H H_S, \tag{4.3a}$$

$$0 = b_N p_{NH}(1-r)N_I H_S - \gamma_H H_I - \mu_H H_I, \tag{4.3b}$$

$$0 = \beta A e^{-\gamma A} - b_L L(1-r) - \mu_L L, \tag{4.3c}$$

$$0 = b_L L(1-r)(1-a)(1-c)(1-p_{HL}H_I) - b_N N_S(1-r) - \mu_N N_S, \tag{4.3d}$$

$$0 = b_L L(1-r)(1-a)\left[c + p_{HL}(1-c)H_I\right] - b_N N_I(1-r) - \mu_N N_I, \tag{4.3e}$$

$$0 = b_N(N_S + N_I)(1-r)(1-a) - \mu_A A, \tag{4.3f}$$

where

$$c = 1 - (1-\delta)^{\frac{N_I}{1-r}}.$$

To analyse the equilibria, we distinguish two cases: $N_I^* = 0$ and $N_I^* > 0$.

1. If $N_I^* = 0$, from (4.3a) we have $H_S^* = 1$, and from (4.3b) $H_I^* = 0$. This coincides with the case with no disease transmission since also $c^* = 0$.

   Furthermore, we can rewrite the conditions for (4.3f), (4.3d) and (4.3c) as:

$$A^* = \frac{b_N(1-r)(1-a)N_S^*}{\mu_A}, \tag{4.4a}$$

$$N_S^* = \frac{b_L(1-r)(1-a)L^*}{b_N(1-r)+\mu_N}, \tag{4.4b}$$

$$L^* = \frac{\beta A^* e^{-\gamma A^*}}{b_L(1-r)+\mu_L}. \tag{4.4c}$$

   Therefore, we study (4.4a) to find N_S^* as a function of A^*, we have

$$N_S^* = \frac{\mu_A A^*}{b_N(1-r)(1-a)},$$

   and we can equate it with (4.4b)

$$\frac{\mu_A A^*}{b_N(1-r)(1-a)} = \frac{b_L(1-r)(1-a)\beta A^* e^{-\gamma A^*}}{(b_N(1-r)+\mu_N)(b_L(1-r)+\mu_L)}.$$

   So $A^* = 0$ is always a solution and is related to the tick-free equilibrium
   $E_T = (H_S^*, H_I^*, L^*, N_S^*, N_I^*, A^*) = (1, 0, 0, 0, 0, 0)$. We want to prove that under certain

conditions, it is not the unique disease-free equilibrium. Therefore, we consider $A^* \neq 0$ and look for conditions that guarantee its existence. Then

$$e^{-\gamma A^*} = \frac{1}{R_T},$$

where

$$R_T := \frac{\beta b_L b_N (1-r)^2 (1-a)^2}{(b_L(1-r)+\mu_L)(b_N(1-r)+\mu_N)\mu_A}.$$

Since A^* represents the adult population, it is a non-negative quantity so this equality is possible only if $R_T > 1$ and this yields the disease-free equilibrium

$$E_D = \left(1, 0, \frac{\beta A^* e^{-\gamma A^*}}{b_L(1-r)+\mu_L}, \frac{\mu_A A^*}{b_N(1-r)(1-a)}, 0, A^*\right),$$

where

$$A^* = \frac{\log(R_T)}{\gamma}.$$

2. Consider the case $N_I^* > 0$. Looking for an equilibrium, we see that $c^* > 0$ for $\delta > 0$ and would depend on N_I^* so $c^* = 1 - (1-\delta)^{\frac{N_I^*}{1-r}} \in [0,1]$. From equation (4.3a), (4.3b), (4.3e), (4.3d) and (4.3f), we get:

$$H_S^* = \frac{\mu_H}{\mu_H + b_N p_{NH}(1-r)N_I^*}, \tag{4.5a}$$

$$H_I^* = \frac{b_N p_{NH}(1-r)N_I^* H_S^*}{\gamma_H + \mu_H}, \tag{4.5b}$$

$$L^* = \frac{[b_N(1-r)+\mu_N]N_I^*}{b_L(1-r)(1-a)[c^* + p_{HL}(1-c^*)H_I^*]}, \tag{4.5c}$$

$$N_S^* = \frac{b_L L^*(1-r)(1-a)(1-c^*)(1-p_{HL}H_I^*)}{b_N(1-r)+\mu_N}, \tag{4.5d}$$

$$A^* = \frac{b_N(N_S^*+N_I^*)(1-r)(1-a)}{\mu_A}. \tag{4.5e}$$

To study if there exists an endemic equilibrium, we compare equation (4.5c) with (4.4c). We look for a positive N_I^* such that the right hand side of both equations equate each

other. Let

$$R_D = \frac{-A + \sqrt{A^2 + 4B}}{2}.$$

where

$$A = \ln(1-\delta)\ln(R_T)\frac{\mu_A}{\gamma b_N (1-r)^2(1-a)},$$

and

$$B = \frac{\mu_A p_{NH} p_{HL} \ln(R_T)}{\gamma(\gamma_H + \mu_H)(1-a)},$$

when $R_T > 1$. Finding the solution analytically proves to be complicated but we show numerically in Figure 4.1 how the endemic solution behaves as the co-feeding probability δ and R_D grows. In particular, we notice that the endemic equilibrium exists when $R_D > 1$ and that R_D is superlinear with respect to δ, showing the importance of co-feeding transmission in the model.

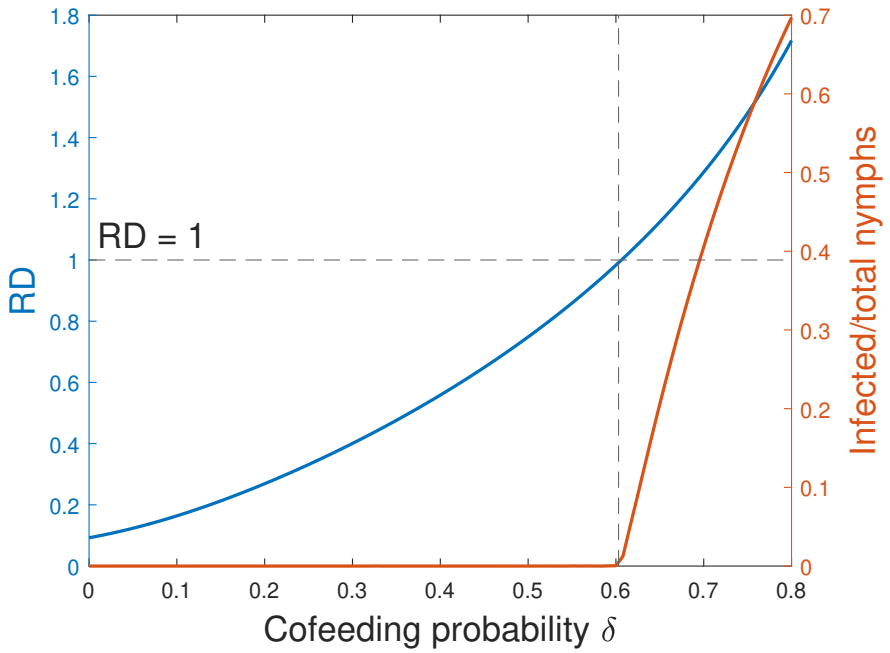

Figure 4.1: Effect of cofeeding probability on disease burden. Numerical computation of the proportion of infected nymphs at the endemic equilibrium as the co-feeding parameter δ grows is shown in red. Computation of the disease reproduction number R_D is shown in blue. Parameters chosen are $\mu_H = 0.001$, $b_N = 0.1$, $p_{NH} = 0.1$, $r = 0.1$, $\gamma_H = 0.1$, $\beta = 0.2$, $b_L = 0.1$, $\gamma = 0.1$, $\mu_L = 0.01$, $p_{HL} = 0.1$, $p_{HN} = 0.1$, $\mu_N = 0.01$, $\mu_A = 0.15$, $a = 0.01$.

4.4 Basic reproduction numbers of the model

In this section, we show how R_T and R_D are also epidemiological thresholds.

4.4.1 Tick growth

Linearizing the system at the tick-free equilibrium E_T, we obtain

$$\begin{cases} H_S' = -b_N p_{NH}(1-r)N_I - \mu_H H_S, \\ H_I' = b_N p_{NH}(1-r)N_I - \gamma_H H_I - \mu_H H_I, \\ L' = \beta A - b_L L(1-r) - \mu_L L, \\ N_S' = b_L L(1-r)(1-a) - b_N N_S(1-r) - \mu_N N_S, \\ N_I' = -b_N N_I(1-r) - \mu_N N_I, \\ A' = b_N(N_S + N_I)(1-r)(1-a) - \mu_A A. \end{cases} \tag{4.6}$$

We calculate the tick basic reproduction number similarly as calculating R_T in Chapter 2. R_T is the spectral radius of the Next Generation Matrix (NGM) where new births are included in the transmission matrix and tick development and deaths in different stages are part of the transition matrix. The sub-system of (4.6) obtained by summing the susceptible and infected nymphs can be written as

$$\begin{pmatrix} L' \\ N' \\ A' \end{pmatrix} = (T + \Sigma) \begin{pmatrix} L \\ N \\ A \end{pmatrix},$$

with the transmission matrix T and the transition matrix Σ being respectively

$$T = \begin{pmatrix} 0 & 0 & \beta \\ 0 & 0 & 0 \\ 0 & 0 & 0 \end{pmatrix},$$

and

$$\Sigma = \begin{pmatrix} -(b_L(1-r)+\mu_L) & 0 & 0 \\ b_L(1-r)(1-a) & -(\mu_N + b_N(1-r)) & 0 \\ 0 & b_N(1-r)(1-a) & -\mu_A \end{pmatrix}. \tag{4.7}$$

Note that the inverse of Σ is

$$\Sigma^{-1} = \begin{pmatrix} -\frac{1}{b_L(1-r)+\mu_L} & 0 & 0 \\ -\frac{b_L(1-r)(1-a)}{(b_L(1-r)+\mu_L)(b_N(1-r)+\mu_N)} & -\frac{1}{\mu_N+b_N(1-r)} & 0 \\ -\frac{b_L b_N(1-r)^2(1-a)^2}{(b_L(1-r)+\mu_L)(b_N(1-r)+\mu_N)\mu_A} & -\frac{b_N(1-r)(1-a)}{\mu_A(b_N(1-r)+\mu_N)} & -\frac{1}{\mu_A} \end{pmatrix}. \tag{4.8}$$

So the next generation matrix is $K = -T\Sigma^{-1}$ with

$$K = \begin{pmatrix} \frac{\beta b_L b_N(1-r)^2(1-a)^2}{(b_L(1-r)+\mu_L)(b_N(1-r)+\mu_N)\mu_A} & k_{12} & k_{13} \\ 0 & 0 & 0 \\ 0 & 0 & 0 \end{pmatrix}, \tag{4.9}$$

where k_{12} and k_{13} are irrelevant in the eigenvalue computation. Therefore, the characteristic equation is

$$\lambda^2 \left(\lambda - \frac{\beta b_L b_N(1-r)^2(1-a)^2}{(b_L(1-r)+\mu_L)(b_N(1-r)+\mu_N)\mu_A} \right) = 0,$$

and the spectral radius is

$$R_T = \frac{\beta b_L b_N(1-r)^2(1-a)^2}{(b_L(1-r)+\mu_L)(b_N(1-r)+\mu_N)\mu_A},$$

which coincides with the computation in the disease-free equilibrium calculation. This quantity represents the average number of female tick that reach the adult stage produced by an adult female tick. So naturally $R_T = 1$ separates the case where tick population decays and leads to the trivial equilibrium (when $R_T < 1$) and the case in which tick population persists (when $R_T > 1$).

4.4.2 Disease transmission

Linearizing the system at the disease-free equilibrium E_D, we get

$$\begin{cases} H_S' = -b_N p_{NH}(1-r)N_I - \mu_H H_S, \\ H_I' = b_N p_{NH}(1-r)N_I - \gamma_H H_I - \mu_H H_I, \\ L' = \beta e^{-\gamma A^*}(1-\gamma A^*)A - b_L L(1-r) - \mu_L L, \\ N_S' = b_L(1-r)(1-a)\left\{L + L^*\left(\dfrac{N_I}{1-r}\ln(1-\delta) - p_{HL}H_I\right)\right\} - b_N N_S(1-r) - \mu_N N_S, \\ N_I' = b_L(1-r)(1-a)L^*\left(p_{HL}H_I - \dfrac{N_I}{1-r}\ln(1-\delta)\right) - b_N N_I(1-r) - \mu_N N_I, \\ A' = b_N(1-r)(1-a)(N_S+N_I) - \mu_A A. \end{cases} \tag{4.10}$$

The infected sub-system of (4.10) can be written as

$$\begin{pmatrix} H_I' \\ N_I' \end{pmatrix} = (T+\Sigma)\begin{pmatrix} H_I \\ N_I \end{pmatrix}.$$

Here the transmission matrix T is directly linked with disease transmission and is made up by both systemic and non-systemic transmission terms within the infected host and nymphs compartment. Note that we consider just the infectious compartments H_I and N_I in the next generation matrix while computing R_D since the other compartments would not affect its computation [88].

Therefore the transmission matrix T and the transition matrix Σ are

$$T = \begin{pmatrix} 0 & b_N p_{NH}(1-r) \\ b_L(1-r)(1-a)p_{HL}L^* & -b_L(1-a)\ln(1-\delta)L^* \end{pmatrix},$$

and

$$\Sigma = \begin{pmatrix} -(\gamma_H+\mu_H) & 0 \\ 0 & -\mu_N - b_N(1-r) \end{pmatrix}. \tag{4.11}$$

Substituting L^* yields

$$T = \begin{pmatrix} 0 & b_N p_{NH}(1-r) \\ b_L(1-r)(1-a)p_{HL}\frac{\beta \ln(R_T)}{\gamma R_T[b_L(1-r)+\mu_L]} & -b_L(1-a)\ln(1-\delta)\frac{\beta \ln(R_T)}{\gamma R_T[b_L(1-r)+\mu_L]} \end{pmatrix}. \quad (4.12)$$

Note that the inverse of Σ is

$$\Sigma^{-1} = \begin{pmatrix} -\frac{1}{\gamma_H+\mu_H} & 0 \\ 0 & -\frac{1}{\mu_N+b_N(1-r)} \end{pmatrix}. \quad (4.13)$$

So the next generation matrix is $K = -T\Sigma^{-1}$ where

$$K = \begin{pmatrix} 0 & \frac{b_N p_{NH}(1-r)}{\mu_N+b_N(1-r)} \\ \frac{b_L(1-r)(1-a)p_{HL}}{\gamma_H+\mu_H}[\frac{\beta \ln(R_T)}{\gamma R_T[b_L(1-r)+\mu_L]}] & -\frac{b_L(1-a)\ln(1-\delta)}{\mu_N+b_N(1-r)}[\frac{\beta \ln(R_T)}{\gamma R_T[b_L(1-r)+\mu_L]}] \end{pmatrix}, \quad (4.14)$$

and the characteristic equation is given by:

$$\lambda^2 + A\lambda - B = 0$$

where

$$A = \frac{b_L(1-a)\ln(1-\delta)}{\mu_N + b_N(1-r)}\left[\frac{\beta \ln(R_T)}{\gamma R_T[b_L(1-r)+\mu_L]}\right]$$

and

$$B = \frac{b_N p_{NH}(1-r)}{\mu_N + b_N(1-r)}\frac{b_L(1-r)(1-a)p_{HL}}{\gamma_H+\mu_H}\left[\frac{\beta \ln(R_T)}{\gamma R_T[b_L(1-r)+\mu_L]}\right].$$

Simplifying this, we get

$$A = \ln(1-\delta)\ln(R_T)\frac{\mu_A}{\gamma b_N(1-r)^2(1-a)}$$

and

$$B = \frac{\mu_A p_{NH} p_{HL}\ln(R_T)}{\gamma(\gamma_H+\mu_H)(1-a)}.$$

The basic reproduction number R_D is defined as the spectral radius of K:

$$R_D = \frac{-A + \sqrt{A^2 + 4B}}{2},$$

whenever $R_T > 1$. We have described in section 4.3 how this quantity determines whether the endemic equilibrium exists or not. In the epidemiological sense, R_D takes into account the average number of infected ticks and hosts produced by a single infected host or tick, and it is relevant only if the tick population persists ($R_T > 1$). So naturally $R_D = 1$ separates the case in which the disease dies out (when $R_D < 1$) and the case in which it remains in the population (when $R_D > 1$).

4.5 Effects of acaricide and repellent application in tick control

We analyse the effect of acaricide and repellent parameters by studying both theoretically and numerically how they would influence tick and disease reproduction numbers.

4.5.1 Dependence of R_T on control measures

We start by studying the impact of control measures such as repellent and acaricide represented respectively by the parameters r and a on the proliferation potential of ticks (R_T). We study R_T as a function of r and a and calculate its partial derivatives with respect to these two parameters.

$$R_T(r, a) = \frac{\beta b_L b_N (1-r)^2 (1-a)^2}{(b_L(1-r) + \mu_L)(b_N(1-r) + \mu_N)\mu_A}.$$

We note that R_T is a decreasing function with respect to r when the natural conditions $R_T > 0$ and $r \in [0, 1)$ take place since

$$\begin{aligned}
\frac{\partial R_T}{\partial r} &= \frac{\beta b_L b_N (1-a)^2}{\mu_A} \frac{\partial}{\partial r} \left(\frac{(1-r)^2}{(b_L(1-r)+\mu_L)(b_N(1-r)+\mu_N)} \right) \\
&= -\frac{\beta b_L b_N (1-a)^2}{\mu_A} \frac{(1-r)[\mu_L b_N(1-r) + \mu_N b_L(1-r) + 2\mu_L\mu_N]}{(b_L(1-r)+\mu_L)^2(b_N(1-r)+\mu_N)^2} \\
&= -\frac{R_T}{1-r} \left(\frac{\mu_L b_N(1-r) + \mu_N b_L(1-r) + 2\mu_L\mu_N}{(b_L(1-r)+\mu_L)(b_N(1-r)+\mu_N)} \right) \\
&< 0.
\end{aligned}$$

Then, we show that R_T is a decreasing function with respect to a when $R_T > 0$ and $a \in [0, 1)$.

$$\begin{aligned}
\frac{\partial R_T}{\partial a} &= \frac{\beta b_L b_N (1-a)^2}{\mu_A (b_L(1-r)+\mu_L)(b_N(1-r)+\mu_N)} \frac{\partial}{\partial a} \left((1-a)^2 \right) \\
&= -\frac{2}{1-a} R_T \\
&< 0.
\end{aligned}$$

We also prove that $R_T(r, a)$ is concave up with respect to a, by observing that when $R_T > 0$ and $a \in [0, 1)$, the second derivative is positive

$$\begin{aligned}
\frac{\partial^2 R_T}{\partial a^2} &= \frac{\partial}{\partial a} \left(\frac{\partial R_T}{\partial a} \right), \\
&= \frac{\partial}{\partial a} \left(-\frac{2}{1-a} R_T \right), \\
&= \frac{2R_T}{(1-a)^2}, \\
&> 0.
\end{aligned}$$

To sum up, we have that

- $\frac{\partial R_T}{\partial a} < 0 \quad \forall a \in [0, 1)$, and R_T is always concave up as a function of a.
- $\frac{\partial R_T}{\partial r} < 0 \quad \forall r \in [0, 1)$. Simulations show that for certain parameter values, there exists a unique change of concavity for R_T with respect to r from concave down to concave

up.

Therefore the partial derivatives show that both control measures effectively reduce the proliferation potential of ticks. Moreover, as a (the proportion of hosts effectively protected through acaricides) increases, its effect of reducing R_T decreases since the second derivative is positive. Just a relatively small application of acaricide therefore becomes relevant to reduce the tick proliferation. In comparison, the concavity of $\frac{\partial R_T}{\partial r}$ may change once in our model and the value of r at the inflection point could be chosen as the effective repellent administration proportion.

4.5.2 Dependence of R_D on control measures

We then focus on the impact of the control measures considered on the tick-borne disease proliferation by seeing the effect of parameters a and r on the disease reproduction number R_D. We write R_T as a function of r and a and study its partial derivatives with respect to these two parameters. We see that

$$R_D(r,a) = \frac{-A(r,a) + \sqrt{A^2(r,a) + 4B(r,a)}}{2},$$

where

$$A(r,a) = \ln(1-\delta)\ln(R_T(r,a))\frac{\mu_A}{\gamma b_N (1-r)^2(1-a)},$$

and

$$B(r,a) = \frac{\mu_A p_{NH} p_{HL} \ln(R_T(r,a))}{\gamma(\gamma_H + \mu_H)(1-a)}.$$

Computations for partial derivatives of R_D are more complicated, but we derive an interesting result which shows the connection between R_D, R_T and acaricide parameter a. In order to describe this, we need

$$\frac{\partial \ln(R_T)}{\partial a} = \frac{1}{R_T}\frac{\partial R_T}{\partial a} = -\frac{2}{1-a}.$$

By using the Chain Rule, we get

$$\frac{\partial R_D}{\partial a} = \frac{1}{2}\left[-\frac{\partial A}{\partial a} + \frac{1}{2}(A^2+4B)^{-\frac{1}{2}}\left(2A\frac{\partial A}{\partial a} + 4\frac{\partial B}{\partial a}\right)\right].$$

so we can examine the partial derivatives of A and B with respect to a:

$$\begin{aligned}\frac{\partial A}{\partial a} &= \frac{\ln(1-\delta)\mu_A}{\gamma b_N (1-r)^2}\frac{\partial}{\partial a}\left(\frac{\ln(R_T)}{1-a}\right)\\ &= \frac{A(1-a)}{\ln(R_T)}\left(\frac{\ln(R_T)-2}{(1-a)^2}\right)\\ &= \frac{A}{\ln(R_T)(1-a)}(\ln(R_T)-2),\end{aligned}$$

and similarly

$$\begin{aligned}\frac{\partial B}{\partial a} &= \frac{\mu_A p_{NH} p_{HL}}{\gamma(\gamma_H+\mu_H)}\frac{\partial}{\partial a}\left(\frac{\ln(R_T)}{1-a}\right)\\ &= \frac{B(1-a)}{\ln(R_T)}\left(\frac{\ln(R_T)-2}{(1-a)^2}\right)\\ &= \frac{B}{\ln(R_T)(1-a)}(\ln(R_T)-2).\end{aligned}$$

Note that there is a threshold where both partial derivatives change sign, which corresponds to $R_T = e^2$. We immediately see that R_D is a non-negative real quantity if and only if $R_T > 1$. Therefore, we conclude that

- If $1 < R_T < e^2$, then $\frac{\partial A}{\partial a} > 0$, $\frac{\partial B}{\partial a} < 0$ and R_D is decreasing;
- If $R_T = e^2$, then $\frac{\partial A}{\partial a} = 0$, $\frac{\partial B}{\partial a} = 0$ and it is a critical point (maximum) of R_D;
- If $R_T > e^2$, then $\frac{\partial A}{\partial a} < 0$, $\frac{\partial B}{\partial a} > 0$ and R_D is increasing.

Change of disease reproduction number R_D with respect to the acaricide parameter a depends on the basic reproduction number of ticks R_T when no acaricide control is applied ($a = 0$). In particular, we know that R_T is a decreasing function with respect to a, therefore

- $R_T(r,0) < e^2 \Rightarrow \frac{\partial R_D}{\partial a} < 0 \quad \forall a \in [0, \hat{a})$ where $\hat{a} := a : R_T(r,a) = 1$.

- $R_T(r,0) > e^2 \Rightarrow \frac{\partial R_D}{\partial a} > 0 \quad \forall a \in [0, a^*), \frac{\partial R_D}{\partial a} < 0 \quad \forall a \in (a^*, \hat{a})$,
  where $a^* := a : R_T(r,a) = e^2$.

The disease reproduction number with respect to the repellent parameter r is mostly increasing from simulations. The analytical computations of this case are done in a similar way and are rather lengthy so they have been omitted in this work. We have instead included a plot in the next section to study the effect of r on R_D together with an explanation of why it may increase disease transmission in certain circumstances and under specific assumptions.

We conclude that when the tick population does not grow fast enough ($R_T(r,0) < e^2$), transmission potential of the disease (R_D) decreases as we increase acaricide treatment (a). If the tick population grows fast without acaricide control ($a = 0$), increasing the level of acaricide control will amplify the transmission potential. This negative effect of acaricide control on disease transmission is related to the fact that acaricides perturb the age structure of the tick population which is explained in detail in the next section.

4.6 Simulations - Control strategies

In this section, we describe how control effects influence tick dynamics and show how these can be counter effective in limiting TBD spread through a series of simulations. The choice of parameters is not entirely realistic and is made in order to show some possible counterintuitive results. Biting rates for larvae and nymphs are $b_L = b_N = 0.5$, parameters related to larval birth rate are $\beta = 15$ and $\gamma = 6.2$. Mortality rates are respectively for ticks $\mu_L = 0.1$ in larval case, $\mu_N = 0.002$ in nymphal case and $\mu_A = 0.1$ in adult case and $\mu_H = 0.001$ for hosts. The probability of systemic infection is $p_{NH} = 0.9$ in the nymph-to-host case and $p_{HL} = p_{HN} = 0.8$ in host-to-tick transmission. Recovery rate of hosts is $\gamma_H = 0.1$ and co-feeding probability is $\delta = 0.7$. Repellent and acaricide parameters r and a are variables in these simulations and are quantities in $[0, 1)$ since they show the constant proportion of effective repellent or acaricide-treated hosts with respect to all hosts.

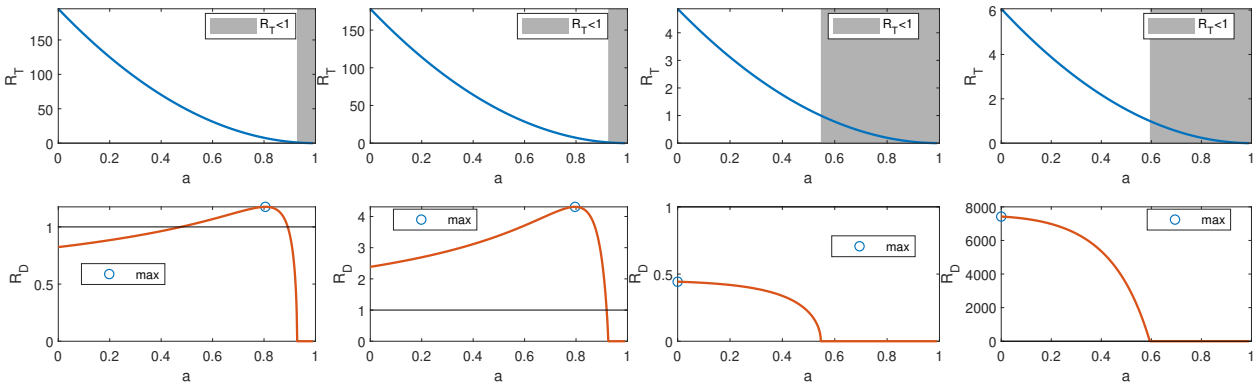

Figure 4.2: Different behaviours of R_D as acaricide control parameter a varies.

4.6.1 Acaricide control

In Figure 4.2, we analyse how R_T and R_D change as we increase the acaricide control depending on the parameters chosen. In the leftmost panel, we see that increasing acaricide control may impact R_D which can become greater than 1 and therefore lead to a persistence of the disease in an area where it was not established before. This indicates that controlling tick population in a non-endemic area may increase the transmission potential of tick borne diseases enough so that the area turns into an endemic area when a disease is introduced. The second panel shows that application of acaricide may also increase the transmission potential (R_D) in endemic areas. In the two panels on the right, control effectively reduces tick population and the potential of TBD spread as R_D is increasing when the acaricide parameter a is increased. The reason why acaricide control can increase disease transmission potential is explained in Figure (4.3). The left panel of Figure 4.3 shows that the adult population decreases as the acaricide parameter is increased (blue curve). As the number of adult decreases, the density-dependent factor in the birth rate of larvae also decreases. This explains why the number of larvae may increase with increased acaricide control (red curve). This larvae overcompensation can result in the increase of susceptible ticks. Therefore, the increased level of acaricide application may increase the disease reproduction number R_D (central panel). After R_D exceeds the threshold value ($R_D = 1$), the disease persists and the number of infected nymphs can also increase with the increased level of acaricide control

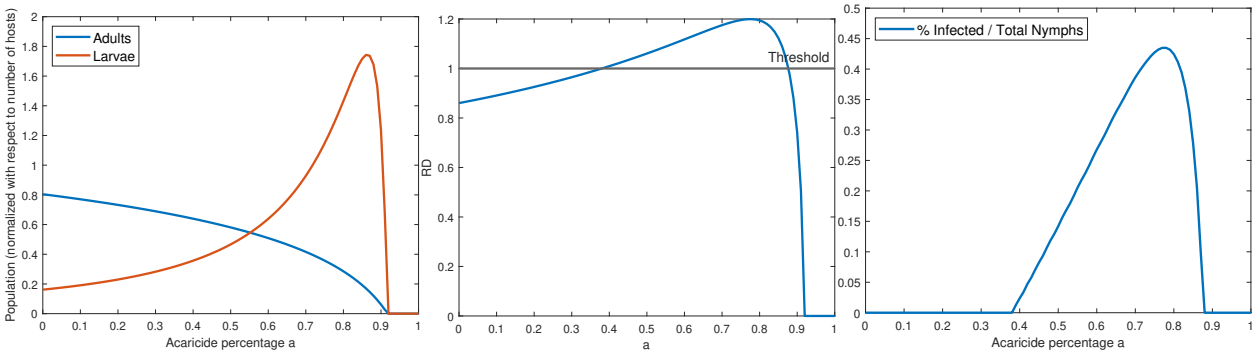

Figure 4.3: Effect of acaricide control on tick population and disease reproduction number R_D.

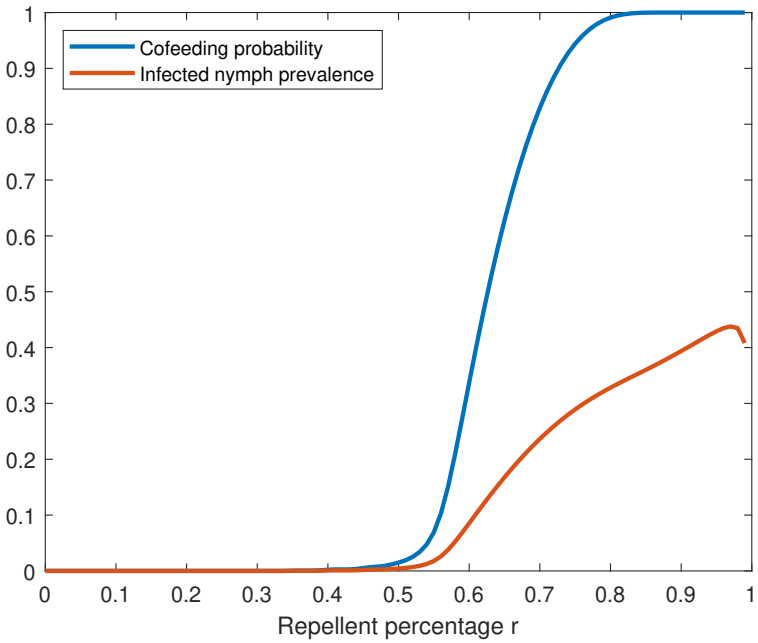

Figure 4.4: Effect of repellent on the co-feeding probability and on the prevalence of infected nymphs.

(right panel).

4.6.2 Repellent control

Figure 4.4 shows how the use of repellent on hosts can be counterproductive to TBD control and lead to a dramatic increase in disease prevalence. In the plot, as the repellent parameter r increases, both co-feeding probability and number of infected nymphs at equilibrium increase.

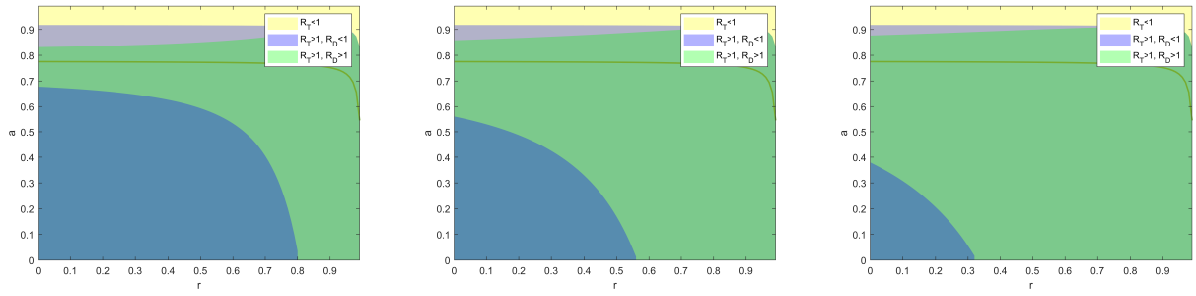

Figure 4.5: Different behaviours of R_D and R_T where co-feeding probability δ is respectively 0.1, 0.4 and 0.7. The green line shows the values of r and a such that $R_T = e^2$ and it is relevant since it will be the line in which R_D reaches the maximum value.

This is a natural consequence since repellent use can lead to a reduction of hosts available to feed the ticks. Since ticks need to feed on hosts in order to develop, they will eventually have to gather around the fewer hosts that are available. So, on average every host will be fed by a larger number of ticks, thus increasing the possibility of co-feeding and disease transmission between ticks. In this case, the number of infected nymphs is very large, thus indicating that repellent control may escalate the disease burden.

4.6.3 Combined acaricide and repellent

In Figure 4.5, we present three plots with varying co-feeding probability parameter δ. Other parameter values are chosen in the same way as the left-most plot of Figure 4.2. The areas with three different colours represent the parameter regions of acaricide and repellent controls with specific solution behaviors:

- Yellow coloured areas represent the percentages of repellent and acaricide control yielding $R_T < 1$ and therefore tick population cannot establish in the region.
- Blue coloured areas represent control values that yield $R_T > 1$ and $R_D < 1$. In this setting, tick population can be established but disease cannot persist.
- Green coloured areas represent control values that yield $R_T > 1$ and $R_D > 1$. In this case, both ticks and disease persist.

There are several aspects that are worth mentioning. First of all, control strategies should be applied only after careful analysis. In the above three plots, we see that if a control strategy cannot be applied extensively, it would be wise not to introduce any acaricide or repellent in the host population since it may lead to disease persistence in previously disease-free areas. Secondly, co-feeding probability δ does not change the plot qualitatively, but it does quantitatively by modifying the area of the disease-free region. This confirms the fact that co-feeding is a relevant mode of transmission and should be considered when designing any tick-control strategy. Finally, there is a difference in control effectiveness between the two strategies analysed. Acaricide is generally more effective than repellent in its ability to control tick spread and it can even lead to tick extinction if applied in high doses.

4.7 Final considerations on control strategies

In this paper, we have shown how different types of host-targeted tick-control strategies affect tick population and tick-borne disease transmission when pathogens can be transmitted both by a systemic and a co-feeding route. In particular, we have demonstrated that control strategies can be counter effective in highly favourable environments for tick growth since these strategies can increase the spread of tick-borne diseases and, in certain cases, even cause a disease outbreak in otherwise disease-free areas. We have also shown how co-feeding and overcompensation play an important role in disease transmission dynamics.

In our model though, one of the assumptions made is that the proportion of controlled hosts remains constant in time. In real life, it is possible for ticks to develop immunity against insecticides making them no longer as effective as before [89]. With a constant effort, this will lead to a decrease in the proportion of hosts effectively protected by insecticides, and therefore may affect tick population dynamics (see Figure 4.5). It is though necessary to consider both non-constant acaricide application and tick immunity for further studies, and to analyse how these two factors would modify tick population and disease transmission dynamics. In addition, it is interesting to further examine different parameter choices in this

model that lead to oscillations and other interesting dynamical behaviours.

In conclusion, applications of acaricide and repellent are effective control measures for the tick population, however, these may result in increasing the transmission potential of the tick-borne diseases if applied without careful analysis.

Chapter 5

Conclusion

5.1 Summary of the work

Using three different mathematical models, we looked into the effect of physiological and environmental factors including tick diapause and control strategies, on tick growth and tick-borne disease spread.

In the second chapter, we studied how mobility and tick-patch suitability affect tick population dynamics. We first studied the isolated model and introduced a patch-specific tick reproduction number $R_{T,i}$. Then we considered unilateral and bilateral migration of ticks between two different patches and showed how parameters affect the dynamics through the general tick reproduction number $R_{T,c}$. We concluded that modifying the environmental conditions and migration probabilities may have a significant impact on tick population depending on the value of $R_{T,c}$ and control strategies may be able to radically change the dynamics from tick-endemic patches to a tick-free state.

In the third chapter, we looked at multi-cycle periodic solutions of a tick-related model including a delay that switches periodically between two different values showing two different development rates for ticks either undergoing or not undergoing diapause. We analysed the model dynamics and determined the cases in which the oscillations of different frequencies produced by the two delays would lead to a periodic persistent pattern.

In the fourth chapter, we studied the effect of acaricide and repellent on hosts with respect to tick population and disease dynamics. We introduced two different basic reproduction numbers: R_T and R_D and showed their relevance in determining a tick-endemic or a tick-free area (R_T) or a tick disease-endemic or a tick disease-free area (R_D). We also studied how it is possible for both repellent and acaricide application to be countereffective and increase disease burden instead of reducing it.

Altogether, these works give further theoretical insight in the attempt to control the tick population and in particular tick-borne diseases which have been a burden worldwide.

5.2 Final thoughts

In general, tick and tick-borne disease models are becoming "hot" topic in the epidemiological community since ticks are considered to be one of the most dangerous vectors after mosquitoes for disease spread. The range of tick-borne diseases is rather wide and can be separated into different categories according to the kind of diseases (viral, bacterial or parasitic) and the tick species involved [1, 4]. One of the strengths of our models is that they are pretty general and therefore can be used with further modifications for different tick vectors and tick-borne diseases. The first two models presented in this thesis study tick population dynamics. In the patchy model, the main focus is to study *Ixodes scapularis*' population dynamics but it can be generalised to any two or three host tick population. In the periodically switching model, there is no further assumption on tick species and therefore may represent any general tick dynamics. The third model instead looks into tick-borne disease dynamics as well. Also in this case, it can capture the dynamics of different tick-borne diseases by including parameters deriving from the specific disease like the probability of transmission and from the tick species responsible for the disease spread like the different birth, death and development rates.

On the other hand, the models proposed present a few limitations and possible improvements or extensions. In chapter 2, some details have been omitted including global stability in the case $e < R_T < e^2$ for both the isolated and interconnected model, which may be proved

using exponential ordering. Also missed are the theoretical conditions for Hopf bifurcation to take place in the asymptotic interconnected model. As a possible step ahead, we could include the effect of control strategies directly into the model and consider parameters to be dependent on some of these strategies. This way, we could be able to analyse and understand how the different control strategies may coexist or if there is an ideal control strategy for a specific environment. Another idea would be to consider temperature and/or humidity-dependent parameters instead of choosing them to be constant, since we have seen in the introduction that these are relevant factors for tick development. In chapter 3, we used function $f(x) = -\text{sgn}(x)$ to represent a density-dependent factor (a large number of ticks would mean there is more competition for resources). This function is one of the simplifying assumptions of the model which in practice should be continuous and monotonically decreasing. Some details have also been omitted in the proof of Theorem 20. In general, we would like to study the effect of perturbations in the model and see if their presence may have a significant impact on tick population dynamics. In chapter 4, we have not included the analytical results regarding the effect of repellent in the disease reproduction number R_D. We should also consider in the future a possible extension of the model by including a non-constant control effort with a time-dependent acaricide and repellent parameter. In this aspect, we may consider tick resistence to acaricides which would lead to a decrease of effectively treated hosts even with a constant effort.

5.3 Future works

A new virus that has been identified in the past few years in the United States is the Heartland virus, caused by lone-star ticks (*Amblyomma americanum*) [90, 91]. This has been identified for the first time in Missouri in 2009 and has been found to be persistent in raccoons and deer in the area. Lone-star ticks have been mainly found in the United States and in Central America and have been responsible for a number of other diseases. Some of them include bacterial infections such as tick-borne relapsing fever and ehrlichiosis, and viral infections

such as the Alpha-gal syndrome, which has recently been identified also in Canada and causes red meat allergies [92]. Public Health Agency of Canada has identified cases of lone-star tick establishment in Canada, thus increased their attention to the study of the effect of global warming in their northward movement [93]. In this framework, possible future work would be to predict the tick basic reproduction number in Canada for this species and to create a map for lone-star ticks similarly to [3] for *Ixodes scapularis*.

In regards to control strategies, we find in literature some models considering one or a few of the aforementioned control strategies [68, 69, 70, 71] and reviews describing general control methods [94, 95]. Another possible future plan would be to consider mathematically all known tick control methods and compare their effectiveness and costs. This could be achieved by introducing a mathematical model similar to that proposed in Chapter 4 and considering additional strategy-dependent parameters and initial conditions. For example, we could consider some habitat-related strategies such as the removal of the mat layer to increase the ticks' development time by reducing their development rates. This general model in addition to the availability of area-specific data (for example tick and host surveillance data and the cost of different control applications) could then be used to validate the model and to give insight to propose an optimal control strategy that tries to minimize both tick-borne disease burden and cost.

Bibliography

[1] *Vector-borne diseases*. 2022. URL: https://www.who.int/news-room/fact-sheets/detail/vector-borne-diseases.

[2] *Global vector control response and its implementation*. 2022. URL: https://www.who.int/docs/default-source/wrindia/presentations-webinar-on-vector-control-strategies/gvcr-implementation-dr-raman.pdf?sfvrsn=a2089c2f_2.

[3] X. Wu et al. "Developing a temperature-driven map of the basic reproductive number of the emerging tick vector of Lyme disease *Ixodes scapularis* in Canada". *Journal of Theoretical Biology* 319 (2013), pp. 50–61.

[4] M. Service. *Medical Entomology for Students*. Cambridge University Press, 2012.

[5] D. Sonenshine and R. Roe. *Biology of Ticks (Vol.1)*. Oxford University Press, 2013.

[6] D. Sonenshine and R. Roe. *Biology of Ticks (Vol.2)*. Oxford University Press, 2013.

[7] J. Gray et al. "Diapause in ticks of the medically important *Ixodes ricinus* species complex". *Ticks and Tick Borne Diseases* 7.5 (2016), pp. 992–1003.

[8] J. Piesman and L. Eisen. "Prevention of tick-borne diseases". *Annual Review of Entomology* 53 (2008), pp. 323–343.

[9] *ECDC - factsheet about tick-borne encephalitis*. 2022. URL: https://www.ecdc.europa.eu/en/tick-borne-encephalitis.

[10] *Vaccine for tick-borne encephalitis*. 2022. URL: https://www.cdc.gov/tick-borne-encephalitis.

[11] G. B. Schoeler and R. S. Lane. "Efficiency of transovarial transmission of the Lyme disease spirochete, *Borrelia burgdorferi*, in the western blacklegged tick, *Ixodes pacificus* (Acari: Ixodidae)". *Journal of Medical Entomology* 30.1 (1993), pp. 80–86.

[12] N. E. Breuner, A. Hojgaard, and L. Eisen. "Lack of evidence for transovarial transmission of the Lyme disease spirochete *Borrelia mayonii* by infected female *Ixodes scapularis* (Acari: Ixodidae) ticks". *Journal of Medical Entomology* 55.3 (2018), pp. 739–741.

[13] A. Harrison and N. C. Bennett. "The importance of the aggregation of ticks on small mammal hosts for the establishment and persistence of tick-borne pathogens: an investigation using the R0 model". *Parasitology* 139.12 (2012), pp. 1605–1613.

[14] M. J. Voordouw. "Co-feeding transmission in Lyme disease pathogens". *Parasitology* 142.2 (2015), pp. 290–302.

[15] K. Nah et al. "Assessing systemic and non-systemic transmission risk of tick-borne encephalitis virus in Hungary". *PLoS ONE* 14.6 (2019), pp. 1–18.

[16] M. Labuda et al. "Tick-borne encephalitis virus transmission between ticks co-feeding on specific immune natural rodent hosts". *Virology* 235 (1997), pp. 138–143.

[17] B. Greenfield. "Environmental parameters affecting tick (*Ixodes ricinus*) distribution during the summer season in Richmond Park". *Bioscience Horizons* 4.2 (2011), pp. 140–148.

[18] J. Gray. "The ecology of ticks transmitting Lyme borreliosis". *Experimental and Applied Acarology* 22.5 (1998), pp. 249–258.

[19] C. A. Cobbold, J. Teng, and J. S. Muldowney. "The influence of host competition and predation on tick densities and management implications". *Theoretical Ecology* 8.3 (2015), pp. 349–368.

[20] J. Gray et al. "Studies on the ecology of Lyme disease in a deer forest in County Galway, Ireland". *Journal of Medical Entomology* 29.6 (1992), pp. 915–920.

[21] T. Levi et al. "Deer, predators, and the emergence of Lyme disease". *Proceedings of the National Academy of Sciences (PNAS)* 109.27 (2012), 10942–10947.

[22] R. S. Ostfeld et al. "Tick-borne disease risk in a forest food web". *Ecology* 99.7 (2018), pp. 1562–1573.

[23] N. Ogden et al. "Investigation of relationships between temperature and developmental rates of tick *Ixodes scapularis* (Acari: Ixodidae) in the laboratory and field". *Journal of Medical Entomology* 41.4 (2004), pp. 622–633.

[24] S. Randolph and G. Steele. "An experimental evaluation of conventional control measures against the sheep tick, *Ixodes ricinus* (L.) (Acari: Ixodidae). II. The dynamics of the tick-host interaction". *Bulletin of Entomological Research* 75 (1985), pp. 501–518.

[25] S. Randolph and K. Storey. "Impact of microclimate on immature tick-rodent host interactions (Acari: Ixodidae): implications for parasite transmission". *Journal of Medical Entomology* 36.6 (1999), pp. 741–748.

[26] A. Lees. "The sensory physiology of the sheep tick, *Ixodes ricinus* L." *Journal of Experimental Biology* 25.2 (1948), pp. 145–207.

[27] C. Boyard et al. "Local environmental factors characterizing *Ixodes ricinus* nymph abundance in grazed permanent pastures for cattle". *Journal of Parasitology* 134.7 (2007), pp. 473–478.

[28] A. Estrada-Pena. "The relationships between habitat topology, critical scales of connectivity and tick abundance *Ixodes ricinus* in a heterogeneous landscape in northern Spain". *Ecography* 26.5 (2003), pp. 661–671.

[29] A. Estrada-Pena. "Distribution, abundance, and habitat preferences of *Ixodes ricinus* (Acari: Ixodidae) in Northern Spain". *Journal of Medical Entomology* 38.3 (2011), pp. 361–370.

[30] N. H. Ogden et al. "Possible effects of climate change on Ixodid ticks and the pathogens they transmit: predictions and observations". *Journal of Medical Entomology* 58.4 (2021), pp. 1536–1545.

[31] A. Walker et al. "Risk factors in habitats of the tick *Ixodes ricinus* influencing human exposure to *Ehrlichia phagocytophila* bacteria". *Medical and Veterinary Entomology* 15 (2001), pp. 40–49.

[32] A. Lindstrom and T. Jaenson. "Distribution of the common tick, *Ixodes ricinus* (Acari: Ixodidae), in different vegetation types in Southern Sweden". *Journal of Medical Entomology* 40.4 (2003), pp. 375–378.

[33] M. Guerra et al. "Predicting the risk of Lyme disease: habitat suitability for *Ixodes scapularis* in the North Central United States". *Emerging Infectious Diseases* 8.3 (2002), pp. 289–297.

[34] J. Medlock et al. "Driving forces for changes in geographical distribution of *Ixodes ricinus* ticks in Europe". *Parasites Vectors* 6.1 (2013).

[35] M. C. Dolan. et al. "Control of immature *Ixodes scapularis* (Acari: Ixodidae) on rodent reservoirs of *Borrelia burgdorferi* in a residential community of Southeastern Connecticut". *Journal of Medical Entomology* 41.6 (2004), pp. 1043–1054.

[36] R. A. Jordan and T. L. Schulze. "Ability of two commercially available host-targeted technologies to reduce abundance of *Ixodes scapularis* (Acari: Ixodidae) in a residential landscape". *Journal of Medical Entomology* 56.4 (2019), pp. 1095–1101.

[37] J. M. Pound et al. "Efficacy of amitraz-impregnated collars on white-tailed deer (Artiodactyla: Cervidae) in reducing free-living populations of lone star ticks (Acari: Ixodidae)". *Journal of Economic Entomology* 105.6 (2012), pp. 2207–2212.

[38] F. Ruis-Fonz and L. Gilbert. "The role of deer as vehicles to move ticks, *Ixodes ricinus*, between contrasting habitats". *International Journal for Parasitology* 40 (2010), pp. 1013–1020.

[39] J. Piesman. "Response of nymphal *Ixodes scapularis*, the primary tick vector of Lyme disease spirochetes in North America, to barriers derived from wood products or related home and garden items". *Journal of Vector Ecology* 31.2 (2006), pp. 412–417.

[40] B. Allan. "Influence of prescribed burns on the abundance of *Amblyomma americanum* (Acari: Ixodidae) in the Missouri ozarks". *Journal of Medical Entomology* 46.5 (2009), pp. 1030–1036.

[41] K. C. Stafford, J. S. Ward, and L. A. Magnarelli. "Impact of controlled burns on the abundance of *Ixodes scapularis* (Acari: Ixodidae)". *Journal of Medical Entomology* 35.4 (1998), pp. 510–513.

[42] H. D. Gaff et al. "TickBot: A novel robotic device for controlling tick populations in thenatural environment". *Ticks and Tick-borne Diseases* 6 (2015), pp. 146–151.

[43] J. Ohlberger et al. "Stage-specific biomass overcompensation by juveniles in response to increased adult mortality in a wild fish population". *Ecology* 92.12 (2011), pp. 2175–2182.

[44] T. Caraco et al. "Stage-structured infection transmission and a spatial epidemic: a model for Lyme disease". *American Naturalist* 160.3 (2002), pp. 348–359.

[45] Y. Zhang and X. Zhao. "A reaction-diffusion Lyme disease model with seasonality". *SIAM Journal of Applied Mathematics* 73.6 (2013), pp. 2077–2099.

[46] Y. Lou and J. Wu. "Modeling Lyme disease transmission". *Infectious Disease Modelling* 2.2 (2017), pp. 229–243.

[47] G. Fan, H. Thieme, and H. Zhu. "Delay differential systems for tick population dynamics". *Journal of Mathematical Biology* 71.5 (2015), pp. 1017–1048.

[48] H. Shu, G. Fan, and H. Zhu. "Global Hopf bifurcation and dynamics of a stage-structured model with delays for tick population". *Journal of Differential Equations* 284 (2021), pp. 1–22.

[49] X. Wang and X. Zhao. "Dynamics of a time-delayed Lyme disease model with seasonality". *SIAM Journal of Applied Dynamical Systems* 16.2 (2017), pp. 853–881.

[50] D. Fisman, A. Tuite, and K. Brown. "Impact of El Niño Southern Oscillation on infectious disease hospitalization risk in the United States". *Proceedings of the National Academy of Sciences (PNAS)* 113.51 (2016), pp. 14589–14594.

[51] N. H. Ogden et al. "A dynamic population model to investigate effects of climate on geographic range and seasonality of the tick *Ixodes scapularis*". *International Journal for Parasitology* 35.4 (2005), pp. 375–389.

[52] N. H. Ogden et al. "Climate change and the potential for range expansion of the Lyme disease vector *Ixodes scapularis* in Canada". *International Journal of Parasitology* 36 (2006), pp. 63–70.

[53] N. H. Ogden et al. "Estimated effects of projected climate change on the basic reproductive number of the Lyme disease vector *Ixodes scapularis*". *Environmental Health Perspectives* 122.6 (2014), pp. 631–638.

[54] M. McPherson et al. "Expansion of the Lyme disease vector *Ixodes scapularis* in Canada inferred from CMIP5 climate projections". *Environmental Health Perspectives* 125.5 (2017), p. 057008.

[55] A. Cheng et al. "Analyzing the potential risk of climate change on Lyme disease in Eastern Ontario, Canada using time series remotely sensed temperature data and tick population modelling". *Remote sensing* 9.6 (2017), p. 609.

[56] K. Clow et al. "Northward range expansion of *Ixodes scapularis* evident over a short timescale in Ontario, Canada". *PLoS ONE* 12.12 (2017), e0189393.

[57] R. Jennings et al. "How ticks keep ticking in the adversity of host immune reactions". *Journal of Mathematical Biology* 78 (2019), pp. 1331–1364.

[58] M. Ghosh and A. Pugliese. "Seasonal population dynamics of ticks, and its influence on infection transmission: a semi-discrete approach". *Bulletin of Mathematical Biology* 66 (2004), pp. 1659–1684.

[59] R. Rosà et al. "Temporal variation of *Ixodes ricinus* intensity on the rodent host *Apodemus flavicollis* in relation to local climate and host dynamics". *Vector-borne and Zoonotic Diseases* 7.3 (2007), pp. 285–295.

[60] A. Ludwig et al. "A dynamic population model to investigate effects of climate and climate-independent factors on the lifecycle of *Amblyomma americanum* (Acari: Ixodidae)". *Journal of Medical Entomology* 53.1 (2016), pp. 99–115.

[61] A. D. M. Dobson, T. J. R. Finnie, and S. E. Randolph. "A modified matrix model to describe the seasonal population ecology of the European tick *Ixodes ricinus*". *Journal of Applied Ecology* 48 (2011), pp. 1017–1028.

[62] X. Zhang and J. Wu. "Critical diapause portion for oscillations: Parametric trigonometric functions and their applications for Hopf bifurcation analyses". *Mathematical Methods in the Applied Sciences* 42.5 (2019), pp. 1363–1376.

[63] X. Zhang et al. "Global continuation of periodic oscillations to a diapause rhythm". *Journal of Dynamics and Differential Equations* (2020), pp. 1–21.

[64] R. Rosà et al. "Thresholds for disease persistence in models for tick-borne infections including non-viraemic transmission, extended feeding and tick aggregation". *Journal of Theoretical Biology* 224 (2003), pp. 359–376.

[65] X. Wu et al. "Stage-structured population systems with temporally periodic delay". *Mathematical Methods in the Applied Sciences* 38.16 (2015), pp. 3464–3481.

[66] X. Zhang, X. Wu, and J. Wu. "Critical contact rate for vector-host-pathogen oscillation involving co-feeding and diapause". *Journal of Biological Systems* 25.4 (2017), pp. 657–675.

[67] X. Zhang and J. Wu. "Implications of vector attachment and host grooming behaviour for vector population dynamics and distribution of vectors on their hosts". *Applied Mathematical Modelling* 81 (2020), pp. 1–15.

[68] R. W. Sutherst et al. "An analysis of management strategies for cattle tick (*Boophilus microplus*) control in Australia". *Journal of Applied Ecology* 16.2 (1979), pp. 359–382.

[69] V. Labarta et al. "Simulation of control strategies for the cattle tick *Boophilus microplus* employing vaccination with a recombinant Bm86 antigen preparation". *Veterinary Parasitology* 63 (1996), pp. 131–160.

[70] H. D. Gaff and L. J. Gross. "Modeling tick-borne disease: a metapopulation model". *Bulletin of Mathematical Biology* 69 (2007), pp. 265–288.

[71] H. D. Gaff, E. Schaefer, and S. Lenhart. "Use of optimal control models to predict treatment time for managing tick-borne disease". *Journal of Biological Dynamics* 5.5 (2011), pp. 517–530.

[72] X. Zhang, B. Sun, and Y. Lou. "Dynamics of a periodic tick-borne disease model with co-feeding and multiple patches". *Journal of Mathematical Biology* 82.27 (2021).

[73] X. Zhang and J. Wu. "Synchronized tick population oscillations driven by host mobility and spatially heterogeneous developmental delays combined". *Bulletin of Mathematical Biology* 83.6 (2021).

[74] S. E. Randolph and D. J. Rogers. "A generic population model for the African tick *Rhipicephalus appendiculatus*". *Parasitology* 115.3 (1997), pp. 265–279.

[75] J. Hale and S. V. Lunel. *Introduction to functional differential equations*. Springer Science + 35 Business Media, LLC, 1993.

[76] H. Smith. *Monotone Dynamical Systems: an Introduction to the Theory of Competitive and Cooperative Systems*. American Matematical Society Ebooks Program, 1995.

[77] P. van den Driessche and J. Watmough. "Reproduction numbers and sub-threshold endemic equilibria for compartmental models of disease transmission". *Mathematical Biosciences* 180 (2002), pp. 29–48.

[78] N. A. Hartemink et al. "The basic reproduction number for complex disease systems: Defining R_0 for tick-borne infections". *The American Naturalist* 171.6 (2008), pp. 743–754.

[79] H. Smith. *An Introduction to Delay Differential Equations with Application to the Life Sciences*. Springer, 2010.

[80] S. Randolph. "Tick ecology: processes and patterns behind the epidemiological risk posed by Ixodid ticks as vectors". *Journal of Parasitology* 129 (2004), S37–65.

[81] *European centre for disease prevention and control: Ixodes ricinus—factsheet for experts*. 2022. URL: https://ecdc.europa.eu/en/disease-vectors/facts/tick-factsheets/ixodes-ricinus.

[82] X. Zhang and J. Wu. *Transmission dynamics of tick-borne diseases with co-feeding, developmental and behavioural diapause*. Springer, 2020.

[83] M. C. Mackey, M. Tyran-Kaminska, and H. O. Walther. "Response of an oscillatory differential delay equation to a single stimulus". *Journal of Mathematical Biology* 74 (2017), pp. 1139–1196.

[84] H. I. Freedman and J. Wu. "Periodic solutions of single-species models with periodic delay". *SIAM Journal on Mathematical Analysis* 23.3 (1992), pp. 689–701.

[85] D. C. De Souza and M. C. Mackey. "Response of an oscillatory differential delay equation to a periodic stimulus". *Journal of Mathematical Biology* 78 (2019), pp. 1637–1679.

[86] B. W. Bissinger and R. M. Roe. "Tick repellents: past, present, and future". *Pesticide Biochemistry and Physiology* 96 (2010), pp. 63–79.

[87] S. Randolph. "Abiotic and biotic determinants of the seasonal dynamics of the tick *Rhipicephalus appendiculatus* in South Africa". *Medical and Veterinary Entomology* 11.1 (1997), pp. 25–37.

[88] O. Diekmann, J. A. P. Heesterbeek, and M. G. Roberts. "The construction of next-generation matrices for compartmental epidemic models". *Journal of the Royal Society Interface* 7 (2010), pp. 873–885.

[89] M. Leschnik et al. "Effect of owner-controlled acaricidal treatment on tick infestation and immune response to tickborne pathogens in naturally infested dogs from Eastern Austria". *Parasites & Vectors* 6.62 (2013).

[90] *Heartland virus disease*. 2022. URL: https://www.cdc.gov/heartland-virus/index.html.

[91] E. M. Esguerra. "Heartland virus: A new virus discovered in Missouri". *Missouri Medicine* 113.4 (2016), pp. 256–257.

[92] *Carnivores beware: tick that causes red meat allergy found in Canada*. 2022. URL: https://nationalpost.com/news/canada/carnivores-beware-tick-that-causes-red-meat-allergy-found-in-canada.

[93] I. Sagurova et al. "Predicted northward expansion of the geographic range of the tick vector *Amblyomma americanum* in North America under future climate conditions". *Environmental Health Perspectives* 127.10 (2019), pp. 1–14.

[94] F. Jongejan and G. Uilenberg. "Ticks and control methods". *Revue Scientifique et Technique (Office International des épizooties)* 13.4 (1994), pp. 1201–1226.

[95] A. White and H. D. Gaff. "Review: application of tick control technologies for black-legged, lone star, and american dog ticks". *Journal of Integrated Pest Management* 9.1 (2018), pp. 1–10.